

IMPACT OF HYDRO- METEOROLOGICAL DRIVERS ON THE STREAMFLOW OF THE USANGU CATCHMENT

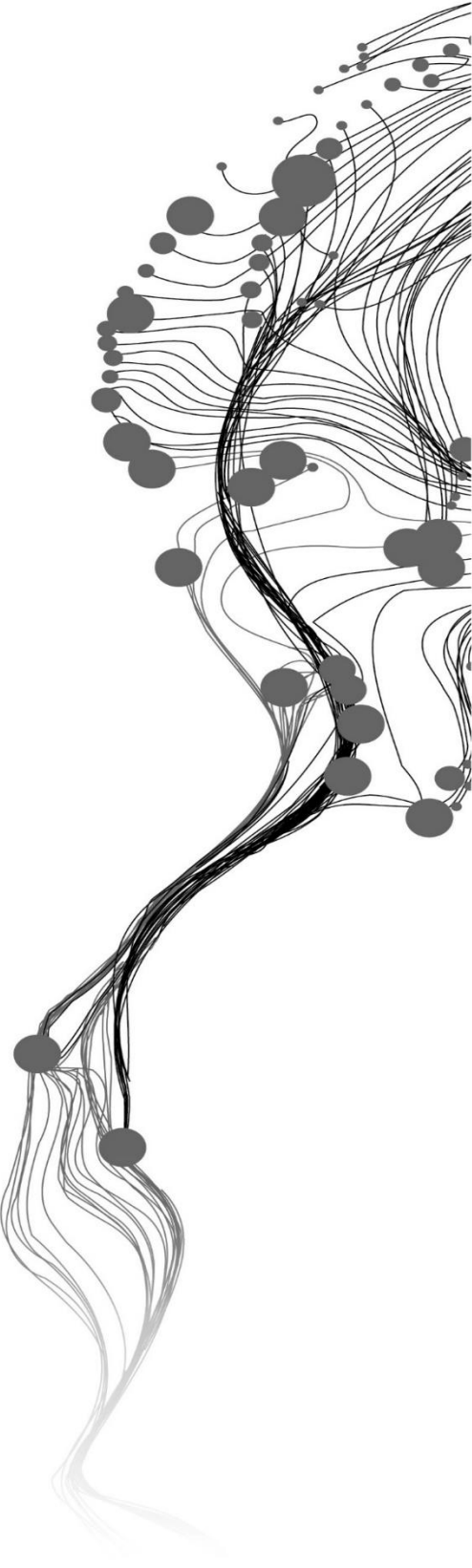
DAMAS PATRICK MBAGA

February, 2015

SUPERVISORS:

Dr. Ir. Rogier van der Velde

Drs. Robert Becht



IMPACT OF HYDRO- METEOROLOGICAL DRIVERS ON THE STREAMFLOW OF THE USANGU CATCHMENT

DAMAS PATRICK MBAGA

Enschede, The Netherlands, February, 2015

Thesis submitted to the Faculty of Geo-Information Science and Earth Observation of the University of Twente in partial fulfilment of the requirements for the degree of Master of Science in Geo-information Science and Earth Observation.

Specialization: Water Resources and Environmental Management

THESIS ASSESSMENT BOARD:

Dr. M.C.Lubczynski (Chair)

Dr.ir. J. Van der Kwast MSc (External Examiner, Unesco-IHE)

Dr. Ir. R. van der Velde

Drs. R. Becht

DISCLAIMER

This document describes work undertaken as part of a programme of study at the Faculty of Geo-Information Science and Earth Observation of the University of Twente. All views and opinions expressed therein remain the sole responsibility of the author, and do not necessarily represent those of the Faculty.

DEDICATIONS

This piece of work is dedicated to my best friend, the lover of my life EVA WILLSON SWILLA.

ABSTRACT

The Coupled Routing Excess Storage (CREST) model. A grid-based distributed hydrological model driven by atmospheric forcings derived from satellite observation is used to evaluate the impact of altered hydro-meteorological drivers on the streamflow of Mbarali sub-catchment. Mbarali sub-catchment is the part of the Usangu basin, which is the major tributary of the Great Ruaha River in Tanzania (GRR). As explained by Shu & Villholth. (2012) the importance of the GRR River in Tanzania economy is built on the fact that almost 51% of the country electricity is produced from the Mtera and Kidatu dams situated downstream of the Usangu catchment and 30% of the Tanzania rice production is form the upstream of the Usangu basin. Furthermore, Ruaha National park placed downstream of the Usangu basin plays a significant role in tourist sector.

Model parameters are calibrated automatically by minimizing the differences between simulated and measured streamflow from 2002 up to 2007 using the Parameter Estimation tool (PEST). The model performance is quite satisfactory, the following model efficiencies are obtained: for calibration period Nash-Sutcliffe efficiency (NSCE = 0.63), Relative bias (Bias% = -0.01) and Correlation of Coefficient (CC= 0.81) for validation period 2008 up to 2012 model performance (NSEC = 0.53, Bias% = -31.12 and CC = 0.78). These results show that satellite data can be used as alternative source of data in ungauged basins.

Subsequently the calibrated model parameters have been utilized to assess the impact of hydro-meteorological drivers on the streamflow of the Mbarali sub-catchment. This has been done by perturbing the RainFact and KE parameters in the CREST model, RainFact is the multiplier on the precipitation field, which is used as a determinant factor to determined precipitation reaching the soil, while KE is the factor used to convert potential evapotranspiration to local actual evaporation, and this factor is used to determine the amount of evapotranspiration in a particular area. This analysis is done for the entire calibration period, further is analysis is done for two selected periods, which are dry year and average year. Within the calibration period 2002/03 is found to be dry year and 2006/07 average year, there is no wet year for the calibration period selected.

As expected, it is found that linearly scaling in rainfall value has positive and negative impact on the streamflow. For example for dry year 2002/03 a decrease in the rainfall to -12 % reduces the runoff volume by 19.64 %, whereas the same increase in rainfall causes an increase in runoff volume by 20.44 %. For average year 2006/07 increase rainfall to +12% resulted in the runoff volume increases by 18.64% and when decreases rainfall by the same value the runoff volume reduces by 18.37 %.

Apparently, it is found that linearly scaling evapotranspiration has negative and positive impact on the streamflow for both average and dry year. For example for dry year 2002/03 decrease evapotranspiration to -12% increase the runoff volume by 6.61%, and increase evapotranspiration by the same value, decrease runoff volume by 6.03%. For average year 2006/07 increase evapotranspiration to +12% the runoff volume decrease by 5.14% and decrease evapotranspiration by the same value runoff volume increases by 5.43 %.

Keywords: CREST distributed hydrological model, Mbarali sub-catchment, RainFact, Streamflow, Satellite data, KE.

ACKNOWLEDGEMENTS

First and foremost I would like to thank the Government of Netherland through Netherland Fellowship Programme (NFP) under the Dutch Ministry of Foreign Affairs for fulfilling my dream of doing my MSc studies abroad particularly in Netherland. I would like also to express my thanks to the University of Twente Faculty of Geo-information Science and Earth observation in particular Department of Water Resources and Environmental Management for granting my admission.

My thanks also are extended to the Government of the United Republic of Tanzania through the Ministry of Water for granting my study leave, special thanks to the Lake Nyasa Basin staff, Lake Nyasa Basin Water Board and Basin Water officer Mr. Witgal Nkondola for his word of encouragement for whole period I was taking my studies.

Am very gratefully to my first Supervisor Dr. Ir. R.van der Velde for his instruction, generous contribution of knowledge and experience, valuable comments and encouragements from the beginning until the end of my research. Drs. R. Becht my second supervisor for his valuable contribution during proposal defence and midterm presentation. I would like also to express my appreciation for the staff and students of the Department of Water Resources and Environmental Management in ITC with them my life in Netherland particularly ITC will always be unforgettable. Special thanks to WREM Course Director Ir. A.M van Lieshout, Student Affairs Office, Department of Finance for timely contributions towards my studies.

With profound gratitude and great humility I would like to thank my wife Eva Willison Swilla for her patience, understanding, love and word of encouragement she has shown during my studies, it was one month after our wedding that I travelled abroad for my studies, she gave birth to our lovely son Derrick while I was away, when I went for field work I had few days to spend with them, for that few days I saw and appreciated that raising a child is not an easy task, through her am dedicating this piece of work to all women in the world because they are doing a good job.

My special thanks goes to Mr. Henry Gathesir ITC MSc student from Kenya for his support and valuable suggestion and his sooner response to my questions. To Mr. David Munkyala Rufiji Basin Water Office Hydrologist for his timely reply to my emails, first time when I decided to undertake my research in Tanzania the first person to contact was him, his assurance about data availability give me confidence to select Usangu as my study area. Since then David gave me maximum cooperation till the time am done with this thesis thank you so much friend.

Lastly, I would like to thank my family members for their prayers and their support. Special thanks to my Father Mr. Mbaga I would like to thank him for the way he has raised me and always stimulated me to keep on aiming highly. Many thanks to Lake Nyasa Basin Water Board and Rufiji Basin Water Board team who participated in my field work to Usangu catchment and for providing me with data which was used to undertake this research. To my colleague form Mwalimu Nyerere land with whom we were studying together at ITC especially, Mr. Omary Mshindo, Mr. Hezron Philip, Mr. Alex Mwamaso and Ms Paskalia Lyimo together we made it happen. Thanks a lot for you cooperation and understanding may the Almighty God continue to bless you in your life after ITC.

TABLE OF CONTENTS

Table of Contents

1.	INTRODUCTION.....	1
1.1.	Background and problem definition	1
1.2.	Objectives	2
1.3.	Specific objectives	2
1.4.	Research questions	3
1.5.	Research method.....	3
1.6.	Thesis outline	4
2.	LITERATURE REVIEW	5
2.1.	Satellite products.....	5
2.1.1.	Rainfall.....	5
2.1.2.	Potential evapotranspiration	6
2.1.3.	Topography.....	7
2.2.	Hydrological modelling	7
2.2.1.	Sensitivity analysis	8
2.2.2.	Calibration and validation.....	8
2.3.	CREST model application	10
3.	CREST MODEL.....	11
3.1.	Background.....	11
3.2.	Model structure.....	11
4.	STUDY AREA	15
4.1.	Location and topographic features.....	15
4.2.	Climate.....	16
4.3.	Drainage pattern	16
4.4.	Land cover and land use.....	16
5.	DATA.....	17
5.1.	Ground measurements and observation	17
5.1.1.	River discharge	17
5.1.2.	Rainfall.....	19
5.2.	Satellite data.....	21
5.2.1.	Potential evapotranspiration	21
5.2.2.	Rainfall.....	21
5.2.3.	Topographic information	24
5.2.4.	Land cover Map	24
5.2.5.	Soil data	25
6.	DATA PROCESSING.....	27
6.1.	TRMM Rainfall	27
6.2.	Potential evapotranspiration.....	28
6.3.	CREST model implementation.....	28
6.3.1.	Input files to the model.....	29
6.3.2.	Output generated by the model.....	31
7.	RESULTS AND DISCUSSION	33
7.1.	Calibration	33
7.2.	Validation.....	36
7.3.	Sensitivity analysis	38

7.3.1. Sensitivity analysis of expM parameter.....	40
7.3.2. Sensitivity analysis of the CoeR parameter.....	42
7.3.3. Sensitivity analysis of the CoeS parameter.....	44
7.4. Impact of hydro-meteorological drivers on the streamflow.....	46
7.4.1. Impact of rainfall on the streamflow.....	46
7.4.2. Impact of evapotranspiration on the streamflow.....	49
8. CONCLUSIONS AND RECOMMENDATIONS.....	53
8.1. Conclusions.....	53
8.2. Recommendations.....	54

LIST OF FIGURES

Figure 1: Flow chart showing research methodology.....	3
Figure 2: Structure of CREST Model version 2.0 (Xue & Hong, 2013).	13
Figure 3: Map showing study area Usangu catchment and Mbarali sub-catchment with stream gauging station at 1ka11a (Mbarali at Igawa gauging station) and rainfall stations.....	15
Figure 4: Double mass curves of average catchment precipitation and discharge (discharge form Mbarali River at Igawa gauging station-AKA11A gauging station).	18
Figure 5: Observed discharge (m^3s^{-1}) versus average gauged rainfall (mmd^{-1}). As shown in the figure during rainy season (November-May) there is peaks in the hydrographs and during dry season (December-June) low flow is reflected in the hydrographs. Observed flow at 15 Feb. 2002 and 30 Dec.2004 record high flow 141.81 and 134.27 m^3s^{-1} , this can be regarded as an outlier and it may affects our modelling results.....	18
Figure 6: Double mass curve for individual rainfall station versus average catchment rainfall for Mbarali sub-catchment. Correlation coefficient Matamba 0.99, Kimani 0.99 and Igawa 0.99.	19
Figure 7: Picture of different activities undertaken during field trip to Mbarali sub-catchment. A= Configuration of current meter which is used to take discharge measurements, B= Taking discharge measurement at Mbarali river at Igawa (1AKA11A), C= Mbarali river at Igawa section, D= River gauging station automatic and manual instruments and E= Igawa meteorological station.	20
Figure 8: Graph of comparison between average in-situ and average satellite rainfall.	22
Figure 9: Scatter plot of ground and satellite rainfall. The correlation of coefficient is 0.13 this show a poor correlation between satellite and in-situ rainfall data.	23
Figure 10: Average satellite rainfall versus time series of discharge data.....	23
Figure 11: Double mass curve of satellite average rainfall vs. discharge.	23
Figure 12: Landcover map Mbarali Sub-catchment. The dominant landcover type is Open bushland (23.59%), sparse forest (19.32%), Water body (14.28%), closed bushland (13.09%), Annual cropland (11.6%) and others as less than 10%.	24
Figure 13: Soil map of Mbarali sub-catchment dominant group is Acrisols, followed by Andosols and Lixols the least group is Leptosols.....	25
Figure 14: Satellite Rainfall data (TRMM) processing. A is window showing rainfall data in 3hrs downloaded, B shows in-situ online toolbox window, C shows the rainfall map with recorded rainfall value (88.4700 mmd^{-1}).	27
Figure 15: Satellite Potential Evapotranspiration data processing. A show global map of satellite potential evapotranspiration with recorded value (12.01 mmd^{-1}), B show the online and in-situ toolbox for PET download and C show the script used to convert PET from MPE format to ASCII format.	28
Figure 16: Basic input file to the CREST model. A is the DEM with lowest elevation and highest elevation of 1129 meters and 2716 meters respectively, B is the FAC with drainage network range of 1 to 1947 square meter of contributing area and C is the FDR map, colour show flow direction with conversion factor increasing by 2 each time these maps are for Mbarali sub-catchment.	30
Figure 17: show the input files to the CREST model. There is 7 input files these includes Basics, Parameters, Initial Conditions, Rainfall, Potential evapotranspiration, States, and Observation files.	30
Figure 18: Shows the output generated by the CREST model, there is simulated flow (R) and observed flow in m^3s^{-1} and date of simulation is shown in the first column.	31
Figure 19: Time series of simulated and measured streamflow (m^3s^{-1}) at 1KA11A Mbarali River at Igawa gauging station for the 2002-2007 and average catchment rainfall mmd^{-1} . As shown simulated flow during dry season is underestimated for whole period.	35

Figure 20: Graph of Cumulative streamflow for observed and measured. Shown in the figure at the middle of 2003 CREST model underestimate the runoff volume records 428.45 Mm³ while the observed runoff volume is 436.12 Mm³ and at the beginning of 2005 simulated streamflow volume is overestimated. Records 906.38 Mm³ for simulated and for observed streamflow volume is 857.89 Mm³36

Figure 21: Scatter plot comparing simulated and measured daily streamflow (m³s⁻¹) for Mbarali River at Igawa, 2002-2007. The graph shows there is good correlation between simulated and observed streamflow as the correlation of determination is 0.76.....36

Figure 22: Hydrographs of the simulated and observed streamflow for the validation period. Graph shows CREST model underestimate the streamflow for both high flow and low flow except for 2011 during high flow CREST model is able to capture the peak flows.....37

Figure 23: Shows the cumulative streamflow for the simulated and observed streamflow for the validation. Total streamflow simulated volume for the entire period of validation is 1413.44 Mm³ while observed streamflow volume is 2051.95 Mm³38

Figure 24: Scatter plot for the validation data. Scatter plot for the observed and simulated for daily streamflow data for Mbarali River at Igawa station, period. As the coefficient determination is 0.71 this shows that the correlation is good.....38

Figure 25: Sensitive parameters and their relative sensitivity. As shown expM has highest sensitivity of 43.67, CoeS ranked the second with 11.50 and the third is CoeR with 5.88 relative sensitivity.40

Figure 26: Hydrographs produced by different values of expM parameter. As seen from the shape of hydrograph produced by expM (1.04) is different from other hydrographs resulted from other parameter value. ExpM (0.72) which is less than other values above calibrated parameter value produces high peak flow. For expM (0.96) the shape of hydrograph for recession and rising limbs are poorly produces.41

Figure 27: Cumulative streamflow volume (Mm³) produced by different values of expM model parameter. ExpM (0.96) produces volume 430.01 Mm³ which is less than volume produced by expM (0.56) 2501.7 Mm³, this indicate sensitivity of that parameter and these results has great effect on the model performance.42

Figure 28: Hydrographs produced by different values of CoeR parameter values. Qsim_refe. Is the calibrated streamflow, which is used as a reference to assess if there is decrease or increase in streamflow when changes the parameter.43

Figure 29: Cumulative streamflow volume (Mm³) produced by different values of CoeR model parameter. CoeR (2.92) which, is higher than CoeR (1.57) but it produces volume 393.50 Mm³ which is less than volume 953.97 Mm³ produced by lower value, this indicate sensitivity of that parameter and these results has great effect on the model performance.43

Figure 30: Hydrographs produced by different values of CoeS parameter. There is sharp decrease in recession limb and sharp increase in rising limb produced by parameter (0.79), (0.89) and (1.08). Qsim_ref is the calibrated streamflow, which is used as a reference to assess if there is decrease or increase in streamflow when changes the parameter.45

Figure 31: Cumulative streamflow volume (Mm³) produced by different values of CoeS model parameter. Low value (0.69) produce high volume 1460.22 Mm³ compared to high value (1.28) produce low volume 1040.43 Mm³, the highest volume is produced lower value (0.79) 22633.420 Mm³. Cum_Qsim_refe. Is the calibrated streamflow, which is used as a reference to assess if there is decrease or increase in streamflow when changes the parameter.45

Figure 32: Graph of the streamflow (runoff ratio) and % change in RainFact parameter values. Graphs for the dry year 2002/03 and average year 2006/07. As shown in the graph when there is increase in RainFact result an increase in streamflow. And when decrease RainFact also there is decrease in the Streamflow both dry year and average year, dry year shown by blue line and average year shown by red line.....47

Figure 33: Hydrographs for lower and upper value of RainFact for Dry year (A) and average year (B). As shown lower RainFact produced low runoff indicated as (Qsim_0.6761) and upper RainFact produced higher runoff indicated as (Qsim_0.8605) compared to calibrated runoff indicated as (Qsim_calibrated). 48

Figure 34: Shows the Cumulative runoff produced by upper and lower values of RainFact, lower value indicated as (Cumm_Qsim_0.6761) produces low cumulative runoff volume, while upper value indicated as (Cumm_Qsim_0.8605) produces higher cumulative runoff volume compared to calibrated cumulative shown as (Cumm_Qsim_calibrated) runoff volume. A shows dry year, while B indicates average year. 49

Figure 35: Graph of the streamflow (runoff ratio) versus % change in KE parameter values. Graphs for the dry year 2002/03 and average year 2006/07. As shown in the graph when there is increase in KE result decrease in streamflow. And when KE decrease there is increase in the streamflow both dry year and average year, dry year shown by blue line and average year shown by red line. 50

Figure 36: Hydrographs for lower and upper value of KE, A for Dry year and B is for average year. As shown lower KE indicated as (Qsim_0.4521) produced high runoff and upper KE indicated as (Qsim_0.5754) produced low runoff compared to calibrated runoff shown as (Qsim_calibrated). 51

Figure 37: Shows the Cumulative runoff produced by upper and lower values of KE, lower value (Cumm_Qsim_0.4521) produced high cumulative runoff volume, while upper value (Cumm_Qsim_0.5754) produced low cumulative runoff volume compared to calibrated cumulative runoff volume (Cumm_Qsim_calibrated). This graphs A is for dry year and B is for average year. 52

LIST OF TABLES

Table 1: CREST v2.0 model parameters for both physical and conceptual parameters also the initialized model parameters are shown (Xue & Hong, 2015).....	13
Table 2: Discharge measurements for Usangu sub-catchments taken during field work 26-29 September 2014. Shows source and location of the river, gauge height in m, measured flow in m^3s^{-1} and flow obtained using rating curve (m^3s^{-1}).....	19
Table 3: Rainfall Stations Usangu catchment.....	20
Table 4: Satellite data sources. It shows satellite product and source of information about the product data are available free of charge.....	21
Table 5: Final calibrated values of CREST model parameters for Mbarali sub-catchment.....	35
Table 6: shows the relative sensitivity of routing parameters produced by sensitivity analysis tool (PEST) column one is the parameter name, second column is the optimized parameter values during automatic calibration process and third column is the relative sensitivity value of optimized parameter.....	39
Table 7: shows the relative sensitivity of physical parameters produced by sensitivity analysis tool (PEST) column one is the parameter name, second column is the optimized parameter values during automatic calibration process and third column is the relative sensitivity value of optimized parameter.....	40
Table 8: Indicated different model performance and values of streamflow volume produced by different values of expM parameter value. Model performance indicators NSEC and Bias % are affected by changing parameter value.....	42
Table 9: Indicated different model performance and values of streamflow volume produced by different values of CoeR parameter value. Model performance indicators NSEC and Bias % are affected by changing parameter value.....	44
Table 10: Indicated different model performance and values of streamflow volume produced by different values of CoeS parameter value. Model performance indicators NSEC and Bias % are affected by changing parameter value.....	45

LIST OF ABBREVIATIONS

ASCII	American Standard Code for Information Interchange
AVHRR	Advanced Very High Resolution Radiometer
CLR	Continuous Linear Routing
CREST	Couple Routing and Excess Storage
DEM	Digital Elevation Model
ESDB	European Soil Database
FAC	Flow Accumulation
FAO	Food and Agriculture Organization
FDR	Flow Direction
FEWSNET	Famine Early Warning System Network
GIS	Geographic Information System
GRR	Great Ruaha River
GSMaP	Global Satellite Mapping Precipitation
HWSD	Harmonized World Soil Database
IIASS	International Institute for Advanced Scientific Studies
ILWIS	Integrated Land and Water Information System
IPCC	Intergovernmental Panel on Climate Change
ITCZ	Intertropical Convergence Zone
IWRMD	Intergraded Water Management and Development plans
JLR	Jumped Linear Routing
MODIS	Moderate Resolution Imaging Spectroradiometer
NASA	National Aeronautics and Space Administration
NOAA	National Oceanic and Atmospheric Administration
PERSIANN Networks	Precipitation Estimation from Remotely Sensed Information using Artificial Neural Networks
PEST	Parameter Estimation tool
PET	Potential Evapotranspiration
PR	Precipitation Radar
RBWBO	Rufiji Basin Water Board Office
SCE-UA	Shuffled Complex Evolution of University of Arizona
SMUWC	Sustainable Management of the Usangu Wetlands and its Catchment
SRTM	Shuttle Radar Topography Mission
TMA	Tanzania Meteorological Agency
TMI	TRMM Microwave Image
TRMM	Tropical Rainfall and Measuring Mission
USGS	United State Geological Survey
WREM	Water Resources and Environmental Management

1. INTRODUCTION

1.1. Background and problem definition

Usangu Catchment is a sub-basin of the Great Ruaha River (GRR) (Figure 3), which is a major tributary of the Rufiji Basin in Tanzania. A number of perennial and seasonal rivers are part of the Usangu catchment. The Great Ruaha, Kimani, Mbarali, Chimala and Ndembera River are the perennial rivers of Usangu catchment, which have their sources of the high rainfall (1000-2000 mm of rain annually) areas. Halali, Kimbi and Kioga are the seasonal rivers that have their sources at lower elevation (below 1100 meters, above mean sea level) in regions with lower rainfall (700-800 mm of rain per year) (SMUWC, 2001a).

Downstream of the Usangu catchment water is used to generate electricity. There are two major dams for hydropower generation; namely Mtera and Kidatu. These dams produce almost 51 percent of the Tanzania's electricity. The river is also very important due to the presence of the National park downstream, which is an important source of water for wildlifes (SMUWC, 2001a).

McCartney et al.(2008) conducted a hydrological modelling study to assist in the water management in the Usangu wetland (Tanzania). The obtainable results indicate that outflow of the Usangu swamp has ceased for extended periods in the dry season. The authors pointed out that between 1958 and 2004 the dry season inflows declined by approximately 60% and that during the dry season the area of the swamp decreased with approximately 40% (i.e. from 160 km² to 93 km²). For instance, the authors concluded that the minimum flow requiring for maintaining the environmental (i.e. environmental flow) is 7 m³ s⁻¹, which is 65% greater than the flow available. Mwakalila (2011) furthered indicated that agriculture are a major water consumer in the study area, his findings is based on the fact that numbers one use of water is for agricultural activities. Consequently, many tributaries dried up, the groundwater table declined leading to reduction of the stream flow of major rivers. This was also noticed in Great Ruaha River in particular as its main water source is the Usangu catchment.

Kashaigili (2008) investigated the impact of land use and land cover changes on the hydrology of GRR. The study illustrates that over the past decades GRR including Usangu catchment has undergone major changes in land use, population growth and agriculture activities. The study furthered demonstrate that the cultivated area increased from 121.2 km² in 1973 to 874.3 km² in 2000 and; the woodland areas have decreased significantly. The study also highlights that this change in land use/cover has resulted in a decrease of runoff within the catchment.

One of the few studies that has assessed impact on land cover changes of the Usangu catchment stream flow has been done by Kashaigili et al.(2006). The authors studied the dynamics of Usangu plains wetlands only and not the entire catchment. No study has been performed on the Usangu catchment that includes the impact on hydro-meteorological drivers (e.g. rainfall, evaporation demand) in the streamflow of an entire Catchment using hydrological model that is driven by satellite forcings.

Currently, the Tanzanian Ministry of Water with assistance from the World Bank is funding a project on the Integrated Water Resources Management and Development (IWRMD) in all river basins in Tanzania including the Usangu catchment. The aim of that project is to study the integrated management of the basin water resources as to meet the demand of the competing users. For this plan to be successful, a hydrological model can be a very useful tool for the water managers and decision makers. However, the model requires input data, such as rainfall. The data must be accurate as well as spatial distribution across the catchment should be a representative. In-situ network of hydrological observations in the catchment is minimal,

unevenly distributed and, in addition, difficult to maintain. So there is scarcity of in-situ measurements in the catchment.

In this research, we investigate the impact of hydro-meteorological drivers on the flow regime of the Mbarali sub-catchment that is part of Usangu catchment using the grid-based Coupled Routing and Excess Storage (CREST) hydrological model forced by satellite observed rainfall and evapotranspiration. The difference of this research with previous studies is that the streamflow is reproduced using meteorological forcing derived from satellite data instead of in-situ measurements. This is advantage because the biggest problem in many catchment in Tanzania is lack of data. Another important difference is that a raster based distributed hydrological model, at 1km grid-resolution is employed for hydrological simulation. An important advantage of spatially distributed hydrological model, such as CREST is that it not only provide estimates of hydrological variable such as streamflow at the catchment outlet, but at any location as represented by a grid-resolution of 1 km as implemented in this research, by knowing the streamflow at any location within the basin will help water managers during water allocation for different water user.

Another important difference of this study with previous studies is that, within the framework of this study two scenarios (rainfall and evapotranspiration demand) are used to assess the impact of hydro-meteorological drivers on the streamflow, we have considered the effect of rainfall and evapotranspiration since there is agricultural activities and urbanization taking place in the study area, these activities may cause land use change, which may affect evapotranspiration as well as rainfall. Another factor that may affect rainfall is climate variability, so this study aim at assessing the impact of rainfall and potential evapotranspiration on the streamflow of the Mbarali sub-catchment.

Indeed, this research intends to take advantage of the available satellite products to perform hydrological modelling, where by the in-situ measured river discharge is used for model calibration and validation. This research has great societal and economic benefits since the Usangu catchment is the main sources of water for hydropower plants downstream of the catchment and agricultural activities upstream, which is the backbone for the socio-economic activities in the Usangu population. Also, the outcome of this research will be useful to support the implementation of IWRMD plans, which are currently being developed by the Tanzanian Ministry of Water.

1.2. Objectives

The main objective of this research is to investigate the impact of hydro-meteorological drivers on the streamflow of Mbarali sub-catchment as part of the Usangu catchment using grid-based CREST distributed hydrological model driven by atmospheric forcing derived from satellite observations. Information on the impact of evapotranspiration on the streamflow and impact of precipitation on the streamflow will help water managers by knowing how much streamflow increase or decrease as the results of changes on evapotranspiration or rainfall. These changes in rainfall or evapotranspiration can arise from climate variability or land use change.

1.3. Specific objectives

- A. To calibrate and validate the CREST model driven by satellite observations using in-situ streamflow data.
- B. To investigate the sensitive parameters of the CREST model for the Mbarali sub-catchment.
- C. To use calibrated model results to assess the impact of rainfall and evapotranspiration on streamflow using hydro-meteorological drivers.

1.4. Research questions

- A. What are the sensitive CREST model parameters for the Mbarali sub-catchment?
- B. How well can the CREST model driven by atmospheric forcing derived from satellite observation simulate streamflow of the Mbarali sub-catchment after model calibration?
- C. Based on hydro-meteorological drivers, what is the impact of rainfall and evapotranspiration on the streamflow of the Mbarali sub-catchment?

1.5. Research method

The method adopted to address the research objectives and answer the research questions is schematically illustrated by the flow chart in Figure 1

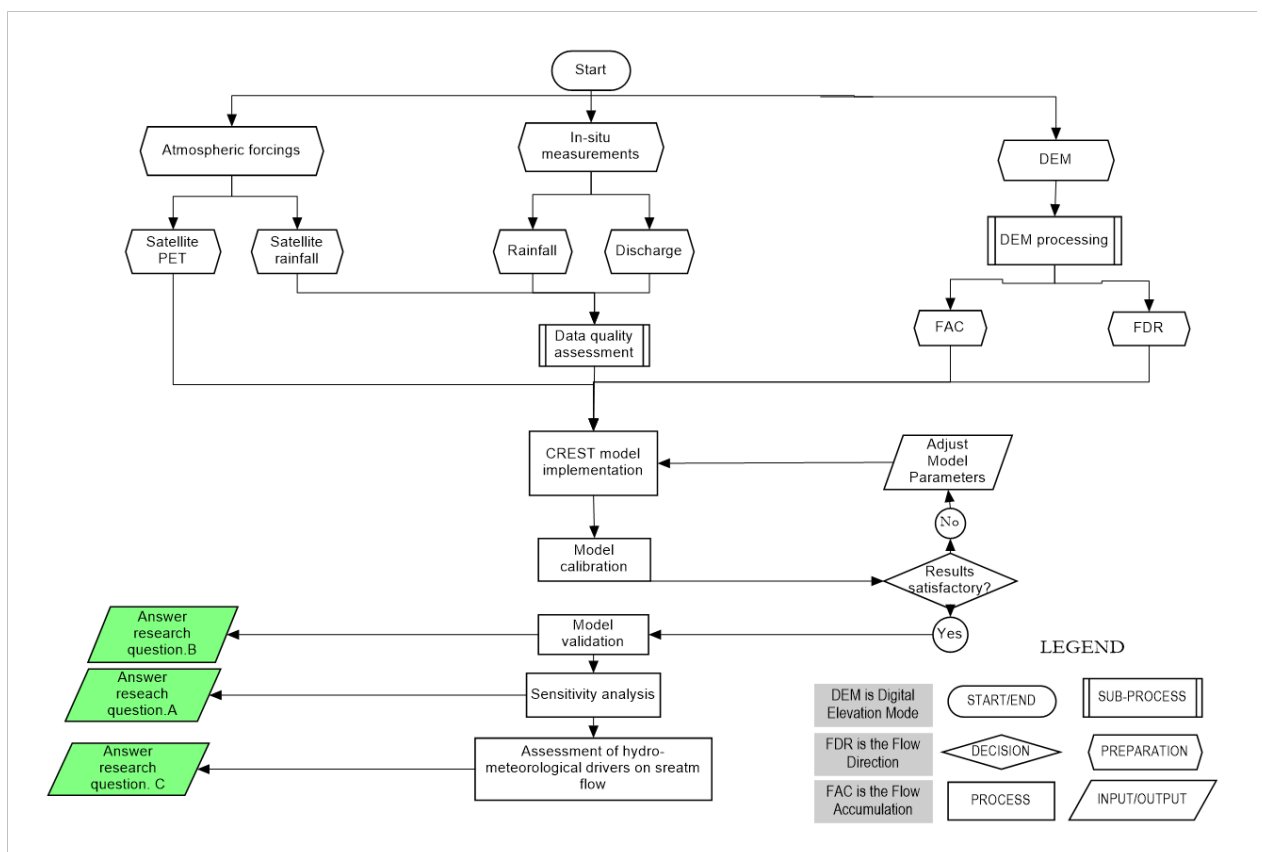


Figure 1: Flow chart showing research methodology

The first step of this research is assessment of the quality and reliability of the in-situ measured discharge and satellite observed rainfall. This is performed by means of double mass curve between river discharge data and rainfall data, double mass curve is used to check the consistency of rainfall and river discharge it is also used to check consistency of each rainfall station with average catchment rainfall. Furthermore, quality check is done by comparing between satellite rainfall and in-situ rainfall, details of this is presented in chapter five. Second step is to set-up and test the CREST model for Mbarali sub-catchment, after setting up the model we run the model from the year 2001 to 2012. This period is chosen based on the availability of satellite potential evapotranspiration from FEWSNET which, start 2001. Data set is then divided into three groups; 2001 is used for model warm-up, 2002-2007 for model calibration and 2008-2012 for model validation. Then, these steps are followed by model calibration, the CREST model parameters for calibration is divided into two groups named; physical group with five parameters calibrated and empirical routing

group with five parameters calibrated. Automatic calibration using PEST (Parameter Estimation Tool) is implemented, where by, we first calibrate physical parameters then, we calibrate empirical routing parameters, and these steps are repeated until no further improvement in model performance is obtained. After obtained optimized model parameters using automatic calibration. Subsequently, the reliability of calibrated model is validated. Additionally, the sensitivity of the simulated streamflow for parameters uncertainties is quantified to provide further confidence in calibration results.

With the CREST model validated for the Mbarali sub-catchment, the impact of hydro-meteorological drivers, which may be caused by land use change and climate variability on the streamflow is studied. This is done by perturbing the CREST model parameters linearly scaling the rainfall and potential evapotranspiration and running the CREST model to reproduce the streamflow based on the assumption that, the changes in hydro-meteorological drivers are results of climate variability or land use change. Changes on the streamflow is assessed for the selected periods inside the calibration period, 2002/03 is selected as dry year and 2006/07 is selected as average year for further analysis.

Changes on land use and climate variability can lead to changes in evapotranspiration and rainfall. To assess the impact of evapotranspiration on the streamflow, CREST model is forced to produce streamflow based on the different values of hydro-meteorological driver called KE, which is the factor used to convert potential evapotranspiration to local actual evapotranspiration. Produced streamflow is compared with the calibrated flow used as a reference so as to assess and analyse flows produced by different values of KE. To assess the impact of rainfall on the streamflow, CREST model is forced to produce streamflow based on the different values of hydro-meteorological driver called RainFact, this is the multiplier on the precipitation field. Produced streamflow is then compared with the calibrated flow used as a reference so as to assess and analyse flows produced by different values of RainFact.

1.6. Thesis outline

This thesis has eight chapters. In the first chapter a brief background and problem definition of the study area is given starting with the entire catchment and its importance in Tanzanian economy. Research objectives and research questions are also described in this chapter. Moreover, the section of research method is also under the same chapter.

Chapter two is describing the literature review, in this chapter, concepts of satellite products are explained. Second, part a brief explanation of hydrological modelling. Third, sensitivity analysis is presented, and fourth model calibration/validation is addressed. Furthermore, the application of CREST model i.e., the places where CREST model has been applied and the results found are also explained. CREST model is presented in chapter three, here background as well as model structure are explained. A general description of the study area is explained in chapter four, where by location and topographic features are presented, climate and drainage pattern are described. We present land use and land cover of the study area.

Chapter five and six describe data collection and data processing respectively. In addition, results and discussion are presented in chapter seven. Furthermore, chapter eight describes conclusion and recommendation.

2. LITERATURE REVIEW

2.1. Satellite products

Remote sensing products used in hydrological modelling are; land cover, topography, soil texture, rainfall, potential evapotranspiration, soil moisture, and water quality parameters. Remote sensing is a promising tool for providing an inexhaustible data and information that is difficult to deduce from in-situ measurement alone. It provides also an important asset for hydrological modelling applications due to the fact that collection of information is unrestricted with wide spatial coverage and temporal resolution (Rango & Shalaby, 1998).

Rango & Shalaby (1998) also explained that in many developing countries, hydrologist most depend on in-situ measurements to carry out hydrological modelling. Notwithstanding, in-situ measurements are scarce in spatial and temporal coverage of the Earth's surface. Remote sensing data with different spatial and temporal coverage has increasingly being used to add-on existing in-situ gauge networks. Despite this, existing technique for remote sensing applications are still mostly research oriented, and the applications of remote sensing products for hydrological modelling is becoming importance in different parts of the world. Rango & Shalaby (1998) further explained that the application of remote sensing in water resources management is becoming of great important due to uniqueness of remote sensing. First, remote sensing techniques has ability to provide spatial information which is not the case to in-situ stations. Secondly, its coverage is very large compared to ground measurements. Finally, remote sensing data can be obtained at low cost compared to the in-situ data. Different remote sensing techniques can be used to retrieval different remote sensing product as explained hereunder.

2.1.1. Rainfall

Precipitation is one of the important variable in hydrological modelling, its availability and distribution in temporal and spatial can always affect land surface and sub-surface hydrological fluxes and states. Precise and dependable precipitation is extremely significant for the real-time monitoring of water caused disasters (flood, drought, and landslide) as well as hydrological modelling and climate change studies. There are three main sources for obtaining precipitation data, which are; ground network observations, ground-radar system and satellite remote sensing retrieval. Satellite remote sensing can provide complete coverage of the global precipitation map (Jiang et al., 2014).

Many satellite-based precipitation products with different resolution are currently available globally, these including; Tropical Rainfall Measuring Mission (TRMM) Multi satellite Precipitation Analysis (TMPA) 3B42 (Huffman et al., 2007), National Oceanic and Atmospheric Administration (NOAA) Climate Precipitation Centre Morphing Technique (CMORPH) (Al, 2004), Precipitation estimates from Remote Sensing information by using Artificial Neural Network (PERSIAN) (Sorooshian, Hsu, Imam, & Hong, n.d.), Precipitation estimates from remotely sensed imagery using Artificial Neural Network-Cloud Classification System (PERSIAN-CCS) (Irvine, 2004) and Global Satellite Mapping of Precipitation (GSMaP) (Kubota et al., 2007).

Satellite rainfall data have been used in many studies. One of the study is explained by (Ochieng & Kimaro, 2009) Their study concluded that satellite derived rainfall products are suitable for water resources management in the Mara River Basin. Dessu & Melesse (2013) did research on satellite rainfall data in Mara River Basin and concluded that satellite rainfall data can fill the gap in data scarce region and they can be used in water resources management. Jeniffer, Su, Woldai, & Maathuis (2010) they estimated spatial

temporal rainfall distribution using remote sensing in Tanzania they concluded that satellite rainfall products gave a good correlation with the available ground data. Liu, Duan, Jiang, & Zhu (2014) compare the performance of three satellite rainfall products TRMM 3B42, CMORPH and PERSIANN with gauge measurements they concluded that TRMM 3B42 and CMORPH performs better at daily temporal scales than PERSIANN satellite product. In hydrological modelling satellite data have been used and in all studies satellite rainfall data shows good performance of the model details of these studies are explained by Behrang et al. (2011); S. I. Khan et al. (2011) they used CREST model and satellite Remote sensing for flood modelling and model performed reasonably with NSCE is 0.873 and Bias % is -0.228; X. Li, Zhang, & Li (2011) they did research on Validation the Applicability of Satellite Based Rainfall Data for Runoff Simulation and Water Balance Analysis using WATLAC model, model performed reasonable with NSCE between 0.61-0.93 and R^2 (Correlation of Coefficient) is between 0.73 and 0.94 and Xue et al. (2013) they evaluated TRMM-based Multi-satellite precipitation over the Wangchu Basin of Bhutan and model performance with TRMM 3B42 performed reasonably with NSCE 0.66 in daily scale and 0.77 in monthly scale.

2.1.2. Potential evapotranspiration

The evapotranspiration is the process by which water is converted into vapour, two terms are described; evaporation water is lost through soil surface, while transpiration water is evaporated by means of stomata of plant. Evapotranspiration is significant component of hydrological and water cycle so its spatial distribution and variation is important in hydrological modelling. According to R. Singh, Senay, Velpuri, Bohms, & Verdin (2014) there are remote sensing techniques that can be used to estimate potential evapotranspiration at different spatial and temporal resolution at local and regional scales. As the result of poor availability of meteorological stations the spatial resolution of potential evapotranspiration estimates are very coarse and the available data are not relevant for many hydrological modelling, integrated water resources management and planning.

Satellite based potential evapotranspiration can be estimated using various method such as MODIS Satellite-based observations and Priestly Taylor formula (J. Kim & Hogue, 2008). Details on how potential evapotranspiration is calculated using satellite products is presented by J. Kim & Hogue.(2008b) they did the study on estimating daily time series of potential evapotranspiration using Moderate Resolution Imaging Spectrometer (MODIS) sensor data obtained from the Terra satellite platform. They proceeds towards the Priestly-Taylor equation, integrating daily net radiation during cloudless days. The Priestley-Taylor equation used is given by $PET = \alpha (R_n - G) \Delta / (\Delta + \gamma)$. Furthermore they applied algorithm using theoretical clear sky net radiation (including daily cloud condition and cloud optical thickness) and PET is finally used for estimating net radiation and PET under cloudy conditions.

Another method is NOAA-Satellite based observation and Penman-Montheith equation (Loukas, Vasiliades, Domenikiotis, & Dalezios, 2005). for NOAA-Satellite based PET the data are available at 1 degree spatial resolution and 1 day temporal resolution, while for MODIS satellite based the data are available at 8 days temporal resolution for ET and PET at 1km spatial resolution from the year 2000 and monthly temporal resolution at 1km spatial resolution.

Satellite Potential evapotranspiration products have been applied for studies in hydrological modelling as explained in detail by Rientjes, Muthuwatta, Bos, Booij, & Bhatti (2013) they used HBV to assess the model performance based on satellite potential evapotranspiration and model performed better with NSCE higher than 0.62. Xue et al. (2013) used both satellite rainfall and satellite potential evapotranspiration and model performance is 0.66 in daily scale and 0.77 in monthly scale and Immerzeel & Droogers (2008) did the study on calibration of a distributed hydrological model based on satellite evapotranspiration using SWAT model and SEBAL evapotranspiration the r^2 increases from 0.4 to 0.81.

2.1.3. Topography

Topography is land-surface characteristics that affects water balance in a watershed, including the production of surface and sub-surface streamflow, the flow paths followed by water as it travels down and through hillslopes and rate of water movements. Distributed hydrological models use topography represented by Digital Elevation Model (DEM). DEM is also used for deriving critical information in fully distributed hydrological models (Anornu & Kortatsi, 2012). Based topography satellite data products are available from different sources such as SRTM 90m Digital Elevation Database v4.1, HydroSHEDS, HYDRO1K and GTOPO30.

SRTM (Shuttle Radar Topography Mission) digital elevation data produced by NASA is a major achievement in global digital mapping with high spatial resolution data starting from 90m for larger portion of the tropics and other parts of the world <http://www.cgiar-csi.org/data/srtm-90m-digital-elevation-database-v4-1>. HydroSHEDS is a topographic product that provides hydrographic information from local scale to global scale. Data from HydroSHEDS are already geo-referenced data sets in raster and vector at various scales, data which can be obtained from this products including river networks, watershed boundaries, Flow Direction (FDR) and Flow Accumulations (FAC). HydroSHEDS products are derived from SRTM and the products are available at different spatial resolution ranging from 3s-90m, 15s-500m and 30s-1000m (Lehner, Verdin, & Jarvis, 2006a). GTOPO30 is a global digital elevation model (DEM) with spatial resolution of 30 arc seconds (approximately 1km) derived from sources of topographic information (N.Yastikli, G. Kocak, 2003). HYDROK1 is database used to provide topographic information including streams, drainage basins at 30 arc second resolution (Karlsson & Arnberg, 2011).

In most distributed hydrological model, the DEM with coarser resolution are used for modelling purpose in order to reduce the computation time. This also enables faster model calibration and model sensitivity analysis. A major drawback in using DEM with coarser resolution is the loss of important small-scales features that can seriously affect modelling results, so the modelling accuracy and reliability of the results can be affected by low resolution DEM since they do not represent the actual on ground topographic features (Mao et al., 2014).

There are numerous research such as Milzow & Kinzelbach, (2010) they used coarser resolution to study flood modelling and they concluded that model results are considered influential using topographic data of coarser resolution. Xue et al. (2013) they used DEM, FDR and FAC derived from HydroSHEDS at 1km spatial resolution in Wangchu Basin to assess the suitability of TRMM 3B42V7 they obtained NSCE 0.66 for calibration period from 2001-205 and NSCE 0.63 during validation period 2006-2010 and Cohen Liechti, Matos, Ferràs Segura, Boillat, & Schleiss (2014) they used DEM derived from HYDRO1k at spatial resolution of 1 km to model larger flood plain of the Zambezi Basin, they obtained NS value higher than 0.5 for calibration period.

2.2. Hydrological modelling

Model is the simplification of the reality. In hydrological models the real systems may be the whole river basin or part of it. Hydrological models are usually used to simulate water balance within a catchment, which usually consists of river network. Hydrological models can be grouped into conceptual models and physically based models, conceptual models; simplified equations represent mass, momentum and energy (Todini, 2007). In physically-based distributed models, is derived from equations of mass and energy conservation for the hydrological process it aims to present (Beven, Warren, & Zaoui, 1980) furthermore, they explained that physically-based models provide predictions at points that are distributed at least one dimension.

In further classification of hydrological model can be either predictive or investigative. Predictive models are used to obtain a specific answer for a specific problem, while investigative models are used for understanding the hydrological processes of catchment. In principle, investigative models require more data,

are more sophisticated in structure and estimate are less robust, but allow more insight into the system behaviour. For both types of models its development follow the following steps; the first step is to collect and analyse data, developing a conceptual model, then the conceptual model is transformed to mathematical model, then the mathematical model is calibrated using various parameters so as the measured data can fit the simulated data, the last stage in model development is model validation using independent data set. If the validation is not satisfied one of the steps above need to be repeated. However, if the simulated and observed results match the model is considered to be ready for use in a predictive mode (Bloschl & Sivapalan, 1995).

2.2.1. Sensitivity analysis

Sensitivity analysis is used to describe how much model output is affected by changing the model input values. It always used to support model calibration and uncertainty analysis by answering the following questions, one, where the data collection efforts should focus? second, level detail that needed to be considered for parameter estimation and third, relative importance of various parameters (Cho, 2002).

Sensitivity analysis can be performed using different methods. The simplest method is to vary one parameter at a time within a certain range and determine the effects on the model output, this method is called One-factor-at-a-time (OAT) method, and this method is efficient when model has several input parameters, details of this method is explained by Morris & May (2007). Another sensitivity analysis method is called global method or multivariate method it is called global sensitivity method because it can investigate input-output sensitivities valid over the full range of parameter variations and combinations. Global sensitivity analysis examine probabilistic model results for multiple goals such as; to identify key contributors to output uncertainty, to determine key factors controlling extreme model outcomes or to determine the presence of non-monotonic input-output patterns (Mishra, 2009). detail of this method can see the work of Herman, Kollat, Reed, & Wagener (2013)

2.2.2. Calibration and validation

Model calibration and validation are important and critical steps in any hydrological model application. Calibration is the process of tuning model parameters, which are sensitive such that the simulated results become equal to the observed results. The goodness of fit is determined by an objective function and the calibration process is stopped when an objective function is not improved any further, calibration techniques can be grouped into single objective or multi objective calibration techniques. Details of these techniques can see the work of Vrugt, Gupta, Bastidas, Bouten, & Sorooshian (2003). According to Yang, Castelli, & Chen (2014) explained that for a good calibration it is always necessary to consider a good fit between simulated, measured catchment runoff volume, the shape of the hydrograph, the peak flow and the base flow. When considering the above mentioned objective function, we refer it as a multi-objective calibration process, but when considering only one objective function we call it single objective function. During the calibration process the multi-objective function is preferred ever than single objective function, Efstratiadis & Koutsoyiannis (2010) did study to assess multi-objective calibration approaches in hydrological modelling for the past one decade they showed examples of research. Model used, how many objective function and calibration method.

Calibration process can be either manual or automatic see the work of Boyle, Gupta, & Sorooshian (2000). There are number of automatic calibration method, such as the Shuffled Complex Evolution-University of Arizona (SCE-UA) (Vrugt, Gupta, Bouten, & Sorooshian, 2003). The SCE-UA has been extensively used for the calibration of various rainfall-runoff models these include CREST model (Xue et al., 2013a), the Soil and Water Assessment Tool (SWAT) model (Birhanu, 2009) and Xinanjiang Model (Lin, Lian, & He, 2014). Genetic Algorithm (AG) is another method for automatic calibration for details can see the work of Shafii & Smedt (2009). The last automatic calibration tool discussed here is the Model-Independent Parameter

Estimation Tool (PEST) as discussed in detail by Doherty (2004). PEST has been used in calibration of various hydrological models such as HBV (Lawrence, Haddeland, & Langsholt, 2009), WetSpa (Shafii & Smedt, 2009), Hydrological Simulation Program-Fortran (HSPF) (S. M. Kim, Benham, Brannan, Zeckoski, & Doherty, 2007), Sacramento and GR4J rainfall runoff models (Zhang, Waters, & Ellis, 2013) and WaSiM-ETH (S. K. Singh, Liang, & Bárdossy, 2012).

In model validation, the calibrated model parameters are used to simulate the flow over an independent datasets for independent period which is outside the calibration period. The main purpose of model validation is to determine the suitability of calibrated model for predicting flow over any period outside the calibration period. One can have confidence that the model is reliable and it can be used for predicting purposes in climatic condition if the model performance is good during the validation period.

During model calibration and validation, the model performance can be tested using either qualitative or quantitative test, in quantitative evaluation a statistical methods are always used. The most commonly used statistical method in hydrological modelling are: the relative bias (%) which is used to measure the agreement between the simulated and observed data, the root mean square error (RMSE) which is used to evaluate the average error magnitude between the simulated and observed data, the Correlation Coefficient (CC) which is used to assess the agreement between the simulated and observed data (a model with CC of 0.8-0.99 is termed as a good model) (Xue et al., 2013a).

Another statistical indices, which is commonly used to assess the performance of model simulation is Nash-Sutcliffe Coefficient of Efficiency (NSCE). The Nash-Sutcliffe model efficiency is usually used to assess the performance of hydrological model. NSCE is recommended for two main reasons: (1) provides useful information on the obtained values, such as ≤ 0.0 shows that the average observed value is better predictor than the simulated value, which indicates that the model performance is unacceptable, values between 0.0 and 1.0 are generally regarded as acceptable model performance (2) best objective function for reflecting the overall performance of a hydrograph (Moriasi et al., 2007b). CREST model performance is always assessed using three commonly-used statistical indices. First, relative bias ratio used to assesses the systematic bias of the simulated discharge. Second, of statistical goodness of fit of simulated flows. Third, the person Correlation Coefficient (CC) is used to assess the agreement between simulated and observed discharge (Xue, 2012).

$$Bias = \left(\frac{\sum_{i=1}^n Sim - \sum_{i=1}^n Obs}{\sum_{i=1}^n Obs} \right) \times 100 \dots \dots \dots \text{Equation 1: Relative Bias (\%)}$$

$$NSCE = 1 - \frac{\sum_{i=1}^n (Obs_i - Sim_i)^2}{\sum_{i=1}^n (Obs_i - \overline{Obs})^2} \dots \dots \dots \text{Equation 2: Nash-Sutcliffe Model efficiency}$$

$$CC = \frac{\sum_{i=1}^n (Obs_i - \overline{Obs})(Sim_i - \overline{Sim})}{\sqrt{\sum_{i=1}^n (Obs_i - \overline{Obs})^2 \sum_{i=1}^n (Sim_i - \overline{Sim})^2}} \dots \dots \dots \text{Equation 3: Correlation Coefficient}$$

Equations 1, 2 and 3 are used to calculate model performance indices. Equation 1 is for calculating Relative Bias %, Equation 2 is used to calculate Nash-Sutcliffe efficiency and Equation 3 is for calculating Correlation Coefficient (Xue, 2012).

Where:

- Obs: is the observed discharge
- Sim: is the simulated discharge
- \overline{Sim} : is the mean of simulated discharge
- \overline{Obs} : is the mean of observed discharge
- N: is the number of observations

2.3. CREST model application

The application of CREST model is explained by Xue et al. (2013), CREST model has been applied in mountainous Wangchu Basin of Bhutan (3559 km²) for assessing the accuracy of satellite rainfall products for TMPA 3B42V6 vs 3B42V7 of 0.25d spatial resolution, the two satellite rainfall products were compared to observed rain gauge datasets at daily and monthly scales. The comparison was done at basin level and at grid cell in terms of bias, correlation coefficient and frequency of occurrence in both cases 3B42V6 shows good improvements compared to 3B42V7.

Xue et al. (2013), further explained that the two satellite rainfall products were used to run CREST model for simulating discharge that is (3B42V6-3B42V7 based simulation), in-situ rainfall data was used as a benchmark for both scenarios, based on 3B42V6 simulation scenarios the simulated discharge was lower than the measured one while for the 3B42V7 simulation scenarios the performance of the model was reasonable the comparison was based on Nash Sutcliff coefficient, CREST model with performed better using satellite rainfall products for mountainous area of Bhutan basin.

The CREST model was also used in East Africa in Nzoia River to produce soil moisture and stream flow using real time satellite rainfall data from TRMM, the produced soil moisture and stream flow enable for flood warning in flood prone areas in East Africa part of Nzoia River. Nzoia River basin covers an area of approximately 12,900 km² with elevation between 1,100m to 3,000m and annual rainfall of about 1500mm (Sadiq I Khan et al., 2009).

Another research which was done using CREST model was Okavango basin Botswana. According to S. I. Khan et al. (2012) concluded that remote sensing products from microwave sensors can be used as alternative for hydrological data in an ungauged basins. They used CREST model for flood prediction in Okavango Basin and the performance of the model was quite well as Nash-Sutcliffe efficiency was 0.84 and Correlation Coefficient of 0.9

3. CREST MODEL

3.1. Background

The Coupled Routing and Excess STorage (CREST) Model is a grid-based distributed hydrological model developed that was developed by the University of Oklahoma(<http://hydro.ou.edu/>) and NASA SERVIR Project Team(<http://www.servir.net/>) (Wang et al., 2011a). CREST model is developed to reproduce the space (spatial) and time (temporal) variations of land surface, and subsurface water fluxes and storage by cell-to-cell simulation, the grid resolution is specified by the user (Wang et al., 2011a).

As explained by Khan et al.(2009) The CREST distributed hydrological model has four main distinctive features that differentiate from other hydrological model. First, its ability to distribute the runoff generated from rainfall and grid-to-grid simulation. Second characteristic is its ability to combine the runoff generation and routing components. Third characteristic is its scalability, the ability to represent the soil moisture variation and routing processes at the grid scale. First time when the CREST Model was developed it was planned to work on global scale for real time flood forecast with courser resolution spatial scales, but now days it is used in small to medium scales catchment.

CREST Model use two main forcing; precipitation and potential evapotranspiration. It can use either forcing form the satellite products or ground observed measurements while there is a number of output variables such as spatial interpolated output of precipitation input forcing, spatial interpolated output of potential evapotranspiration data, actual evaporation, streamflow, soil moisture, overland reservoir depth and interflow reservoir depth (Wang et al., 2011b)

Further explanation is given by Xue and Hong. (2013). They explained that there are two version of CREST model, the first one is CREST v1.6c and the second one is CREST v2.0. This research use the current version CREST v2.0, the main difference between the two versions is that CREST v1.6c has 17 parameters, only allow input of uniform parameter values, only calibrate the uniform parameter dataset, auto-calibrated the parameters slowly, inefficient because did not use matrix manipulation and difficult for beginners to add new processes. CREST v2.0 is rebuild to better suit for distributed hydrological modelling, with 12 parameters and 11 outputs available at any location and any time within a catchment, different input file formats , five model run style are available, which are (Simulation, Real time, Automatic calibration, return period and forecast) for real time model simulation the user can get the real time streamflow, another advantage of CREST v2.0 is that it include both distribute and uniform parameters for both simulation and calibration and simulation speed is high because of enhanced computation capability using matrix manipulation, some bugs were fixed and inclusion of the optimization scheme Shuffled Complex Evolution of University of Arizona (SCE-UA) to enable automatic calibration.

3.2. Model structure

In this research, a simplified version of the CREST (Coupled Routing and Excess STorage (Wang et al. 2011)) is applied. The model structure is shown in Figure 2. Before precipitation reaching the soil, some is intercepted and evaporation occurs, RainFact (multiplier on the precipitation field) is used to determine the amount of rainfall reaching the soil and is given by $P_{soil} = RainFact \times rain$. Once precipitation passes the canopy layer, the amount of precipitation that exceed reaches the soil surface is P_{soil} . P_{soil} reaching the soil is separated into two components, excess rainfall R (water that is not infiltrated) and infiltration water I (infiltration occurs when infiltration capacity is more than amount of rainfall) by using Variable Infiltration Curve (VIC, (Bao et al., 2011)). The excess rainfall R is additionally separated into two main components,

which are overland excess rainfall (R_O) this is the amount of water that will be contributing to the quick runoff and interflow excess rainfall (R_I) this is the amount of water that will be contributing to the slow runoff, and this subroutine is controlled by K and P_{soil} , K closely comparable to the saturated soil hydraulic conductivity. The conditions for overland excess rainfall and interflow excess rainfall to occur is explained below.

If $P_{soil} > K$, then equation 4 and 5 applies;

$$R_I = K \frac{R}{P_{soil}} \quad \text{Equation 4: Interflow excess rainfall}$$

$$R_O = R - R_I \quad \text{Equation 5: Overland flow excess rainfall}$$

If $P_{soil} < K$, then equation 6 and equation 7 applies;

$$R_I = R \quad \text{Equation 6: Interflow excess rainfall}$$

$$R_O = 0 \quad \text{Equation 7: Overland flow excess rainfall}$$

The separation of overland and interflow excess rain produce quick and slow streamflow responses to the precipitation. The overland excess rainfall R_O flows through overland reservoir, meanwhile the interflow excess rainfall R_I flows through interflow reservoir. Those two procedures are controlled by the overland reservoir discharge parameter (KS) and the interflow reservoir discharge parameter (KI) respectively.

The overland streamflow is given by Equation 8 and the Interflow streamflow is shown by Equation 9.

$$R_{O,out} = KS * R_O. \quad \text{Equation 8: Overland streamflow}$$

$$R_{I,out} = KI * R_I. \quad \text{Equation 9: Interflow streamflow}$$

$$Q = R_{O,out} + R_{I,out} . \quad \text{Equation 10: Total streamflow}$$

After obtain the quick and slow flow then routing process at the overland flow is controlled by $CoeM$ parameter, while the routing mechanism at the interflow flow is governed by $CoeS$ parameter and the channel routing is controlled by $CoeR$ model parameter.

Where:

KS is the overland reservoir discharge parameter

KI is the interflow reservoir discharge parameter

R_O is the overland excess rain (mmd^{-1})

R_I is the interflow excess rain (mmd^{-1})

$R_{O, out}$ is the overland streamflow (mmd^{-1})

$R_{I, out}$ is the interflow streamflow (mmd^{-1})

Q is the total streamflow produced by the overland and interflow streamflow (mmd^{-1})

For each grid is treated as sub basin, the water balance is solved per grid cell as:

$$\frac{dS_{to}}{dt} = P - E_a - \sum R_{O,in} - R_{O,out} + \sum R_{I,in} - R_{I,out}. \quad \text{Equation 11: Water balance equation for each grid}$$

Where:

P is the precipitation

E_a is the actual evaporation

$R_{O, in}$ is the overland flow going in to the cell

$R_{O, out}$ is the overland flow going out from the cell

$R_{I, in}$ is the interflow flow going in to the cell

$R_{I, out}$ is the interflow flow going out from the cell

Table 1: CREST v2.0 model parameters for both physical and conceptual parameters also the initialized model parameters are shown (Xue & Hong, 2015).

Module	Symbol	Description
Initial condition	WO	Initial value of soil moisture
	SSO	Initial value of overland reservoir
	SIO	Initial value of interflow reservoir
Physical parameters	Ksat	Soil saturated hydraulic conductivity
	RainFact	Multiplier on the precipitation field
	WM	Mean water capacity
	B	Exponent of variable infiltration curve
	IM	Impervious area ratio
	KE	Factor to convert PET to local actual evaporation
	CoeM	Overland runoff velocity coefficient
	expM	Overland flow speed exponent
Conceptual parameters	CoeR	Multiplier used to convert overland flow speed to channel flow speed
	CoeS	Multiplier used to convert overland flow speed to interflow speed
	KS	Overland reservoir discharge parameter
	KI	Interflow reservoir discharge parameter

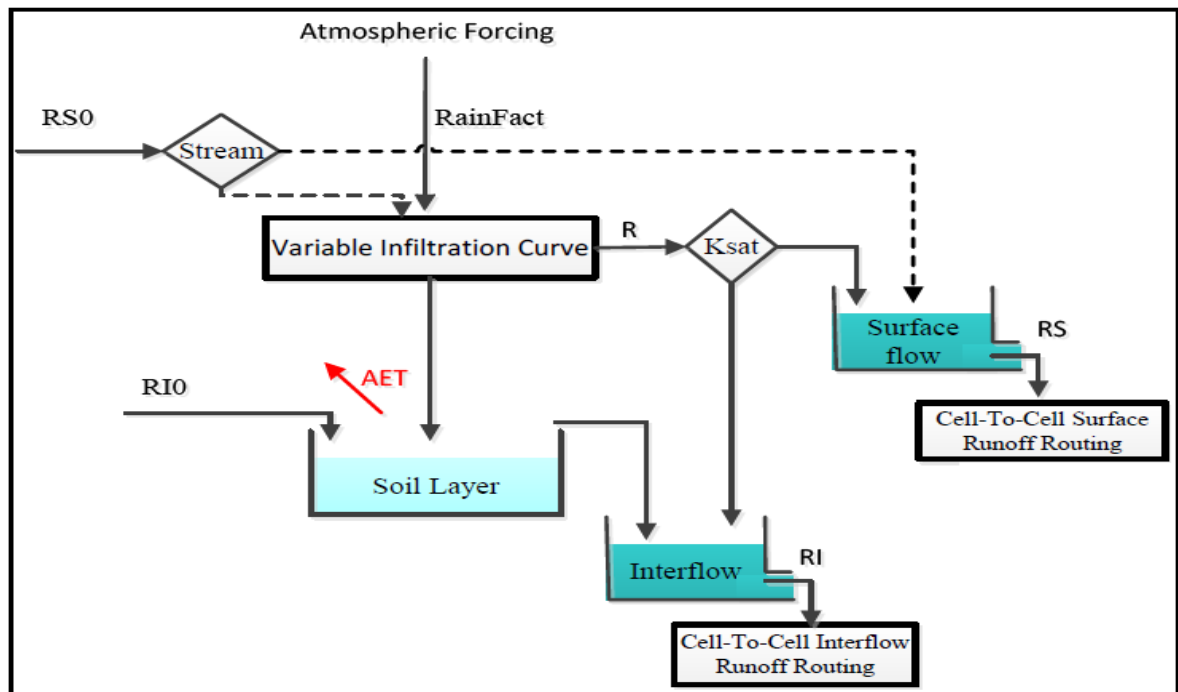


Figure 2: Structure of CREST Model version 2.0 (Xue & Hong, 2013).

4. STUDY AREA

4.1. Location and topographic features

Usangu catchment is positioned in the south-west of the United Republic of Tanzania within -7.56- -9.47 N latitude and 32.56 -35.90 E longitude Figure 3. The catchment is within the eastern arm of rift valley contained in Mbeya and Iringa regions, it is described by the boundary of the drainage basin that drains to N'Giriama where the Great Ruaha River efflux from the Usangu Plains. The area covers 20,800 km² of which 4,840 km² (23%) is in alluvial plains below about 1100 m above sea level (masl). The remaining 77% of the catchment area lies in the high altitude areas, which ranges in elevation from about 1100 m above sea level (masl) to over 2000 m above sea level (masl). The catchment of the Usangu wetland forms the sources of the Great Ruaha river, which is the major tributary of the Rufiji River (SMUWC, 2001a). The area which will be covered by this research is the Mbarali sub-catchment 1553 km², which is 7.47% of the entire area of the Usangu catchment, the selected catchment contribute between 69.17% and 47.78% of the inflow to Usangu catchment (Mwakalila, 2011b).

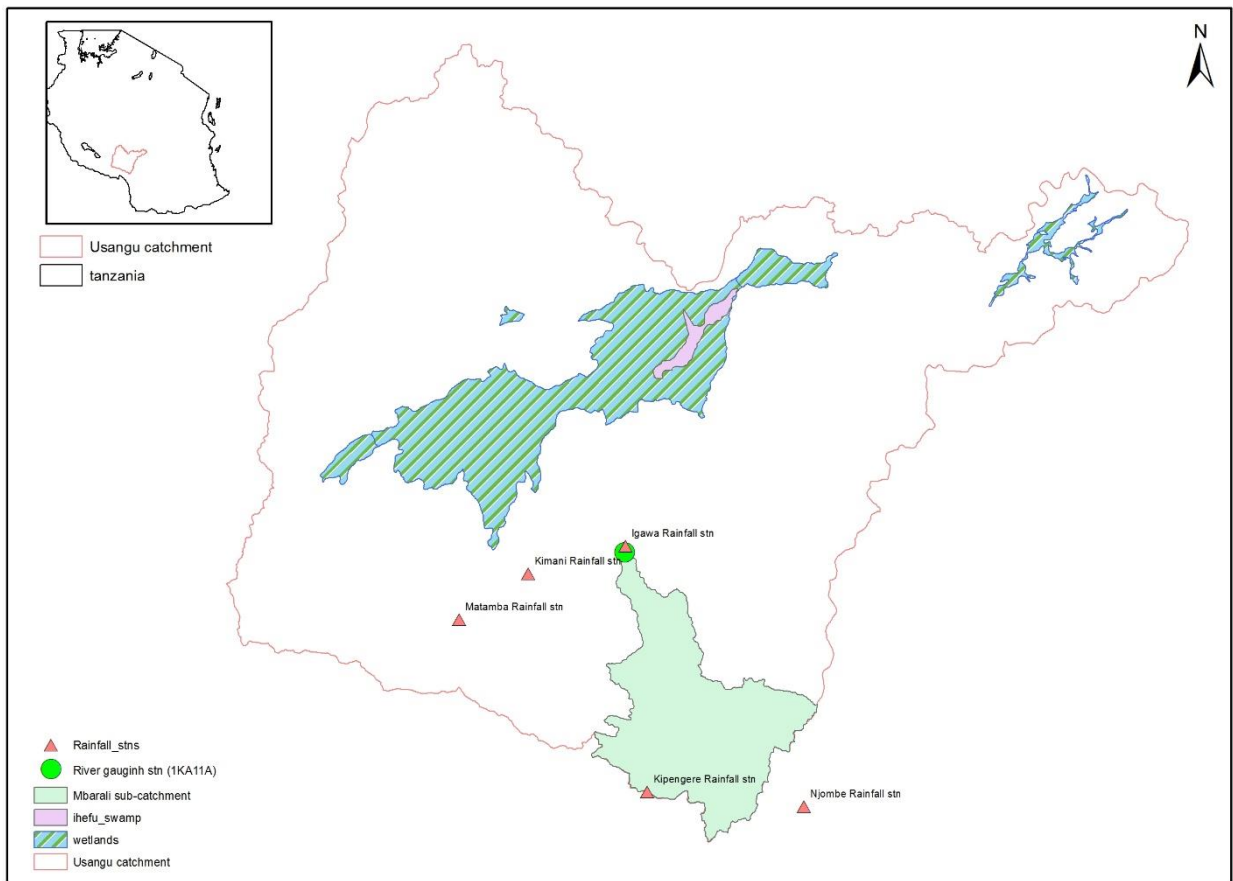


Figure 3: Map showing study area Usangu catchment and Mbarali sub-catchment with stream gauging station at 1ka11a (Mbarali at Igawa gauging station) and rainfall stations.

4.2. Climate

The general climate of the study area is controlled by the Inter-Tropical Convergence Zone (ITCZ), and rainfall is highly seasonal, with a unimodal type of rainfall period from the end of November to April, and indicated by high intensity rain events and dry season is between May to November. This rainfall pattern is echoed in the hydrology, with rivers indicate extremely peak runoff patterns and clearly distinguishable high and low flow seasons. High altitude areas receive between 1000-2000 mm of annually rainfall, while the low altitude areas receive around 700-800 mm annual rainfall. The average annual temperature ranges from 18 °C at higher altitude (above 2000 m above sea level) to about 28 °C in the lower altitude (below 1100 m above sea level) and drier parts of the catchment. The mean annual potential evapotranspiration is about 1900 mm (SMUWC, 2001b).

4.3. Drainage pattern

According to Mwakalila (2011a) the significant rivers that drains to Usangu catchment are the Great Ruaha (supplying between 25% to 2.96% inflow), Ndembera (supplying between 25% to 13.83% of the inflow), Kimani (contributing between 25% to 8.33% of the inflow), Chimala and Mbarali (its contribution is about 69.17% to 47.78% of the inflow). These rivers are permanent and they contribute to almost 70% of the available average annual streamflow at the outlet of the catchment. There are number of small rivers, which are periodic rivers in the catchment and in the time of dry season the contribution to the catchment is zero. These rivers include; Umrobo, Mkoji, Lunwa, Mlomboji, Kioga, and Mswiswi.

4.4. Land cover and land use

There is well define variability in land cover, use and vegetation patterns from the high elevation areas to the low elevation areas. In the highland areas excluding those of high altitude the area is dominated by Savanna woodland. At the higher altitude more than 2000 m above meter sea level, there is remains montane humid forest. Cultivation activities are extensive in the two sub-catchment of the Usangu basin, which are Mbarali Sub-catchment and Mkoji Sub-catchment as well as in the lower rolling hills north east in Iringa Region. In the catchment areas, which are below 1100 m above meter sea level are described as relatively low areas are grouped into two areas (i) the wetlands areas and (ii) the fans areas, which contains different vegetation formation and features. The southern fans are usually occupied by spiny woodland and/or wooded grassland. After all, most of this has been removed and replaced by cultivation. Most of agricultural activities are conducted in the fans areas because of its fertility. The Usangu wetlands have mixed of seasonally flooded swamps open grassland, seasonally flooded woodland, and a smaller perennially flooded swamp called Ihefu swamp. The permanent swamp is controlled by plant with non-woody stems called Herbaceous vegetation and Vossia, which is indicative of unstable hydrological regime has been found (McCartney et al., 2008).

5. DATA

5.1. Ground measurements and observation

Field work was done for three weeks period September 14 to October 5, 2014. The main activities carried out during field visit were:

- collecting runoff and rainfall data
- Taking discharge measurements

The field visit team composed of

1. Damas Patrick Mbagi – MSc student-University of Twente (ITC)
2. Abisai Chilunda -Rufiji Basin Hydrology Technician
3. Ally Diwani - Rufiji Basin Gauge reader and Meteorological station observer
4. Philemon Sinienga-Lake Nyasa Basin-Driver

The team travelled part of the Usangu catchment to check the status of river gauging stations, meteorological stations and different water user abstraction points. Due to limited time and financial resources, the team did not travel the whole catchment, after interview with staff of the Rufiji Basin Water Board office about the status of discharge data we decided to concentrate on the Mbarali sub-catchment, which is the sub-catchment of the Usangu basin. So for the selected sub-catchment discharge measurement were taken for 4 days to confirm if the rating curve developed correlate with the measurement we took.

5.1.1. River discharge

Discharge data is used for model calibration and validation. The gauging station for Mbarali sub- catchment is shown in Figure 3. The station is named as Mbarali River at Igawa AKA11A, some of the data is collected from the Ministry of Water headquarter Dar es salaam, Tanzania and other data were obtained from Rufiji Basin Office. The gauging station has good record of discharge data from 1955 to 2013, the station is equipped with automatic water level recorder and manual reading. The rating curve established is used to convert water level to discharge data. During field visit we took discharge measurement so as to check if what is obtained using rating curve is the same as what we measured on site, Table 2 shows the comparison of the result we measured to that obtained using rating curve. As shown in the table the results are almost similar, rating curve is still valid since no change in river cross section and the discharge data can be used for calibration and validation in our modelling purposes. Model calibration and validation we used discharge data from 2001-2012 at daily time scale. Discharge measurements in Mbarali sub-catchment is always done during high and low flow periods, the area-velocity method, commonly known as current meter method is mostly used. Mbarali River at Igawa station always provide water level recorded every morning at 9:00 am. Using the water level and discharge data rating curve is constructed, which is then used to convert daily recorded water level into discharge data.

Figure 4 shows the relationship between the cumulative observed discharges (m^3s^{-1}) at the outlet of Mbarali catchment (1KA11A Mbarali River at Igawa) and cumulative average rainfall ($mm d^{-1}$) from three stations. The relationship is shown by means on double-mass curve for the period of 2001 to 2010 at daily time step. Double mass curve is used to check the consistency and reliability of rainfall and observed discharge. The graph shows that there is a relationship between the rainfall and the discharge in the catchment, the graph is not such a straight line this may be due to seasonal variations which cause the fluctuations in the discharge,

inconsistency in rainfall data, change of rainfall station, changes in method of recording rainfall data and changes in the ecosystem due to natural calamities such as forest fires landslide. Figure 5 shows average rainfall (mmd^{-1}) at Mbarali sub-catchment obtained from three stations (Igawa, Kimani and Matamba) and the hydrograph measured at the outlet of the Mbarali catchment (1KA11 Mbarali at Igawa River) (m^3s^{-1}). From the graphs it shows that observed discharge responds quite well with the rainfall events in both period of rain and dry seasons. Rain season from mid-November to May and dry season from June to December.

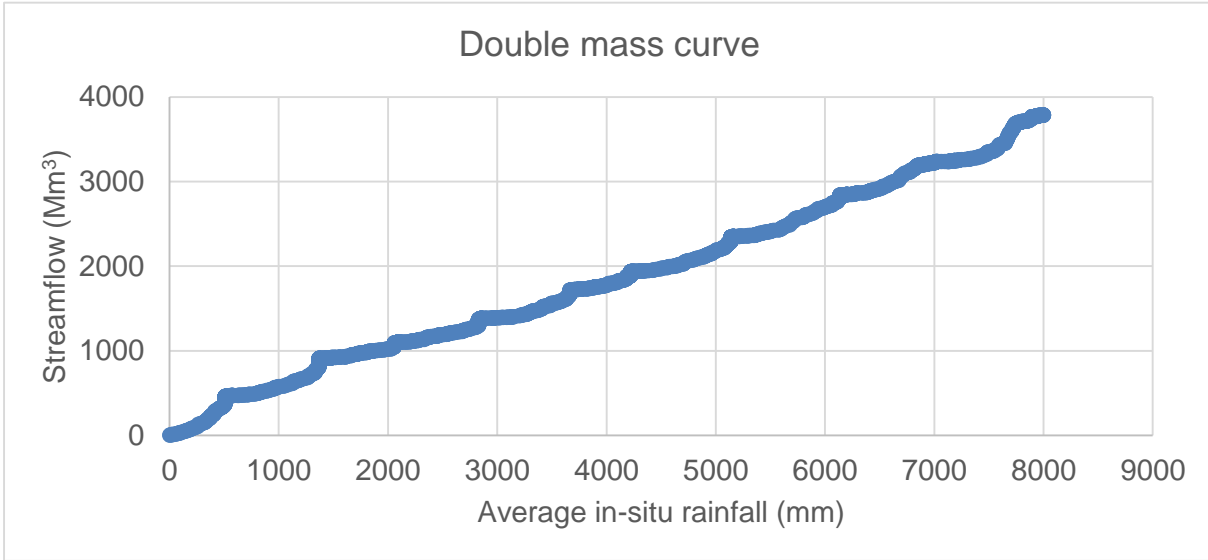


Figure 4: Double mass curves of average catchment precipitation and discharge (discharge form Mbarali River at Igawa gauging station-AKA11A gauging station).

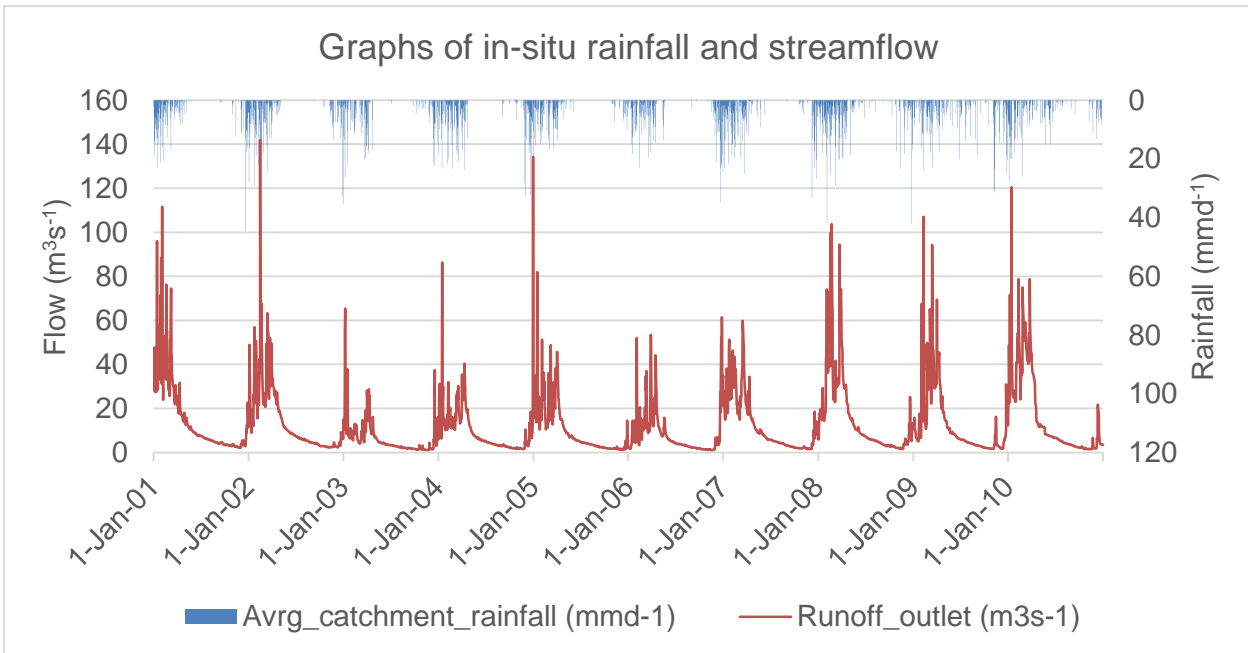


Figure 5: Observed discharge (m^3s^{-1}) versus average gauged rainfall (mmd^{-1}). As shown in the figure during rainy season (November-May) there is peaks in the hydrographs and during dry season (December-June) low flow is reflected in the hydrographs. Observed flow at 15 Feb. 2002 and 30 Dec.2004 record high flow 141.81 and 134.27 m^3s^{-1} , this can be regarded as an outlier and it may affects our modelling results.

Table 2: Discharge measurements for Usangu sub-catchments taken during field work 26-29 September 2014. Shows source and location of the river, gauge height in m, measured flow in m^3s^{-1} and flow obtained using rating curve (m^3s^{-1}).

Stn No	Location	Source	Date	GH (m)	Q_m (m^3s^{-1})	A (m^2)	V (ms^{-1})	Q_{RC} (m^3s^{-1})
1KA11A	Igawa	Mbarali	26/9/2014	0.25	3.091	15.107	0.205	3.076
1KA11A	Igawa	Mbarali	27/9/2014	0.24	2.96	15.11	0.196	2.76
1KA9	Kimani	Kimani GNR	28/9/2014	0.34	0.695	1.305	0.533	0.689
1KA9	Kimani	Kimani GNR	29/9/2014	0.340	0.695	1.290	0.639	0.687

5.1.2. Rainfall

The in-situ rainfall data in this study is used to check the relationship between rainfall and discharge recorded at the outlet of the catchment and we did quality-check of rainfall data. There are six rainfall stations within and around Usangu catchment. Since this research will concentrate on part of the Usangu catchment that is Mbarali sub-catchment, in that sub-catchment there are three rainfall stations within and around the sub-catchment. Rainfall data is obtained from Ministry of Water Dar es salaam-Tanzania, Tanzania Meteorological Agency (TMA) and from Rufiji Basin Water Board Office (RBWB). During field visit we visited some of the rainfall stations, and there are two types of rainfall stations used in the study area, including; manual reading where the meteorological station observer is reading the measurement every morning at 9:00 am, and the other type is the, automatic rainfall station, is included in the automatic meteorological station, this automatic station record rainfall every 1 hr. The automatic meteorological station is newly constructed as part of the World Bank project in the basin. In this research we use rainfall data obtained from manual reading station, they have data recorded for long period of time from 1970s to 2013. Rainfall data used in this research are from 2001-2010 daily data. Detail for the rainfall station are provided in Table 3.

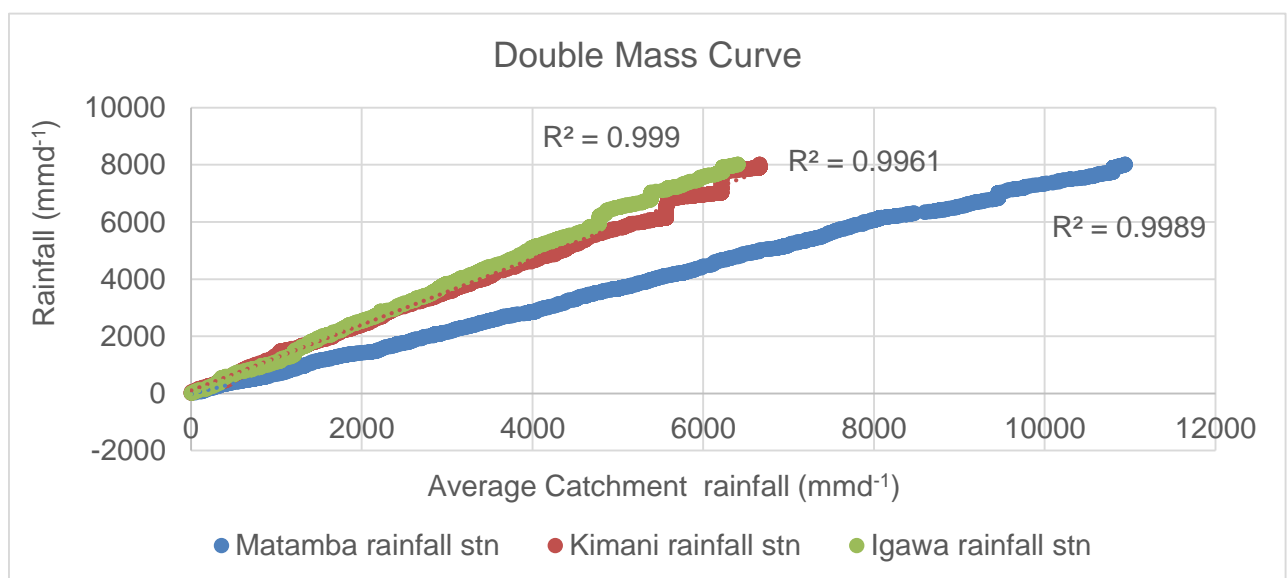


Figure 6: Double mass curve for individual rainfall station versus average catchment rainfall for Mbarali sub-catchment. Correlation coefficient Matamba 0.99, Kimani 0.99 and Igawa 0.99.

Figure 6: shows the double mass curve for the individual rainfall station and catchment average rainfall. The double mass curve is used to check the consistency of precipitation records in the Mbarali sub-catchment. The straight double mass curve indicates a consistent precipitation within the mean record and a bend in the curve indicates that the records have been affected, the bend indicates that the rainfall data is not consistent. This may be caused by either the station location has changed, error in recording or recording method has changed, but since the correlation coefficient in all stations are good (shown in Figure 6) we can conclude that data quality is acceptable. Table 3 shows location, date of data available, % of data missing, altitude of each station, station name and World Meteorological Organization station code for each station. Ground rainfall data is not used as forcing to the model because there is only one station within Mbarali sub-catchment while other stations are outside of the catchment.

Table 3: Rainfall Stations Usangu catchment.

WMO Code	Station Name	Lat.	Long	Alt	Data	% Missing
09834006	Igawa	-8.77	34.38	1067	1981-2013	1.67
09834010	Kimani	-8.83	34.17	1189	1981-2010	5.67
09834013	Matamba Pr. School	-8.93	34.02		1990-2010	3.56
09934001	Njombe District Office	-9.33	34.77	1829	1940-1989	5.87
09934001	Kipengere Pr.School	-9.30	34.43	2164	1953-1995	2.35



Figure 7: Picture of different activities undertaken during field trip to Mbarali sub-catchment. A= Configuration of current meter which is used to take discharge measurements, B= Taking discharge measurement at Mbarali river at Igawa (1AKA11A), C= Mbarali river at Igawa section, D= River gauging station automatic and manual instruments and E= Igawa meteorological station.

5.2. Satellite data

The satellite data sets used in this study are:

1. TRMM rainfall
2. Potential evapotranspiration (FEWSNET)
3. Shuttle Radar Topographic Mission (SRTM) Digital Elevation Model (DEM)
4. Land cover and Soil data

All these data are obtained from open source internet (Table 4)

Table 4: Satellite data sources. It shows satellite product and source of information about the product data are available free of charge.

Data	Source
TRMM	ILWIS-ISOD-Global Rainfall
PET	ILWIS-ISOD-FEWSNET Global PET
DEM	http://hydrosheds.cr.usgs.gov/index.php
Land Cover	http://servir.rcmrd.org/ArcGIS/rest/services/landcover/tanzania/MapServer
Soil data	http://webarchive.iiasa.ac.at/Research/LUC/External-World-soil-database/HTML/

5.2.1. Potential evapotranspiration

The Potential Evapotranspiration (PET) is obtained from National Oceanic and Atmospheric Administration (NOAA) Famine Early Warning System Network (FEWSNET). The daily global potential evapotranspiration (PET) that is used in this research is calculated from climate data (air temperature, atmospheric pressure, wind speed, relative humidity and solar radiation), which is obtained from Global Data Assimilation System (GDAS). The GDAS data are produced after every 6 hrs. PET is calculated By the NOAA for each 6 hour period and then daily total is obtained by summation, data produced has 1 degree spatial resolution. The daily PET is calculated on pixel basis using the Penman-Monteith formulation is by (Allen, 2006).

$$ET_o = \frac{0.408\Delta(R_n - G) + \gamma \left(\frac{900}{T + 273} \right) u_2 (VPD)}{\Delta + \gamma (1 + 0.34u_2)} \quad \text{Equation 12: Penman-Monteith equation}$$

Where:

- ET_o = daily reference ET (mm d⁻¹)
- T = air temperature at 2 m high (°C)
- VPD = vapour pressure deficit (KPa)
- U_2 = wind speed at 2 m high (m s⁻¹)
- R_n = net radiation at crop surface (MJ m⁻² d⁻¹)
- G = soil heat flux density (MJ m⁻² d⁻¹)
- Δ = slope vapour pressure curve (KPa °C⁻¹)
- γ = psychometric constant (KPa °C⁻¹)

5.2.2. Rainfall

The Tropical Rainfall Measuring Mission (TRMM) is a joint U.S.-Japan satellite mission to monitor tropical and subtropical precipitation. The rainfall measuring instruments on the TRMM satellite include the Precipitation Radar (PR), TRMM Microwave Image (TMI), with a nine-channel passive microwave radiometer; and Visible and Infrared Scanner (VIRS), with a five-channel visible/infrared radiometer. TMPA products provide precipitation for the spatial coverage of 50° N-S at the 0.25° x 0.25° latitude-longitude resolution as explained in detail by (Proposal, 2011). In this research the TRMM-3B42V7 with

the temporal resolution daily and spatial resolution 0.25deg is used. The TRMM-3B42 is calibrated and merged with monthly rainfall data. More detailed information regarding the processing and generation of on TRMM 3B42 can be found on J.Huffman.(2007). The temporal resolution of TRMM 3B42 is 3-hourly, on that account allowing us to acquire daily precipitation for estimation. There are two category of TRMM 3B42 data available, 3-hourly precipitation (correlate with eight time period per day, i.e., 00, 03, 06, 09, 12, 15, 18, 21) and daily aggregated precipitation. The daily aggregated precipitation is acquired by summation of all 8 sets of 3-hourly totals for a given day (Liu et al., 2014).

Figure 8 the comparison between catchment average in-situ rainfalls and satellite rainfall data as shown in the figure satellite overestimate rainfall in 2001, 2003, 2004, 2005, 2006 and 2007, Figure 9 show a scatter plot of in-situ and satellite rainfall data both in (mmd^{-1}), this plot is used to check if there is a correlation between satellite and in-situ rainfall data. As shown coefficient of correlation is very poor this may be caused by error in ground rainfall data, error due to recording or method used to find average rainfall in the catchment another error can be in the satellite rainfall data, Figure 10 Shows the spatial satellite rainfall and the observed discharge for the period 2001-2010. It shows that rainfall responding to the discharge at the outlet of the catchment, during rainy season January to May (2001-2010) it show high flows at the outlet of the catchment and during dry season June- to December (2001-2010) it also reflected by low flow at the outlet of the catchment. Figure 11 double mass for cumulative satellite rainfall and cumulative runoff at the outlet of the catchment. The double mass curve is used to check if there is consistency in runoff and response rainfall. The graph show there is inconsistency since the line is not straight line this may be caused by error in satellite rainfall data.

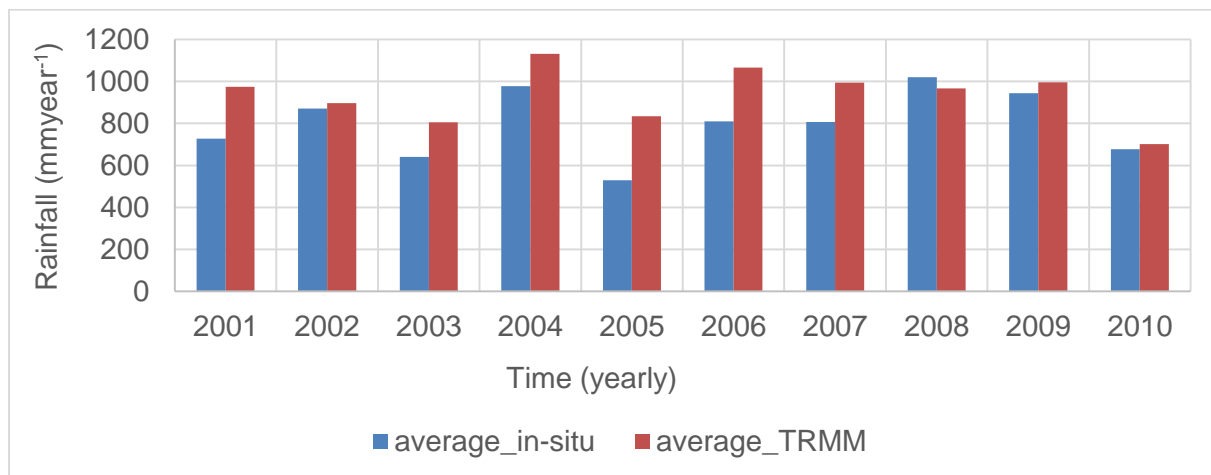


Figure 8: Graph of comparison between average in-situ and average satellite rainfall.

The satellite rainfall data are extracted using point to pixel method form global rainfall map. And the in-situ stations used as point are Igawa, Kimani and Matamba rainfall stations, then the average of the three station is found using normal average method. The following method is used to extracted satellite rainfall data for ten years. We made the maplist of the downloaded rainfall map using Integrated Land and Water Information System (ILWIS) software, then we displayed the rainfall stations on the maplist created to find which station fall to which pixel, thereafter open the pixel information and from the pixel information the rainfall values is seen and copied.

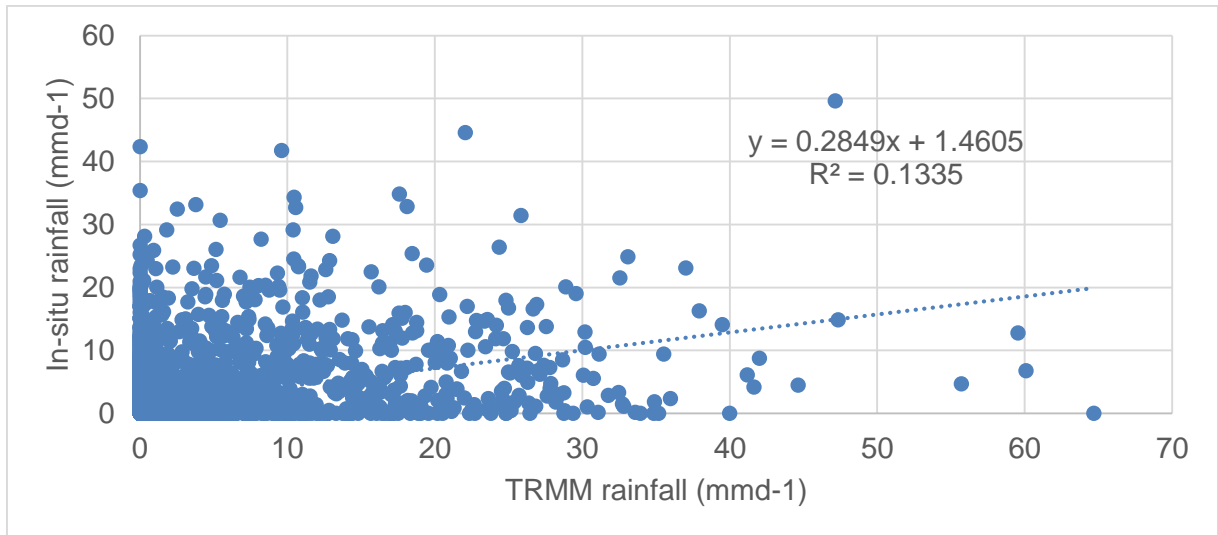


Figure 9: Scatter plot of ground and satellite rainfall. The correlation of coefficient is 0.13 this show a poor correlation between satellite and in-situ rainfall data.

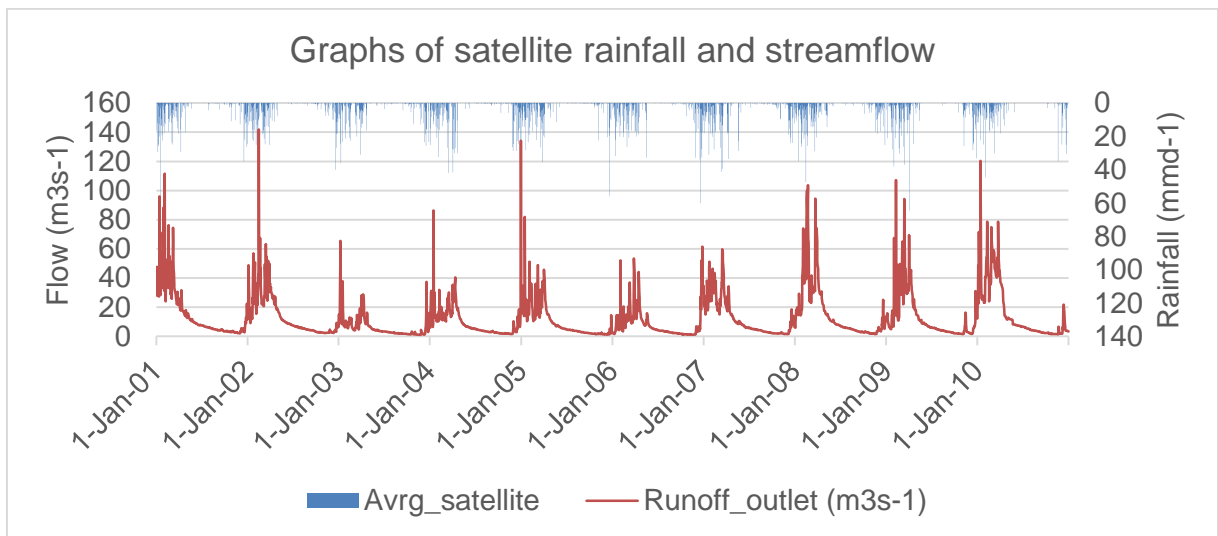


Figure 10: Average satellite rainfall versus time series of discharge data.

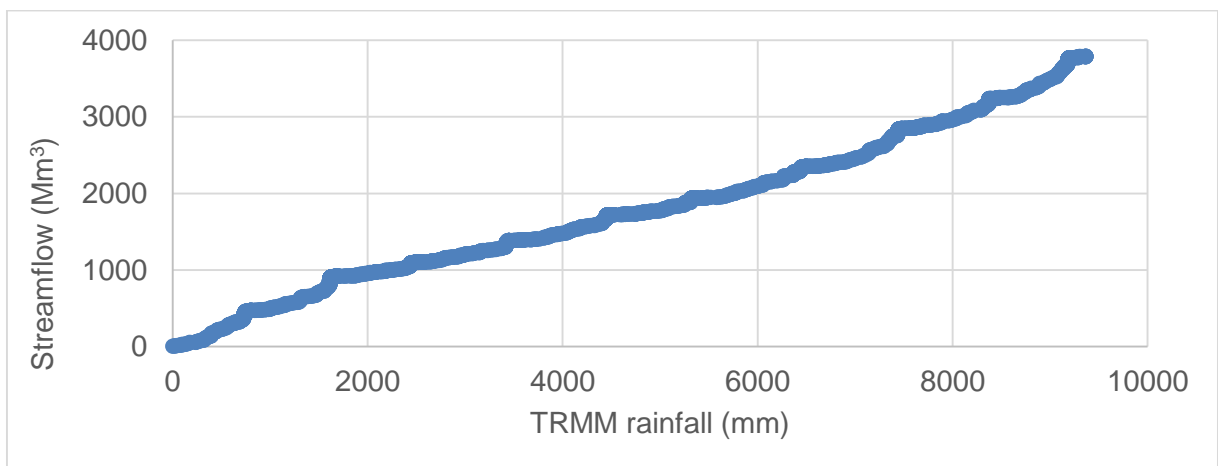


Figure 11: Double mass curve of satellite average rainfall vs. discharge.

5.2.3. Topographic information

The Digital Elevation Mode (DEM) obtained from SRTM is used to derive HydroSHEDS products. HydroSHEDS (**H**ydrological data and maps based on **S**huttle **E**levation **D**erivatives at multiple **S**cales) the products are geo-referenced and including; stream networks, watershed boundaries, drainage direction, and other products provides are: flow accumulations, flow direction, distances, and river topology information. HydroSHEDS is derived from elevation data of the Shuttle Radar Topography Mission (SRTM) at 30 arc-seconds (1000 m) resolution. Existing methods of data improvements and newly developed algorithms have been applied, including void-filling, filtering, stream burning, and upscaling techniques (Lehner et al., 2006a).

5.2.4. Land cover Map

Landcover map used in this research is obtained from SERVIR Eastern and Southern Africa Open Datasets. SERVIR is a joint venture between NASA and the U.S.Agency for International Development (USAID), which provides satellite-based Earth observation data and science application to help developing nations to improve their environmental decision making (Crew, Vehicle, Summary, & Module, 2010). The landcover map is developed from Landsat imagery 30m by 30m spatial resolution and this is accomplished using supervised classification method. The standard used to classify the image is built on seasonality and dry season is considered as the best period because during dry period of no cloud. This research we used land cover map Scheme II 2010 this land cover map help us to obtain the Mean Water Capacity (WM), which is used as input parameter to CREST model these parameters is not calibrated is obtained from site information. The WM for Mbarali sub-catchment range between 88-124 mm this values are derived from Global Land Cover Map look up table. Figure 12 shows the landcover map of the Mbarali sub-catchment there are thirteen landcover classes with the dominant land cover being open bush bushland, which occupies 23.59% of the total area of the Mbarali.

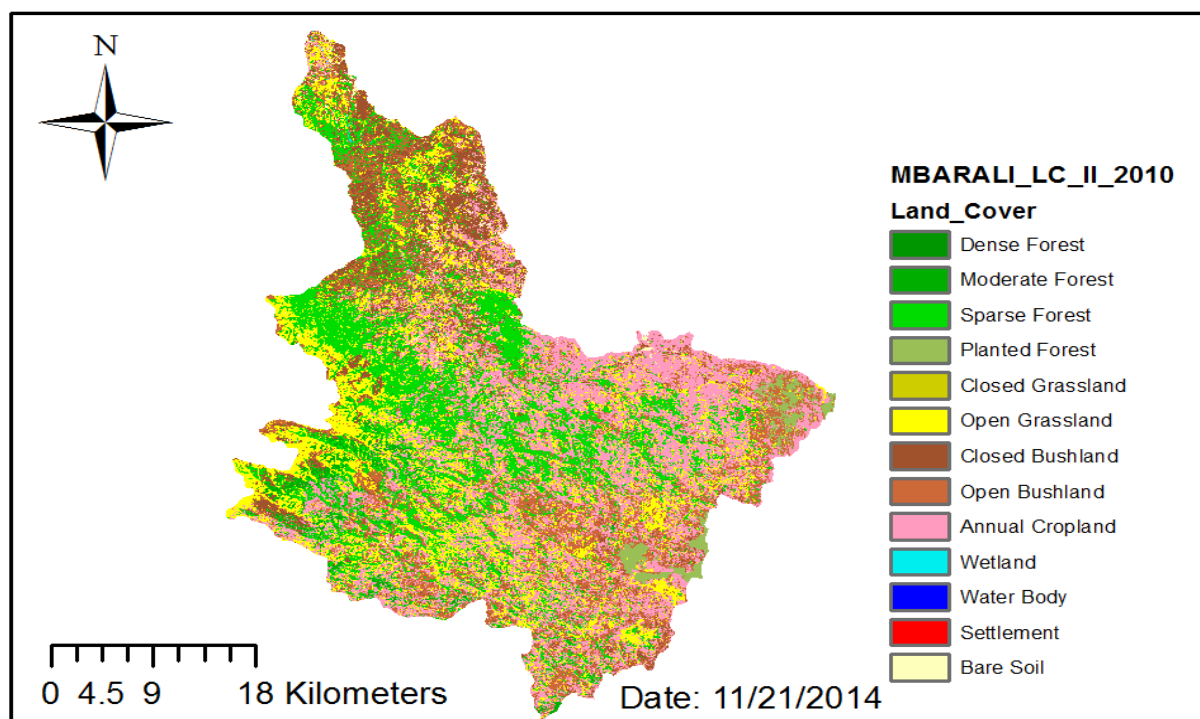


Figure 12: Landcover map Mbarali Sub-catchment. The dominant landcover type is Open bushland (23.59%), sparse forest (19.32%), Water body (14.28%), closed bushland (13.09%), Annual cropland (11.6%) and others as less than 10%.

5.2.5. Soil data

In this research we used soil data from Harmonized World Soil Dataset (HWSD), this database is developed by Food and Agriculture Organization (FAO) and International Institute for Applied System Analysis (IIASA). They used the already available soil information already contained within the 1:5,000,000 scale FAO-UNESCO Digital Soil Map of the world. The soil data is needed in the model as it will provide the saturated hydrologic conductivity (Ksat), which is the parameter to the model. The spatial resolution of this dataset is 1km. There are four main sources of version 1.2 of HWSD, these are; the European Soil Database (ESDB), 1:1 million soil map of China, the various regional SOTER database (SOTWIS) and Soil Map of the World. The soil information from HWSD is obtained using Arc GIS and the HWSD VIEWR. Figure 13 shows the soil map of the study area clipped from HWSD map, The study area consists of these type of soil as shown, with the dominant group being Acrisols which take 60.16%, followed by Andosols which take 25.75% the third group is Lixosols which take 13.44% while the last group which take less percentage is Leptosols that contains 0.665%. Based on the HWSD map the Ksat of the Mbarali sub-catchment Ksat range between 146-266 mmd^{-1} .

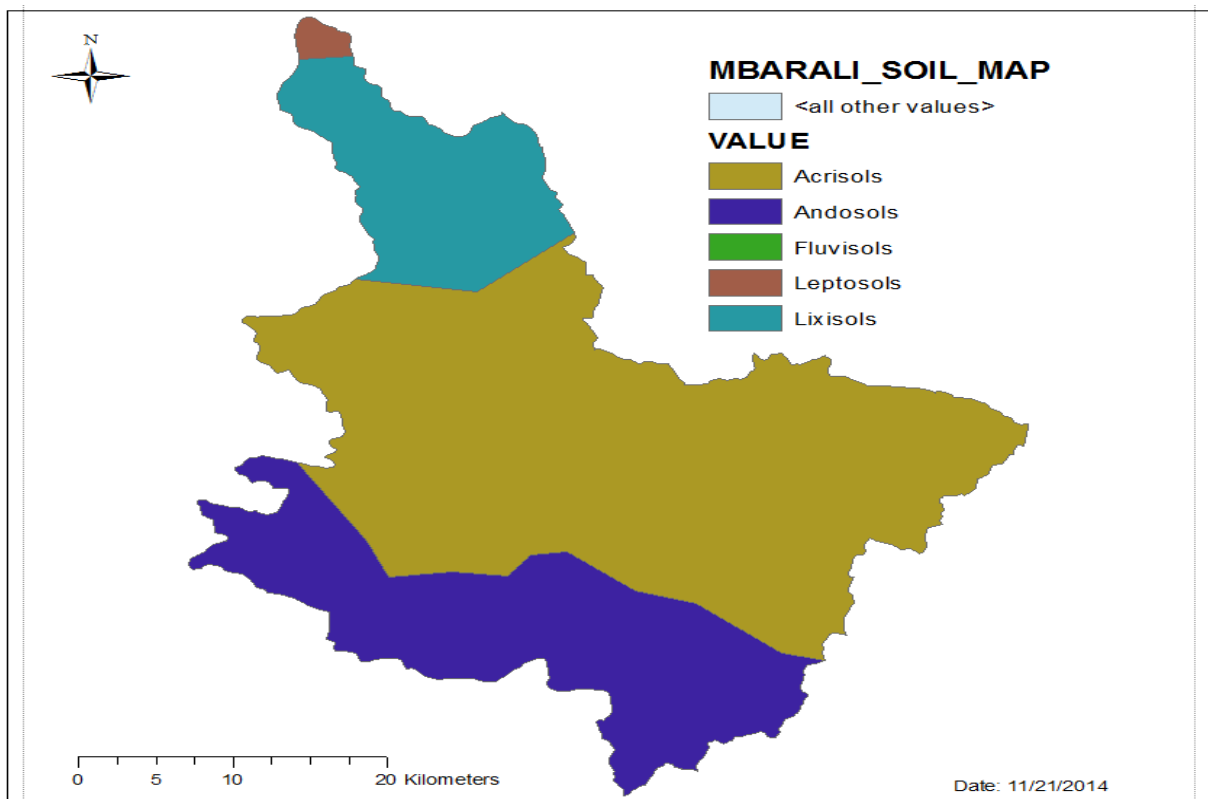


Figure 13: Soil map of Mbarali sub-catchment dominant group is Acrisols, followed by Andosols and Lixols the least group is Leptosols.

6. DATA PROCESSING

6.1. TRMM Rainfall

TRMM 3B42V7 is obtained from Integrated Land and Water Information System version 3.7.2 (ILWIS 3.7.2) using In Situ and Online Data (ISOD) toolbox. The following sequence is adopted to download the TRMM rainfall data. Open ILWIS 3.7.2 then go ISOD Toolbox followed by Gauge Satellite derived Rainfall Data then go to Global Rainfall data followed by TRMM Global and the last one is to choose the TRMM 3B42 day archive. The rainfall data downloaded are in 0.25 degree spatial resolution and 3 hrs temporal resolution. This is aggregated to daily temporal resolution. Rainfall data from 1st January 2001 to 31st December 2012 is downloaded in Multi sensor Precipitation Estimate (MPE) format. Since data is in 3hrs temporal resolution batch file is created to ease the work of downloading data (Attached in annex Appendix A). Then the data is converted from MPE format to American Standard Code for Information Interchange (ASCII) format using script (attached in annex Appendix B), which is made in ILWIS because this is the format used by CREST model. Figure 14 shows different procedure that is adopted to download rainfall data, A is the DOS command prompt window that is used to download data in 3 hrs interval time then it is aggregated to daily data, as shown there is processing time steps after every 3 hrs. C shows the global rainfall map with pixel information as seen, there is recorded rainfall on 20020202 with rainfall value of 88.47 mmd⁻¹ and B is In Situ and Online Data Toolbox window it explains how to access rainfall data.

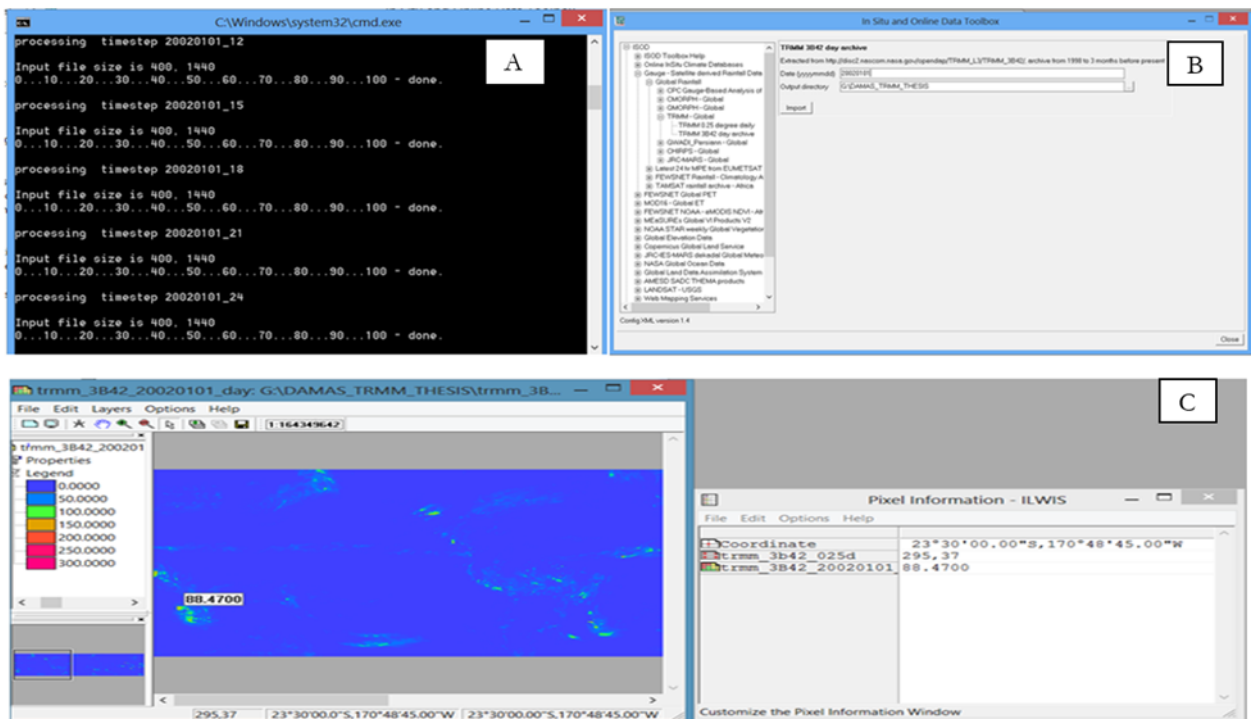


Figure 14: Satellite Rainfall data (TRMM) processing. A is window showing rainfall data in 3hrs downloaded, B shows in-situ online toolbox window, C shows the rainfall map with recorded rainfall value (88.4700 mmd⁻¹).

6.2. Potential evapotranspiration

Potential Evapotranspiration data is obtained from ILWIS 3.7.2 ISOD Toolbox. The following sequence is followed to obtain the data format that is required by CREST model. First ISOD Toolbox is opened in ILWIS 3.7.2 then FEWSNET Global PET is used to download PET of 1 degree spatial resolution and daily temporal resolution. Data from 1st of January 2001 to 31st of December 2012 is downloaded. Batch file is created so as to ease the work of downloading data for 11 years collected on daily basis, the data obtained is in MPE format it is converted to ASCII format using script (Attached annexes in Appendix C) which is created in ILWIS so as we can use them in CREST model. Figure 15 is the steps how PET data is obtained, B is the In Situ and Online Toolbox it gives the details on how to get access to PET data, A is the global map with displayed pixel information using ILWIS software there is recorded PET data on 20020722 is 12.01 mmd⁻¹ and C is the script that is made so to change data format from MPE format to ASCII format, the aim of this conversion is enable CREST model to read PET data.

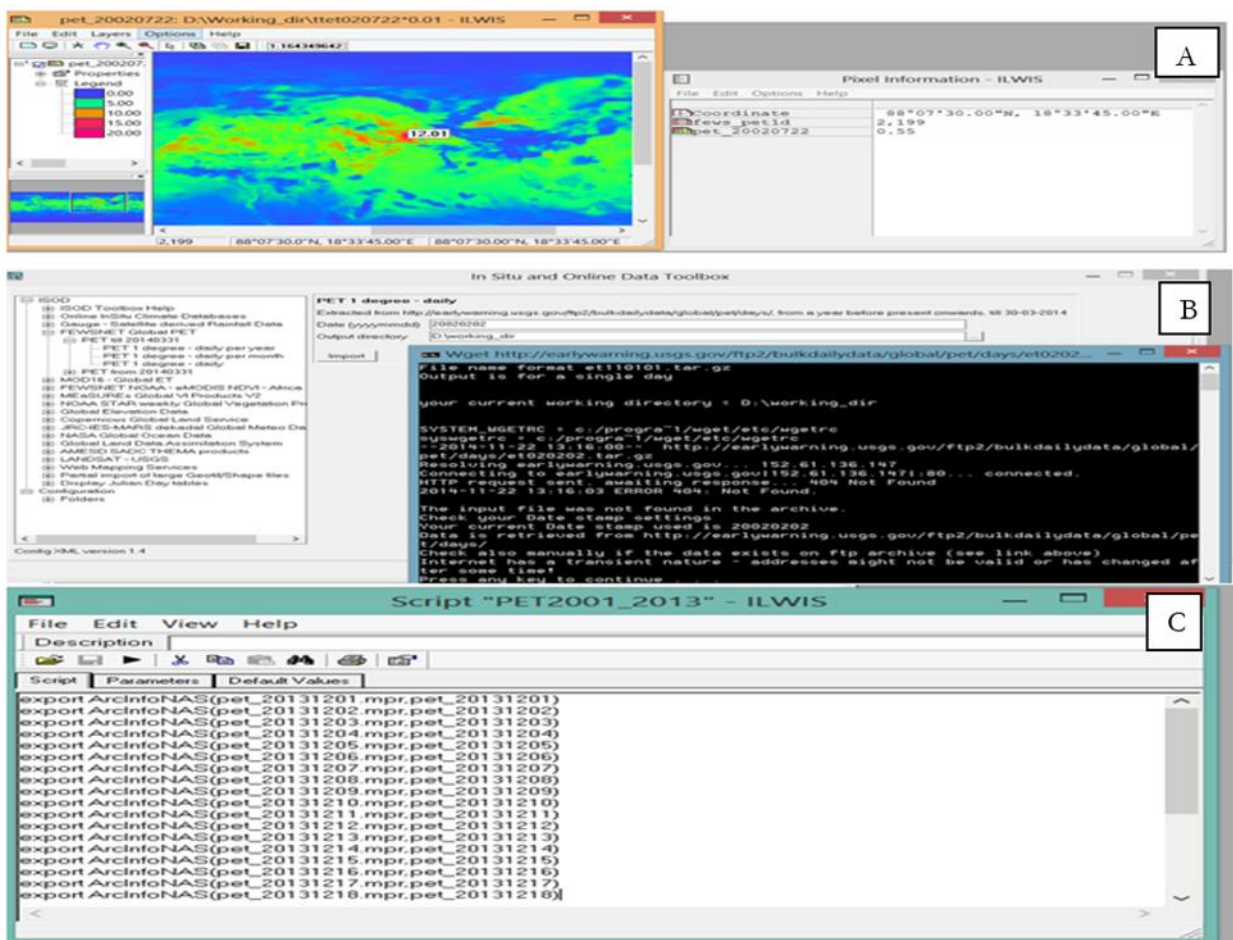


Figure 15: Satellite Potential Evapotranspiration data processing. A show global map of satellite potential evapotranspiration with recorded value (12.01 mmd⁻¹), B show the online and in-situ toolbox for PET download and C show the script used to convert PET from MPE format to ASCII format.

6.3. CREST model implementation

Model setup is done including the preparation of different folders with different files. Folders are Basics that consists of (DEM, FAC and FDR), forcing folder includes (potential evapotranspiration and rainfall data), Parameters (Parameter value), Observation (Flow data) and ICS with (Values for model initialization). ProjectName.Project is the control file including the information about Model Area (location of the study

area and size of your grid area), Run Time Information (show the time span for model run i.e., simulation period and warm up period), Configuration Directory (setting of different file format e.g. asc, txt, biffit, dbif), Run Style (you can specify if model run in; simulation, automatic calibration and real time), and Outputs Information for specified Pixels and outlets (catchment outlet location), Output States and Output Date (specify which date you are interested in the results are in Grid outputs) . The final stage is to run CREST mode “crest_v2_0.exe” in this research we used version 2.0 which is more advanced than version 1.6.

6.3.1. Input files to the model

CREST model has about 7 input files, which enable to run the model. How the input file is prepared are explained in detail in the following paragraph. The first input file is Basic file, this file consists of Digital Elevation Model (DEM), Flow Direction Map (FDR), and Flow Accumulation Map (FAC). These datasets are downloaded from HydroSHEDS website (<http://hydrosheds.cr.usgs.gov/index.php>). Data are in 1 km spatial resolution, Arc GIS for Desktop version 10.1 is used to clip DEM, FDR and FAC for the study area based on the map of Africa DEM, FAC and FDR the output is raster it is projected to Arc_1960_UTM_Zone 36S to specify study area. The downloaded map is in raster format then by using Arc Toolbox in Arc GIS the map is converted from Raster to ASCII format so that it can be read by CREST model. As explained by Lehner, Verdin, & Jarvis (2006b) HydroSHEDS its accuracy is better than HYDRO1k, a global hydrographic data set at 1-km resolution this is because the HydroSHED is based on superior Digital Elevation Model. HydroSHEDS is based on elevation data of the SRTM at 3 arc-second (90 meter) resolution while HYDRO1K is derived from 30 arc-second (1 km) DEM of the world (GTOP30) (Shook, 2012).

The second input file to the CREST model is the Observation file (OBS), this file contain flow data from the study area, which is used for model calibration and model validation. The third file is the parameter file (params) this file contains the configuration and parameters values that is used during model calibration to compare the simulated and observed flow there are 12 parameters. The fourth file is initial condition file (ICS).this file contains the values used for model initialization. Important files are rainfall file and potential evapotranspiration file. There is also Calibration folder (Calibs), which contains all the configuration and values of calibration for the model. Figure 16. Shows the basic input files to the CREST model, these basics are Digital Elevation Model (DEM), Flow Direction map (FDR) and Flow Accumulation map (FAC). For the DEM cell size is established and the elevation of the study area, elevations information describe about where water comes from and where it is going across any grid of a raster data. Flow direction is used to identify the water flow direction on a surface or identify the steepest descending direction of each cell in a DEM. Flow Accumulation is used to create a network to show accumulated flow into each cell. Figure 17 show the input data required to the CREST model all the data are explained above.

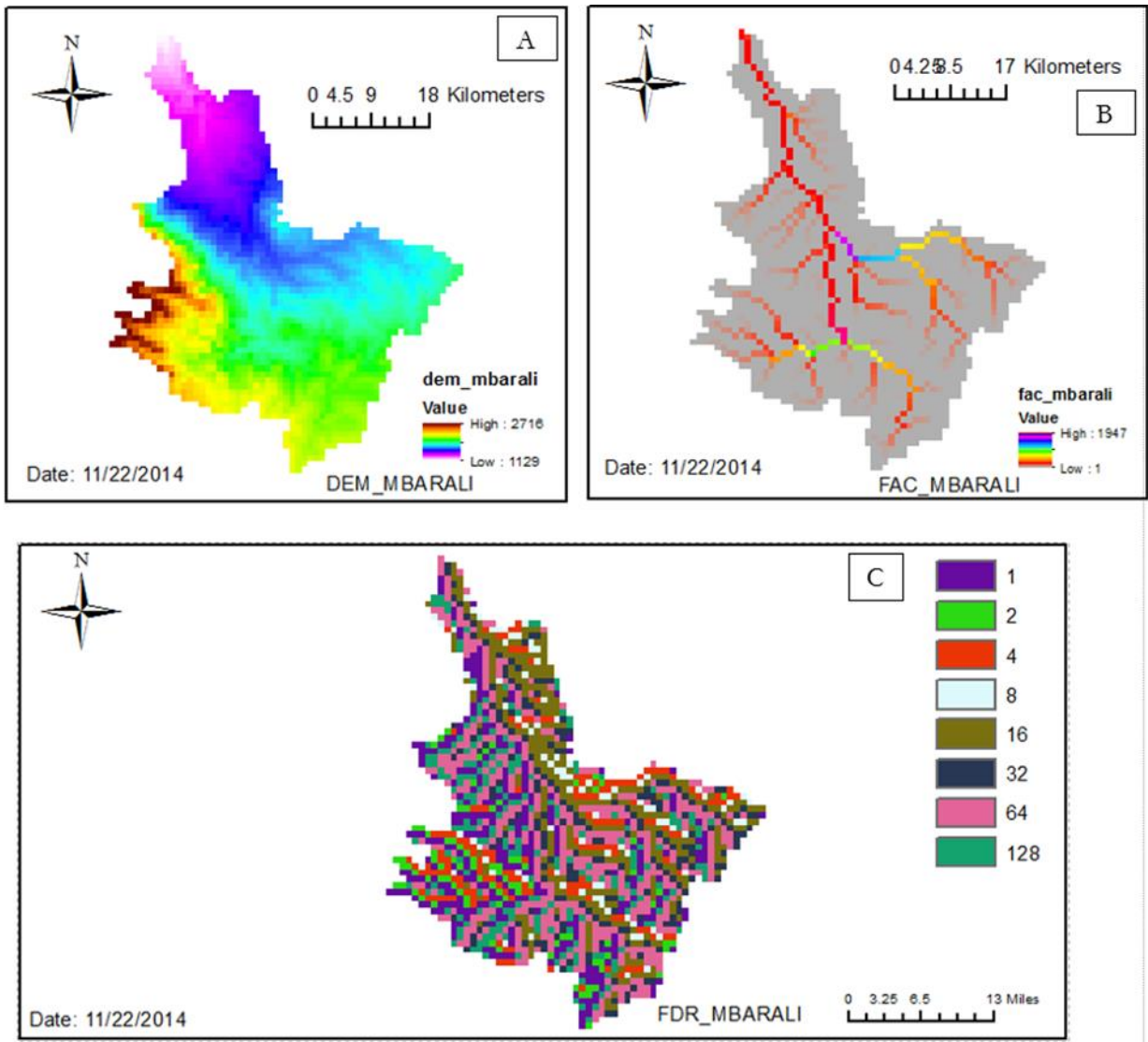


Figure 16: Basic input file to the CREST model. A is the DEM with lowest elevation and highest elevation of 1129 meters and 2716 meters respectively, B is the FAC with drainage network range of 1 to 1947 square meter of contributing area and C is the FDR map, colour show flow direction with conversion factor increasing by 2 each time these maps are for Mbarali sub-catchment.

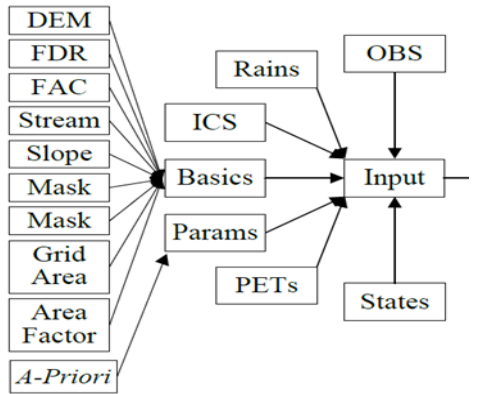


Figure 17: show the input files to the CREST model. There is 7 input files these includes Basics, Parameters, Initial Conditions, Rainfall, Potential evapotranspiration, States, and Observation files.

6.3.2. Output generated by the model

CREST model results are produced in format shown in Figure 18. There are twelve output results, starting with column two; Rain is the average rainfall of precipitation forcing (mmd^{-1}), PET is the average potential evapotranspiration (mmd^{-1}), EPot is the product of factor used to convert PET to local actual ET (KE) and PET, EAct actual evapotranspiration, W is the soil mean water capacity, SM is soil moisture, RS is the overland reservoir depth, RI is the interflow reservoir depth, ExcS is the surface runoff, excI is the sub-surface runoff, R is the simulated discharge (m^3s^{-1}) and RObs is the observed discharge (m^3s^{-1}).

DateTime	Rain	PET	EPot	EAct	W	SM	RS	RI	ExcS	ExcI	R	RObs
1/1/2002 0:00	8.781	4.064	2.088	1.828	72.661	0.727	9.45	5.558	0.958	3.089	3.213	14.929
1/2/2002 0:00	3.812	2.483	1.275	1.112	73.619	0.736	9.346	5.679	0.37	1.226	19.7	11.901
1/3/2002 0:00	11.941	3.873	1.99	1.99	77.286	0.773	10.17	6.27	1.414	4.87	17.07	12.972
1/4/2002 0:00	11.103	0.22	0.113	0.113	80.959	0.81	10.796	6.969	1.562	5.755	22.614	23.842
1/5/2002 0:00	5.621	2.594	1.333	1.202	82.08	0.821	10.324	7.252	0.649	2.574	39.717	48.853
1/6/2002 0:00	3.959	4.479	2.301	1.87	82.136	0.821	9.264	7.379	0.366	1.377	41.881	34.464

Figure 18: Shows the output generated by the CREST model, there is simulated flow (R) and observed flow in m^3s^{-1} and date of simulation is shown in the first column.

7. RESULTS AND DISCUSSION

7.1. Calibration

Calibration of the model is performed by comparison of the simulated and measured flow. Measured flow data at the outlet of the Mbarali sub-catchment (1KA11A Mbarali river at Igawa station) for the period of 2001-2012 are divided into three groups; 2001 period is used for model warming-up, duration between 2002-2007 is used for calibration and 2008-2012 interval is used for model validation. The calibration process is done by automatic calibration method using Parameter Estimation Tool (PEST). First step we run the model using default parameter values and the model is initialized using initial conditions supplied with the model. Initial value of Soil Moisture (WUO = 53.53), Initial value of Overland Reservoir (SSO = 5.89) and Initial value of Interflow Reservoir (SIO = 17.31). Using default parameter values and initial condition supplied, the model performance is; Nash-Sutcliffe model efficiency coefficient (NSCE) = -1026.21, Relative Bias (Bias %) = 3426.79 and Coefficient of Correlation (CC) = -0.21. Second step is to divide parameter into two groups; physical parameter (these parameters are to be derived by a-priori parameter method and/or to be calibrated) and empirical routing parameter/conceptual parameters (these parameters are obtained by calibration) the model is calibrated automatically using PEST tool and is initialized with these initial conditions (WUO =70, SSO = 10 and SIO = 40) the model performance results is NSCE = 0.63 Bias % = -0.01 and CC = 0.81

For the model calibration, PEST program is used to perform automatic calibration. PEST is a nonlinear parameter estimation and optimization techniques, it appeals well formulated Gauss-Marquardt-Levenberg algorithm, which incorporate the advantages of the inverse Hessian method and steep descent method hence allow quickly and more efficient convergence toward the objective function minimum (a. Bahremand & De Smedt, 2007). Table 5 shows the final list of calibrated value of model parameters. Figure 19 shows time series plot of simulated and measured streamflow in m^3s^{-1} daily, the magnitude and trend in the simulated streamflow closely follow the measured data most of the simulation period. The measured and simulated discharge volume are 1884.35 Mm^3 and 1884.19 Mm^3 respectively for the entire calibration period. The statistical model performance indicator shows that, Nash-Sutcliffe model efficiency coefficient (NSCE) = 0.63, Relative Bias (%) = -0.01 and Correlation of Coefficient (CC) = 0.81 values indicating satisfactory performance of the CREST model in Mbarali sub-catchment. Judgment of whether model performance is poor, satisfactorily or good is given by Moriasi et al. (2007b).

CREST model has twelve parameters and ten parameters are calibrated, two parameters (K_{sat} and WM) are obtained from site data, which are; land cover map we obtained water mean capacity (WM) and soil map saturated soil hydraulic conductivity (K_{sat}) is obtained. We started to calibrate the physical parameters with calibrated physical parameters we calibrated empirical routing parameters, then we calibrate again the physical parameters using calibrated parameters from empirical routing parameters, this process is repeated until no further improvements on the model results is achieved. This is how we did automatic calibration using PEST. Then, the optimal calibration parameters are obtained and are shown in Table 5. Parameter name, description of each parameter, numerical range, default value supplied with the model and final calibrated values for Mbarali sub-catchment are shown.

During the calibration period 2002-2007 CREST model underestimate the baseflow for the whole period of calibration as shown in Figure 19. Graph shows that peaks flow is well captured between simulated and observed streamflow except that there is mismatch at the beginning of 2003 where CREST model overestimate the streamflow ($22.67 \text{ m}^3\text{s}^{-1}$) compared to the observed ($14.19 \text{ m}^3\text{s}^{-1}$). Middle of 2004 also

CREST model overestimate the streamflow ($26.61 \text{ m}^3\text{s}^{-1}$), while the observed streamflow is ($23.68 \text{ m}^3\text{s}^{-1}$) on the same date, at April of 2007 CREST model overestimate the streamflow ($47.504 \text{ m}^3\text{s}^{-1}$) while the observed streamflow is ($34.39 \text{ m}^3\text{s}^{-1}$) during the same period, this overestimated streamflow it may be caused by overestimation of rainfall recorded by satellite as shown in Figure 8 where TRMM overestimate rainfall in 2003, 2004, 2005, 2006 and 2007 compared to rainfall recorded by in-situ measurement. During calibration period the simulated baseflow is underestimated compared to the observed one, for example July 2005 observed baseflow is $4.59 \text{ m}^3\text{s}^{-1}$, while the simulate baseflow $0.88 \text{ m}^3\text{s}^{-1}$, August 2003 observed streamflow $2.48 \text{ m}^3\text{s}^{-1}$, while the simulated streamflow is $0.34 \text{ m}^3\text{s}^{-1}$ these are examples on how the CREST model underestimate baseflow for the whole entire period of calibration as seen from Figure 19, this underestimation of baseflow by the CREST model may be caused by the routing method used by the CREST hydrological model. The Coupled Routing and Excess Storage (CREST) version 2.0 hydrological model use Jumped Linear Routing (JLR) as routing method during routing process, the disadvantage of this method is that in some application where the grid cell is large and time scale is very small, JLR will underestimate the streamflow this explanation is given by Xue & Hong. (2015) in their user manual. In this research we used 1 km as grid resolution for each grid cell, to overcome the problem of underestimation of the streamflow CREST 2.1V is developed, the new version use another routing method called Continuous Linear Routing (CLR). Generally we can conclude that the CREST model simulate satisfactorily the streamflow of the Mbarali sub-catchment this conclusion is based on the model performance indicator, which are NSCE = 0.63, Bias % = -0.01 and CC = 0.81. Explanations is given by (Moriassi et al., 2007b) concluded that model can be judged as satisfactory if NSCE > 0.5 and Bias $\pm 25\%$.

S. I. Khan, Adhikari, Hong, Vergara, Adler, et al. (2011) they did study on hydrological modelling using CREST model and automatic calibration of the model was done using Adaptive Random Search (ARS) the model performance is NSCE = 0.87 and bias = -0.23% for the period between 1985 and 1999. Model was forced using in-situ measurements, furthermore they did validation form 1999-2003 using in-situ measurements with NSEC = 0.65 and Bias = 1.04% and using satellite observed rainfall TRMM 3B42 V6 NSCE = 0.48 and bias = -4.58, this study was done in Lake Victoria basin at the sub-basin of Nzoia river. Another study performed using CREST model was at Okavango basin in Botswana by Sadiq I. Khan et al. (2012) they study was to find if satellite data can be used in ungauged basins and model performance during validation period yield Nash-Sutcliffe efficiency of 0.84. They concluded that remote sensing data can be used in ungauged basins. By comparing the calibration results from CREST model in Mbarali sub-catchment with these two studies we found that our results are within the performance of CREST model in other areas.

Figure 20 shows the cumulative simulated and observed streamflow volume for the period 2002-2007. As shown in the figure, most of the period the streamflow volume between simulated and observed is well captured except at the end of 2002, where CREST model underestimate streamflow volume; for example simulated volume in December 2002 is 363.03 Mm^3 , while observed volume is 431.01 Mm^3 and April to May 2004 CREST model overestimate streamflow volume. Figure 21 shows scatter plot for simulated and observed streamflow for the calibration period. The coefficient of determination form the plot is 0.76, this implies that there is good correlation between simulated and observed streamflow.

Table 5: Final calibrated values of CREST model parameters for Mbarali sub-catchment.

Parameter	Description	Numerical Range	Default Value	Final Calibrated Value
K_{sat}	Soil saturated hydraulic conductivity (mmd^{-1})	0-2827.2	500	150
RainFact	Multiplier on the precipitation field	0.5-1.2	1	0.77
WM	Mean soil water capacity	80-200	120	100
B	Exponent of VIC	0.05-1.5	0.25	1.5
IM	Impervious area ratio	0-0.2	0.05	0.14
KE	Ratio of PET to actual evapotranspiration	0.1-1.5	1	0.51
CoeM	Overland runoff velocity coefficient	1-150	90	138.11
CoeR	Multiplier used to convert overland flow speed to channel flow speed	1-3	2	2.24
CoeS	Multiplier used to convert overland flow speed to interflow flow speed	0.001-1	0.3	0.99
KS	Overland reservoir discharge parameter	0-1	0.6	0.86
KI	Interflow reservoir discharge parameter	0-1	0.25	0.13
expM	Overland flow speed exponent	0.9-1.2	0.95	0.80

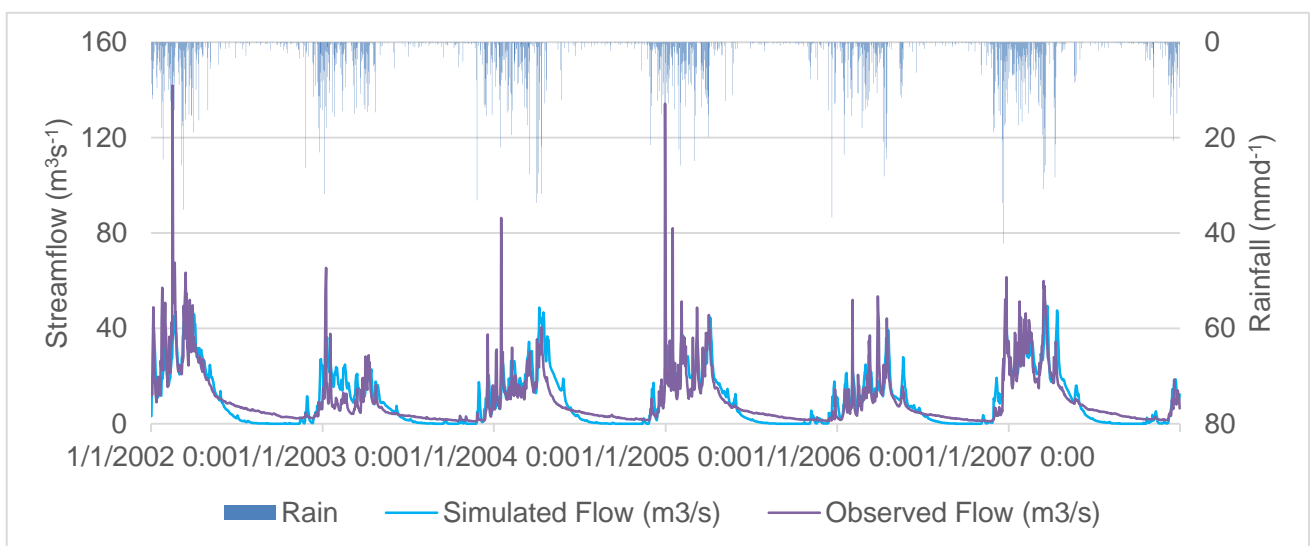


Figure 19: Time series of simulated and measured streamflow (m^3s^{-1}) at 1KA11A Mbarali River at Igawa gauging station for the 2002-2007 and average catchment rainfall mmd^{-1} . As shown simulated flow during dry season is underestimated for whole period.

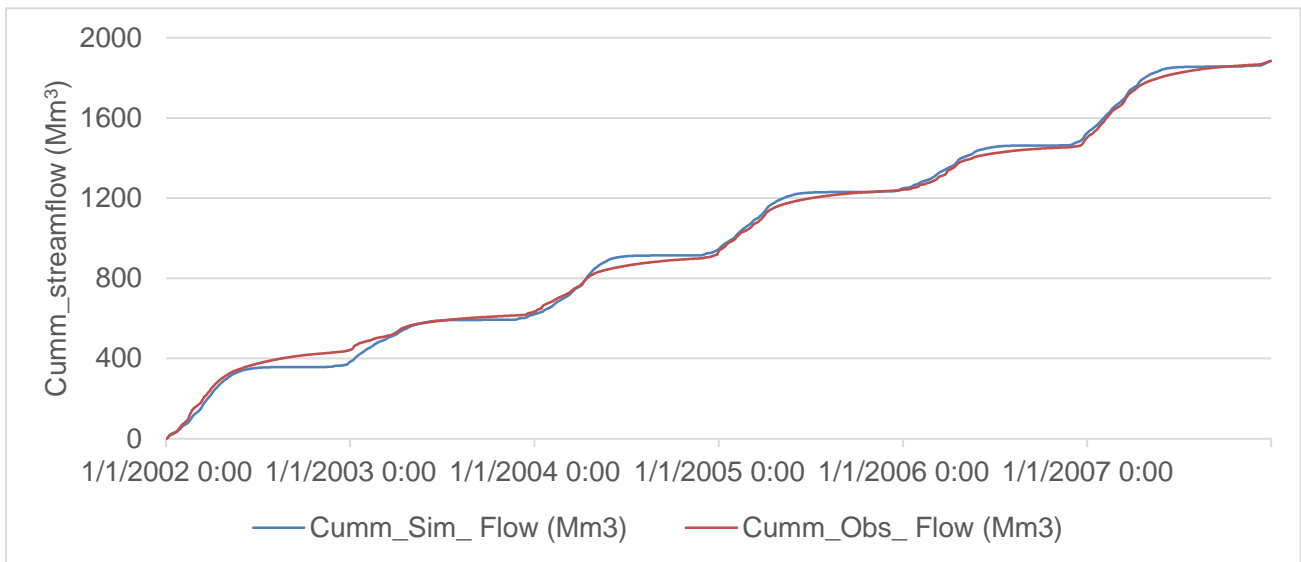


Figure 20: Graph of Cumulative streamflow for observed and measured. Shown in the figure at the middle of 2003 CREST model underestimate the runoff volume records 428.45 Mm³ while the observed runoff volume is 436.12 Mm³ and at the beginning of 2005 simulated streamflow volume is overestimated. Records 906.38 Mm³ for simulated and for observed streamflow volume is 857.89 Mm³

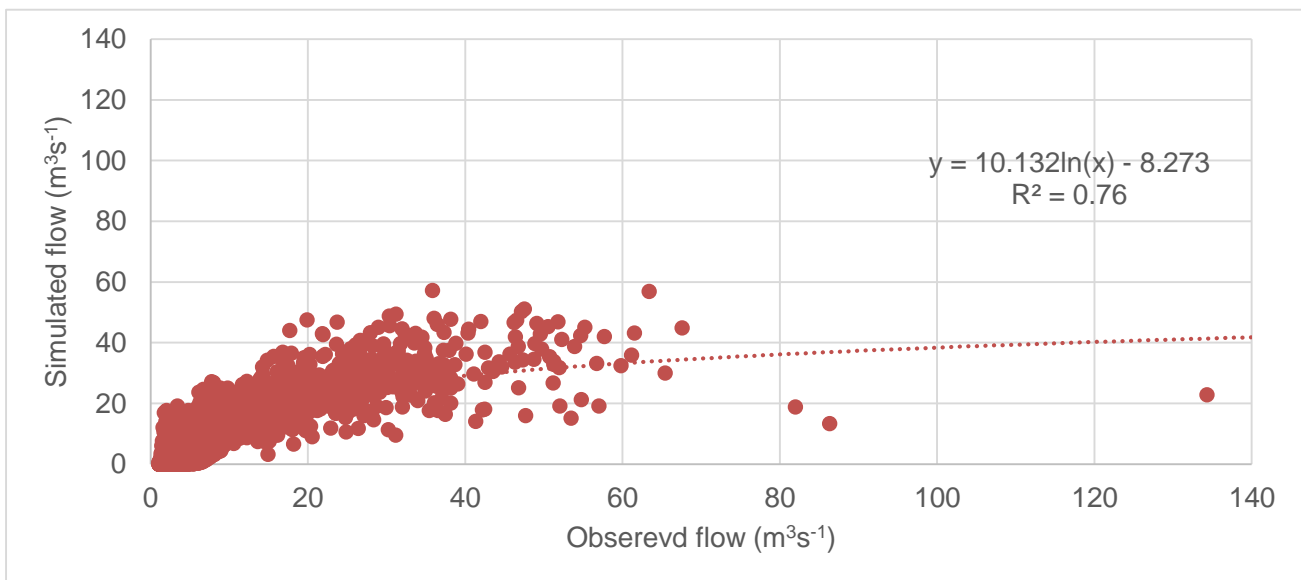


Figure 21: Scatter plot comparing simulated and measured daily streamflow (m³s⁻¹) for Mbarali River at Igawa, 2002-2007. The graph shows there is good correlation between simulated and observed streamflow as the correlation of determination is 0.76

7.2. Validation

During validation process, CREST model is forced to run with the calibrated parameter values obtained during calibration procedure. All the input data to the model including basics (DEM, FDR, and FAC) are assumed to be stationary except the hydro-meteorological inputs (Rainfall, PET). Figure 22 shows the time series plot of measured and simulated streamflow for the period 2008-2012 at daily time scale. The measured and simulated streamflow volume for the validation period are 2051.95 Mm³ and 1413.44 Mm³ respectively.

Model performance are shown by performance indicators, which are NSCE = 0.53, Bias% = -31.12 and CC = 0.78.

Figure 22 shows hydrograph of the validation results for the period 2008-2012. From the hydrograph, the CREST model underestimate both high and low flows; for example for high flow periods; January 2008 simulated flow is $3.21 \text{ m}^3\text{s}^{-1}$ while observed is $6.55 \text{ m}^3\text{s}^{-1}$, for May 2008 simulates is $11.48 \text{ m}^3\text{s}^{-1}$ while the observed is $17.01 \text{ m}^3\text{s}^{-1}$, during April 2009 simulated is $25.29 \text{ m}^3\text{s}^{-1}$ and observed is $33.17 \text{ m}^3\text{s}^{-1}$ furthermore, March 2010 simulated is $23.69 \text{ m}^3\text{s}^{-1}$ and observed is $59.57 \text{ m}^3\text{s}^{-1}$. During low flow period July 2008 simulated is $2.16 \text{ m}^3\text{s}^{-1}$ and observed is $7.14 \text{ m}^3\text{s}^{-1}$ for July 2009 simulated is $1.36 \text{ m}^3\text{s}^{-1}$ and observed is $5.91 \text{ m}^3\text{s}^{-1}$ in July 2010 simulated is $0.99 \text{ m}^3\text{s}^{-1}$ and observed $6.64 \text{ m}^3\text{s}^{-1}$ while July 2011 simulated is $3.29 \text{ m}^3\text{s}^{-1}$ and observed is $5.15 \text{ m}^3\text{s}^{-1}$. model performance indicator show that the overall performance during validation period in terms of NSCE is satisfactory, for Bias % CREST model perform poorly this is according to (Moriassi et al., 2007a).

Figure 23 shows the cumulative runoff volume for both simulated and observe flow, as shown in the figure simulated volume is underestimated compared to observed flow. CREST model underestimate the volume in Mbarali sub-catchment during the validation period, and this underestimation of volume is reflected in the model performance indicator in terms of the relative bias, which is -31.46% this values is out of range from according to (Moriassi et al., 2007a) suggest that model perform satisfactorily if relative Bias % is within $\pm 25\%$. Figure 24 shows scatter plot for simulated and observed streamflow for the period 2002-2007. As the coefficient of determination is 0.71 this implies that there is good correlation between simulated and observed streamflow.

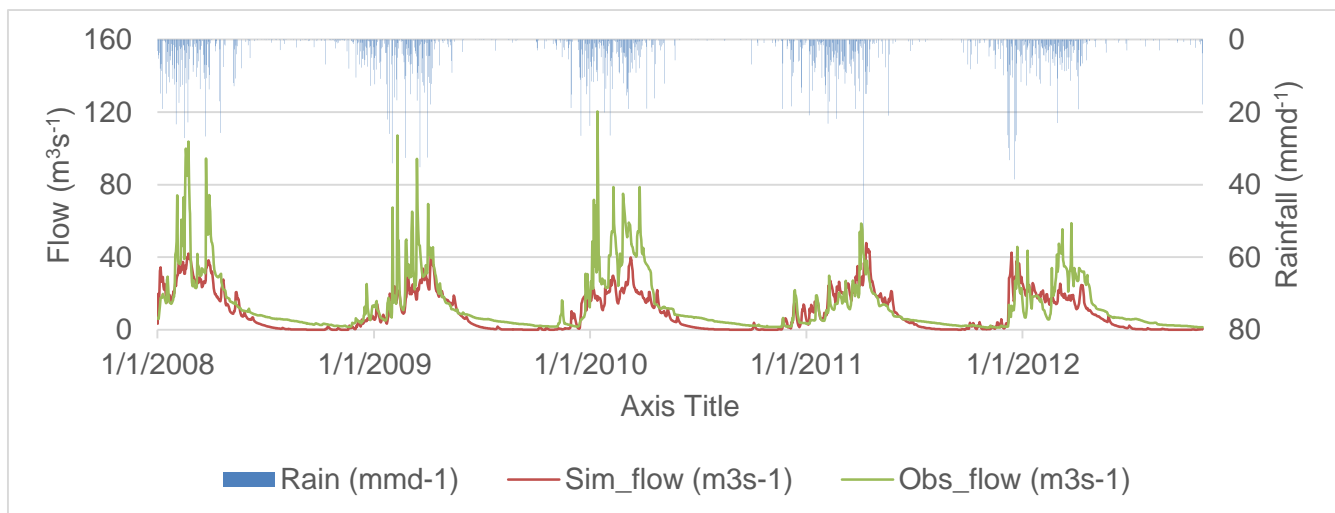


Figure 22: Hydrographs of the simulated and observed streamflow for the validation period. Graph shows CREST model underestimate the streamflow for both high flow and low flow except for 2011 during high flow CREST model is able to capture the peak flows.

This underestimation of streamflow can be caused by the routing method used by the CREST model. Jumped Linear Routing (JLR) is the routing method used in routing process by the CREST model, the disadvantage of this method is that it underestimate streamflow.

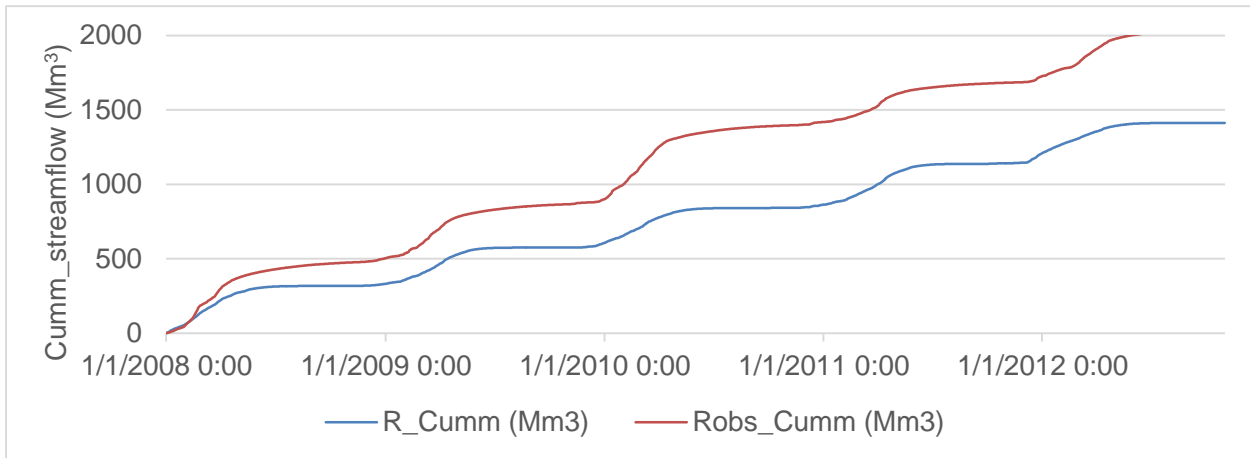


Figure 23: Shows the cumulative streamflow for the simulated and observed streamflow for the validation. Total streamflow simulated volume for the entire period of validation is 1413.44 Mm³ while observed streamflow volume is 2051.95 Mm³.

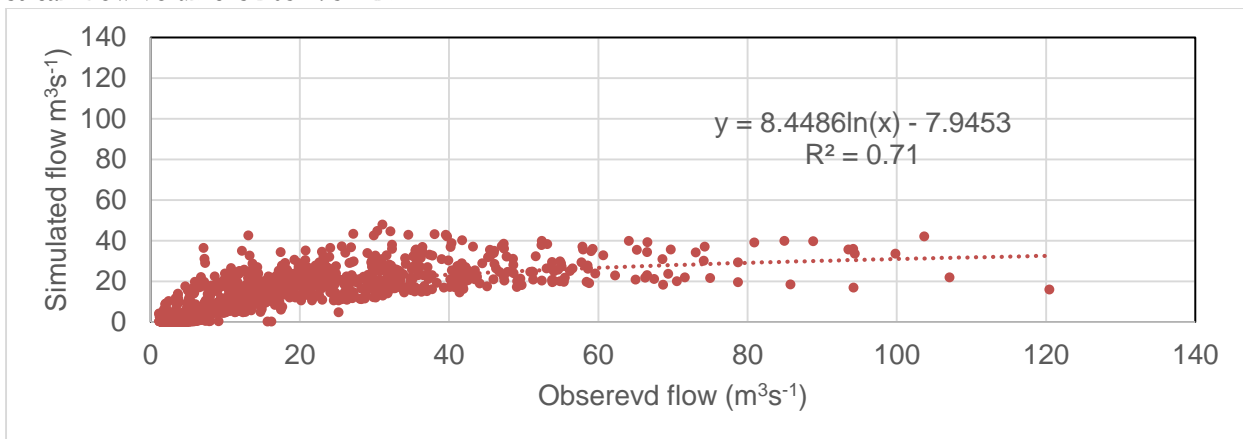


Figure 24: Scatter plot for the validation data. Scatter plot for the observed and simulated for daily streamflow data for Mbarali River at Igawa station, period. As the coefficient determination is 0.71 this shows that the correlation is good.

7.3. Sensitivity analysis

The sensitivity analysis is performed on the CREST model parameters for the Mbarali sub-catchment, the purpose of sensitivity analysis is for model improvements, calibration efficiency and improve measurement program. In this study sensitivity analysis is performed using two methods. The first sensitivity analysis is done using automatic calibration method and this is done using PEST, PEST uses a nonlinear estimation technique known as the Gauss-Marquardt-Levenberg method. The robustness of this method is built in the fact that it normally estimate parameters using less model run than any other estimation method, an explicit bonus for distributed models whose run times may be considerable. For nonlinear problems, parameter estimation is an iterative process (Tang, Reed, Wagener, & van Werkhoven, 2006). A. Bahremand & de Smedt.(2010) they explained that PEST uses a local calibration approach and determine the optimal values of model parameters by minimizing the sum of squares of the differences between measured and simulated model results. Sensitivity analysis using automatic procedure is done together with calibration of the model parameters. Parameters are divided into two groups; routing group shown in Table 6 and physical group see Table 7 . After model parameter optimization, PEST provide relative sensitivities of each model parameters

in each group, see Table 6 and Table 7 for their relative sensitivities values, the relative sensitivity are obtained by multiplying composite sensitivity by the magnitude of the value of model parameters for details of this, see the work of A. Bahremand & de Smedt. (2010). Based on this relative sensitivities we identified, which parameter are more sensitive than others, find details in Figure 25. With the guidance from Figure 25 and by the study done by Lijalem Zeray Abraham, Jackson Roehrig. (2007) they provided Relative Sensitivity (RS) range: Small to Negligible $0 \leq RS < 0.05$, Medium $0.05 \leq RS < 0.2$, High $0.2 \leq RS < 1.0$ and Very High $RS \geq 1.0$. We found that, three parameters with higher relative sensitivities values are more sensitive than other parameters. After finding these parameters with very high relative sensitivity, the next step is to perform sensitivity analysis using manual procedure, the aim of this manual sensitivity analysis is to evaluate the effect of sensitive parameters to the model performance based on model performance indicator NSCE, Bias % and CC. The automatic calibrated parameters and the results of parameter sensitivity analysis after the optimization process are presented in Table 6 for routing parameters and Table 7 for physical parameters.

As can be seen in the Table 6 relative sensitivity of the 5 calibrated parameters varies within the range (0.2-44). Parameter expM, which is the overland flow speed exponent has highest relative sensitivity. Parameter CoeS, used to convert overland flow speed to interflow speed has the second highest sensitivity. Parameter CoeR, used to convert overland flow speed to channel flow speed has the third place highest sensitivity. Parameters KS and KI which, are overland flow discharge parameter and interflow discharge parameter respectively has high relative sensitivity in this group. As shown in Table 7 relative sensitivity of the 5 calibrated parameters varies within the range (0.0065-0.79). Parameter RainFact, which is the multiplier on the precipitation field is ranked the second parameter with high relative sensitivity. B that is the exponent of variable infiltration curve its relative sensitivity is negligible. IM is the impervious area ratio is the first parameter with high relative sensitivity in this group. CoeM is the overland runoff velocity coefficient it is ranked fourth with medium relative sensitivity. And KE factor used to convert potential evapotranspiration to local actual evapotranspiration is placed as the third parameter with high relative sensitivity. These classification is according to Lijalem Zeray Abraham, Jackson Roehrig (2007) they gave range of parameter relative sensitivity from very high sensitivity to negligible relative sensitivity see Figure 25 for interpretation.

PEST also provides a parameter correlation coefficient matrix of the calibrated parameters. For Routing parameters, this matrix shows that there are no significant correlation between parameters, except there is strong positive correlation between expM and CoeR ($R = 0.99$), high negative correlation between CoeR and KS ($R = -0.62$) and moderate negative correlation between expM and KS ($R = -0.60$), expM and KI ($R = -0.53$) and CoeR and KI ($R = -0.56$). In the case of physical parameters, this matrix also show that, there are no significant correlation between parameters, except there is high positive correlation between RainFact and KE ($R = 0.80$) and high negative correlation between RainFact and CoeM ($R = -0.66$), RainFact and IM ($R = -0.63$) and IM and KE ($R = -0.62$). Because sensitivities are obtained by changing the parameters one by one, they are not influenced by parameters correlation this is according to A. Bahremand & Smedt. (2006).

Table 6: shows the relative sensitivity of routing parameters produced by sensitivity analysis tool (PEST) column one is the parameter name, second column is the optimized parameter values during automatic calibration process and third column is the relative sensitivity value of optimized parameter.

Parameter name	Calibrated value	Relative sensitivity value
expM	0.80	43.70
CoeR	2.24	5.89
CoeS	0.99	11.50
KS	0.86	0.22
KI	0.13	0.99

Table 7: shows the relative sensitivity of physical parameters produced by sensitivity analysis tool (PEST) column one is the parameter name, second column is the optimized parameter values during automatic calibration process and third column is the relative sensitivity value of optimized parameter.

Parameter name	Calibrated value	Relative sensitivity value
RainFact	0.71	0.64
B	1.5	0.01
IM	0.14	0.79
CoeM	138.11	0.12
KE	0.51	0.25

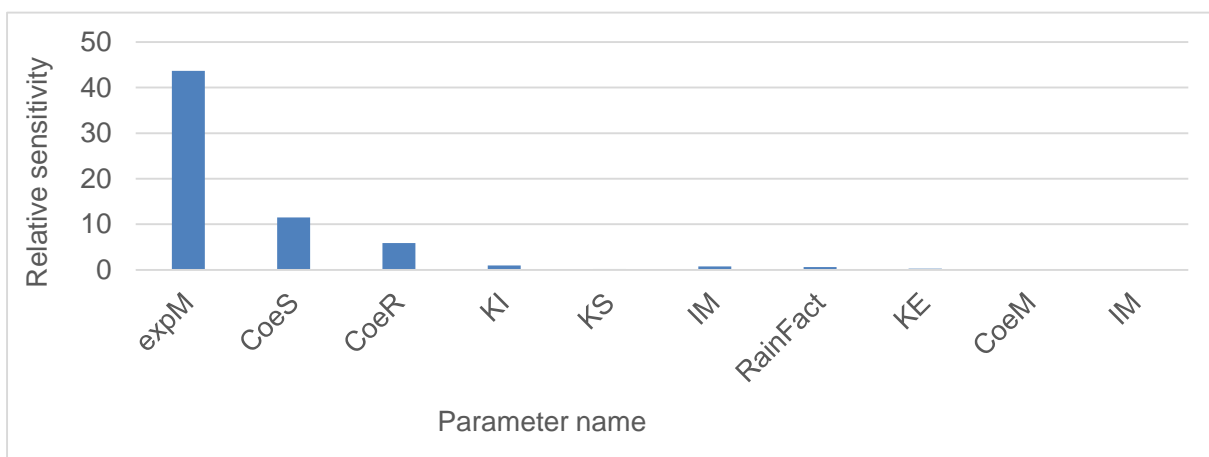


Figure 25: Sensitive parameters and their relative sensitivity. As shown expM has highest sensitivity of 43.67, CoeS ranked the second with 11.50 and the third is CoeR with 5.88 relative sensitivity.

7.3.1. Sensitivity analysis of expM parameter.

Table 8: shows how the sensitivity of the CREST model to changes in the expM parameter has affected the model performance in terms of model performance indicators NSCE, Bias % and CC. The sensitivity analysis is done by varying the parameter in the selected range of $\pm 30\%$ of the calibrated model parameter value. In this case expM is changed, while other calibrated model parameter are kept constant, as indicated in the table model performance in terms of Bias and NSCE is affected largely.

Figure 26 shows hydrographs produced when changing different parameter values, hydrographs further shows that both peak flow and low flow changed drastically when the values changed from 0.56 to 1.04 ($\pm 30\%$ of the calibrated value). Both the shape and peaks of the hydrographs change quite drastically when the expM parameter is varied. For the lower value of expM (i.e. 0.56, 0.64 and 0.72), the peak flow are much larger than the higher values of expM (i.e. 0.88 and 0.96). for example in March 2002, with expM set as 0.72, the peak flow is $102.66 \text{ m}^3\text{s}^{-1}$ but for the higher value of expM like 0.96 the peak flow becomes $7.11 \text{ m}^3\text{s}^{-1}$. This is the same as for March 2003 where expM (0.72) record peaks of $50.26 \text{ m}^3\text{s}^{-1}$ and expM (0.96) records peaks of $2.39 \text{ m}^3\text{s}^{-1}$. As shown in the figure higher value of expM more than one, for example expM (1.04) produces hydrograph, which is not like hydrographs produced by other expM values, the falling limb is very sharp this shows that the proportional of rainfall that reaches the outlet via overlandflow increases. The expM is the overland flow speed exponent and it implies that any increase of expM more that one will have large impact on the overland flow speed which in turn will cause the rising and faling limbs of

hydrographs to change drastically. During low flow period lower values of expM produce high runoff compared to high values of expM, for example July 2002 expM (0.72) record flow of $9.76 \text{ m}^3\text{s}^{-1}$ while expM (0.88) and expM (0.96) produces flow of $0.01\text{m}^3\text{s}^{-1}$, $0.00 \text{ m}^3\text{s}^{-1}$ respectively. The same as July 2003 and 2004 expM (0.72) records $4.93 \text{ m}^3\text{s}^{-1}$ and $9.76 \text{ m}^3\text{s}^{-1}$ respectively, while expM (0.96) produces flow of 0.05 and $0.06 \text{ m}^3\text{s}^{-1}$ respectively on the same year. Higher values of expM more than one produces higher values of runoff even during dry season, for example July 2002, 2003 and 2004 expM (1.04) records runoff of 96.63 , 49.33 and $74.16 \text{ m}^3\text{s}^{-1}$ respectively, expM is the overland flow speed exponent and values more than one will produce more runoff that is the reason why expM (1.04) produces higher runoff even during dry season.

Figure 27: shows the commulative runoff for the different values, the higher value more than one produce high value of runoff volume of 9957.87 Mm^3 while the lower value produces less runoff volume of 2501.7 Mm^3 these values are recorded during calibration period. This changes in parameter values which, has resulted in changes in streamflow during high and low flow has great impact on the model performance these impact is seen in Table 8, which shows the statistical indices for the different values of expM, the upper value next to the calibrated value gives better NSCE as close to the calibrated one, while the other value gives poor value of NSCE as compared to the calibrated one and this effect can be seen in the shape of hydrographs in terms of peak and low flow as well as recession and rising limbs. Also for the Bias (%) model performance is poor and this is reflected in the shape of hydrographs in terms of streamflow volume and for CC higher expM value leads to poor performance of the model.

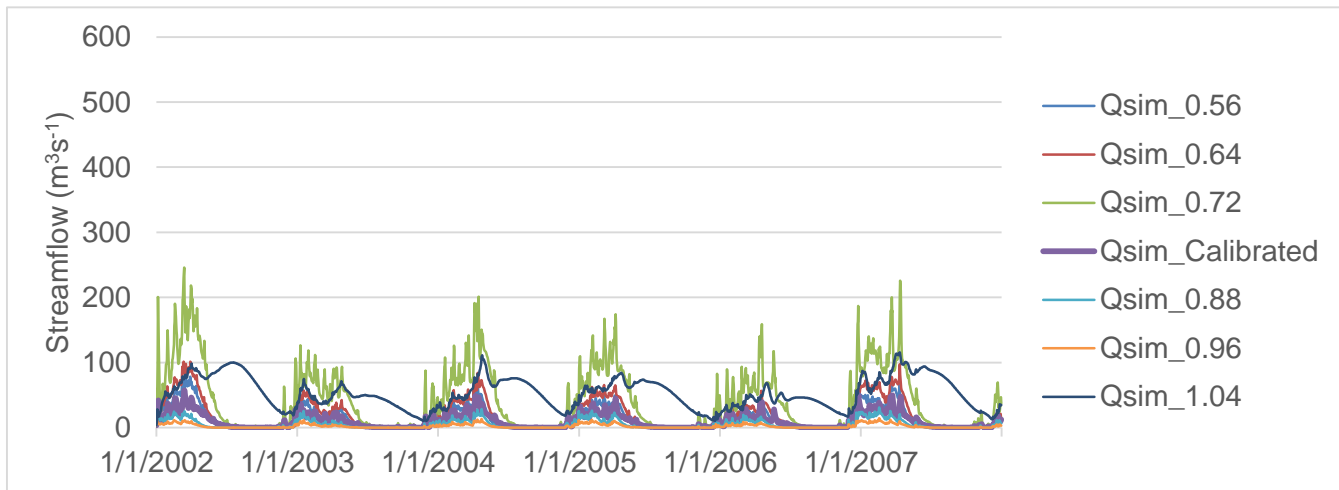


Figure 26: Hydrographs produced by different values of expM parameter. As seen from the shape of hydrograph produced by expM (1.04) is different from other hydrographs resulted from other parameter value. ExpM (0.72) which is less than other values above calibrated parameter value produces high peak flow. For expM (0.96) the shape of hydrograph for recession and rising limbs are poorly produces.

Qsim_calibrated is the calibrated streamflow, which is used as a reference to assess if there is decrease or increase in streamflow when changes the parameter.

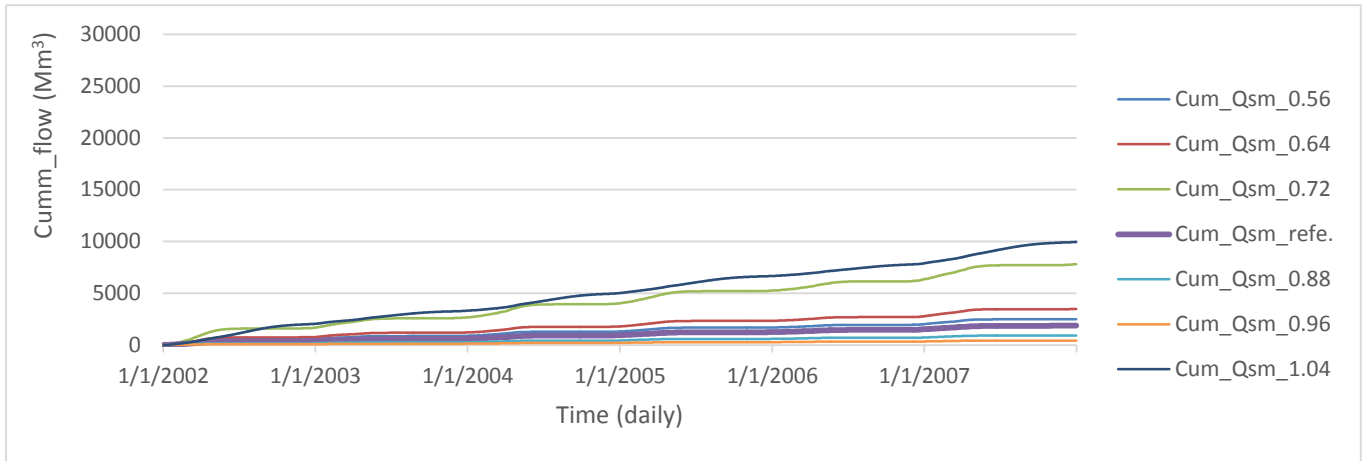


Figure 27: Cumulative streamflow volume (Mm^3) produced by different values of expM model parameter. ExpM (0.96) produces volume $430.01 Mm^3$ which is less than volume produced by expM (0.56) $2501.7 Mm^3$, this indicate sensitivity of that parameter and these results has great effect on the model performance.

Table 8: Indicated different model performance and values of streamflow volume produced by different values of expM parameter value. Model performance indicators NSEC and Bias % are affected by changing parameter value.

expM Parameter value	0.56	0.64	0.72	0.80	0.88	0.96	1.04
NSCE	0.08	-1.41	-18.39	0.63	0.40	-0.08	-16.57
Bias %	32.76	84.93	314.40	-0.01	-51.18	-77.18	428.45
CC	0.80	0.79	0.77	0.81	0.81	0.81	0.32
Cumm_flow volume (Mm^3)	2501.70	3484.75	7808.61	1884.19	919.88	430.01	9957.87

7.3.2. Sensitivity analysis of the CoeR parameter

Table 9: shows how the sensitivity of the CREST model to changes in the CoeR parameter has affected the model performance in terms of model performance indicators NSCE, Bias % and CC. The sensitivity analysis is done by varying the parameter in the selected range of $\pm 30\%$ of the calibrated model parameter value. In this case CoeR is changed while other calibrated model parameter are kept constant as indicated in the table model performance in terms of Bias and NSCE is affected largely.

Figure 28: shows the hydrographs produced when changing the CoeR parameter values, the shapes and the peak of hydrograph both show changes from the original hydrograph. High and low flow components of the hydrograph have been examined to better understand the effects of CoeR parameter, also the runoff volume and statistical indices have been examined as shown in Figure 29 and Table 9 respectively to better understand the effects of CoeR parameter in Mbarali sub-catchment. As shown in Figure 29 it cannot be concluded if higher value produce high flow or low value produce low flow, for example CoeR (1.57) produces flow of $3.49 m^3s^{-1}$, $15.95 m^3s^{-1}$ and $0.003 m^3s^{-1}$. CoeR (1.79) produces $520.51 m^3s^{-1}$, $352.32 m^3s^{-1}$ and $14.88 m^3s^{-1}$. CoeR (2.92) produces $1.28 m^3s^{-1}$, $6.38 m^3s^{-1}$ and $0.001 m^3s^{-1}$ and CoeR (2.69) produces 31.79

m^3s^{-1} , $29.88 \text{ m}^3\text{s}^{-1}$ and $0.17 \text{ m}^3\text{s}^{-1}$ these flow are recorded 2002 during high flow, 2007 high flow season and 2006 low flow period respectively.

In Table 9 the model performance drops drastically when parameters changes either by increases or by reduces. In general, peak flows are much affected when changes CoeR than the low flow, Figure 29 shows the runoff volume produced by low value (1.57) as 953.97 Mm^3 where by the runoff volume produced by high value (2.92) as 393.50 Mm^3 and for value (2.02) produces runoff volume of 11309.18 Mm^3 and value (2.47) produces runoff volume of 22164.38 Mm^3 it can be concluded that there is no clear relationship between CoeR and runoff volume production, higher CoeR can produce low runoff volume or vice versa. CoeR is the conceptual model parameter that is used to convert overland flow speed to channel flow speed, as seen from the hydrographs changes in the parameter values affect the shape and volume of the hydrographs, which in turns affect model performance.

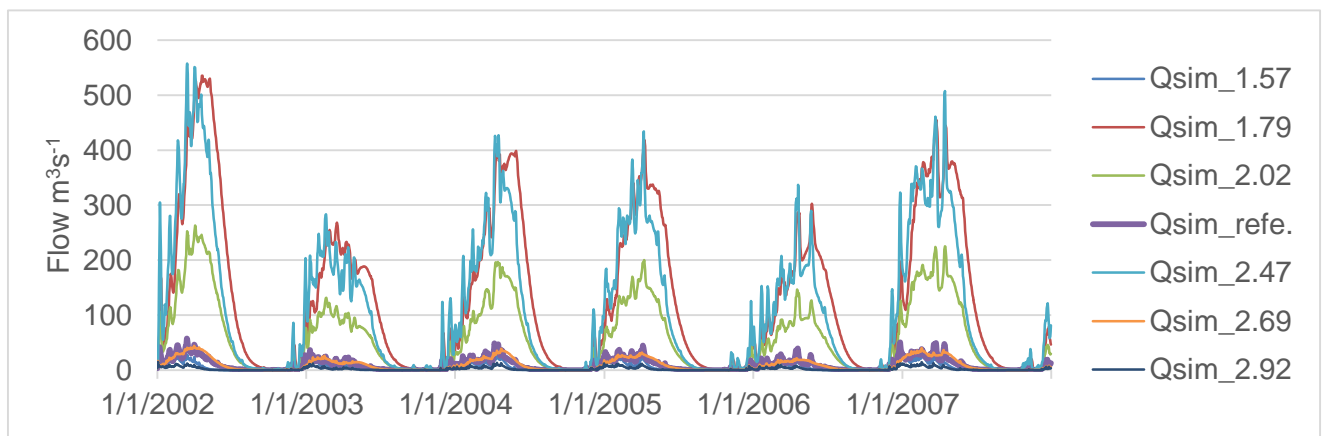


Figure 28: Hydrographs produced by different values of CoeR parameter values. Qsim_refe. Is the calibrated streamflow, which is used as a reference to assess if there is decrease or increase in streamflow when changes the parameter.

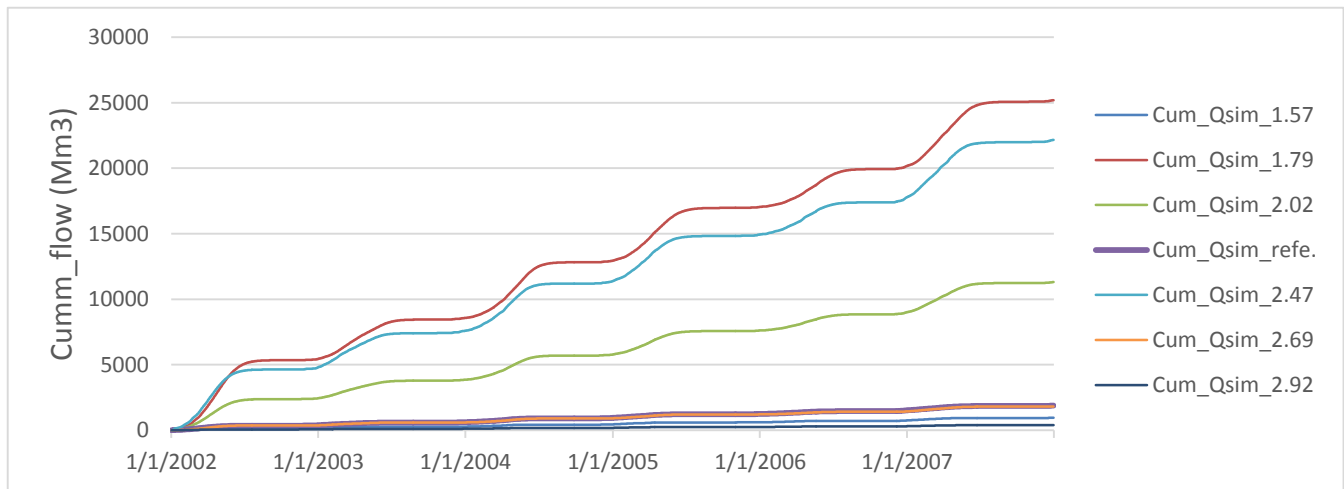


Figure 29: Cumulative streamflow volume (Mm^3) produced by different values of CoeR model parameter. CoeR (2.92) which, is higher than CoeR (1.57) but it produces volume 393.50 Mm^3 which is less than volume 953.97 Mm^3 produced by lower value, this indicate sensitivity of that parameter and these results has great effect on the model performance.

Cumm_Qsim_refe. Is the calibrated streamflow, which is used as a reference to assess if there is decrease or increase in streamflow when changes the parameter.

Table 9: Indicated different model performance and values of streamflow volume produced by different values of CoeR parameter value. Model performance indicators NSEC and Bias % are affected by changing parameter value.

CoeR Parameter value	1.57	1.80	2.02	2.24	2.47	2.69	2.92
NSCE	0.43	-246.95	-42.34	0.63	-196.32	0.47	-0.12
Bias %	-49.37	1236.95	500.16	-0.01	1076.24	-3.61	-79.12
CC	0.81	0.55	0.67	0.81	0.71	0.73	0.81
Cumm_flow volume (Mm ³)	953.97	25192.80	11309.18	1884.19	22164.38	1816.36	393.50

7.3.3. Sensitivity analysis of the CoeS parameter

Table 10: Shows the CREST model performance in terms of statistical indices that is NSEC, Relative Bias % and Correlation Coefficient (CC). In terms of NSCE model performance dropped drastically when the parameter changed to $\pm 20\%$ of the calibrated value, and when parameter value change to -30% of the calibrated valued the model performance in terms of NSCE is reasonably. CREST model performance in terms of Relative Bias (%) dropped drastically when the parameter was changed to $\pm 20\%$ of the calibrated value and in terms of CC the model performance is reasonably when the parameter values are changed to $\pm 30\%$ of the calibrated value.

Figure 30: shows hydrographs as the results of different values of CoeS parameter values. Hydrographs produces high flow during rainy season period and low flow during dry season, shape of hydrographs are affected by different values of CoeS parameter. It is not possible to conclude the relationship between different values of model parameter and streamflow produced, for example low value of CoeS (0.69) produced $4.08 \text{ m}^3\text{s}^{-1}$, $0.003 \text{ m}^3\text{s}^{-1}$ and $16.95 \text{ m}^3\text{s}^{-1}$ while higher value (1.28) produces streamflow of $1.85 \text{ m}^3\text{s}^{-1}$, $0.001 \text{ m}^3\text{s}^{-1}$ and $7.32 \text{ m}^3\text{s}^{-1}$. And CoeS of (0.79) and (1.18) produces flow of $515.81 \text{ m}^3\text{s}^{-1}$, $14.98 \text{ m}^3\text{s}^{-1}$, $347.12 \text{ m}^3\text{s}^{-1}$ and $32.47 \text{ m}^3\text{s}^{-1}$, $0.17 \text{ m}^3\text{s}^{-1}$, $31.99 \text{ m}^3\text{s}^{-1}$ respectively, these flow are recorded from Figure 30 for the period May 2002, September 2006 and March 2007 respectively. These inconsistency of streamflow production is reflected in shape of hydrographs, peak and low flow and in terms of model performance are represented by NSCE as shown in Table 10 NSCE is affected by different value of CoeS parameter values.

Figure 31: Shows the runoff volume produced by CREST model for Mbarali sub-catchment when changing parameter values, low value CoeS (0.69) produces the runoff volume of 1460.22 Mm^3 , which is higher than the runoff volume produced by high value (1.28) it produces 1040.43 Mm^3 , the highest runoff volume is produced CoeS (0.79) 22633.40 Mm^3 while other high values such as (1.18) and (1.09) produce streamflow volume of 2483.12 Mm^3 and 17753.55 Mm^3 respectively. This difference in volume is reflected model performance in terms of relative Bias % as model performance indicator see Table 10.

CoeS is the conceptual model parameter that is used to convert overland flow speed to interflow flow speed, changes in the parameter will affect both peaks and baseflow as well as the volume of the hydrographs.

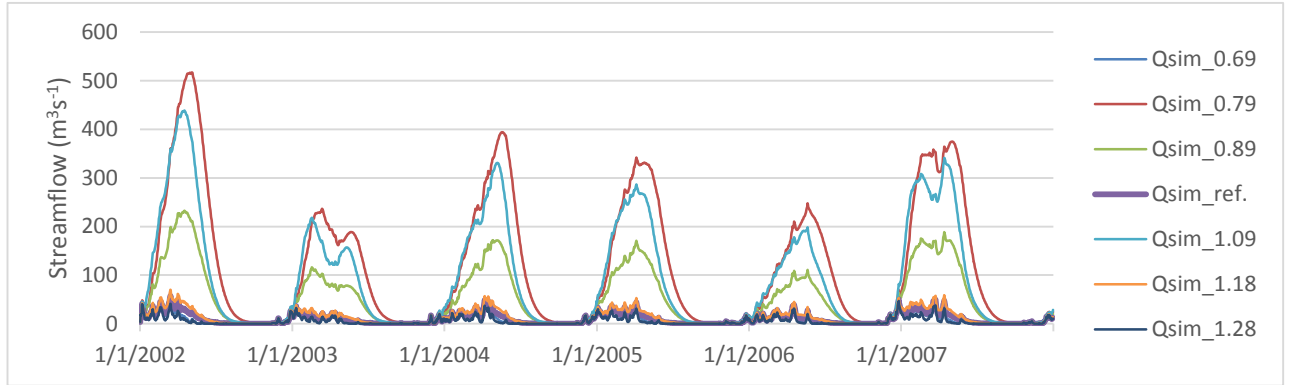


Figure 30: Hydrographs produced by different values of CoeS parameter. There is sharp decrease in recession limb and sharp increase in rising limb produced by parameter (0.79), (0.89) and (1.08). Qsim_ref is the calibrated streamflow, which is used as a reference to assess if there is decrease or increase in streamflow when changes the parameter.

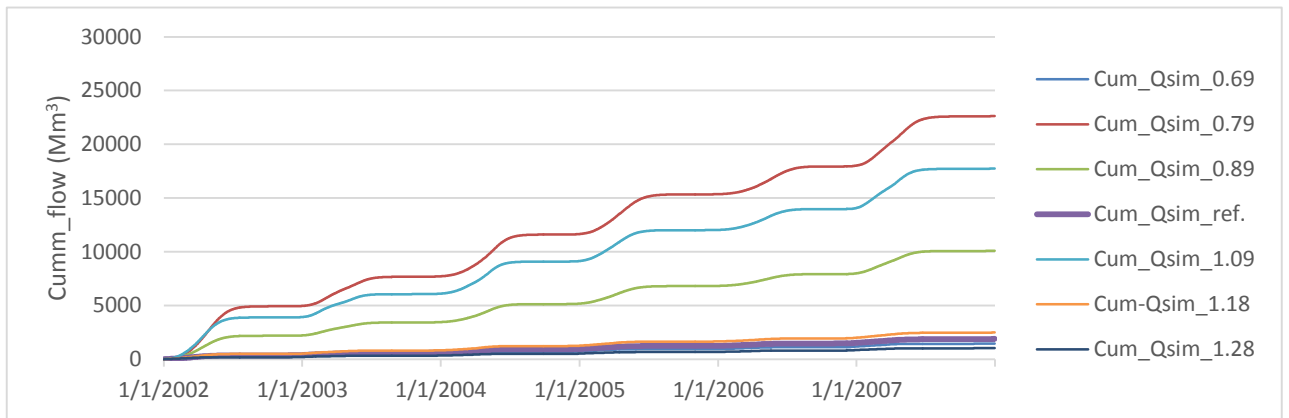


Figure 31: Cumulative streamflow volume (Mm³) produced by different values of CoeS model parameter. Low value (0.69) produce high volume 1460.22 Mm³ compared to high value (1.28) produce low volume 1040.43 Mm³, the highest volume is produced lower value (0.79) 22633.420 Mm³. Cum_Qsim_ref. Is the calibrated streamflow, which is used as a reference to assess if there is decrease or increase in streamflow when changes the parameter.

Table 10: Indicated different model performance and values of streamflow volume produced by different values of CoeS parameter value. Model performance indicators NSEC and Bias % are affected by changing parameter value

CoeS Parameter value	0.69	0.79	0.89	0.99	1.09	1.18	1.28
NSCE	0.58	210.60	-34.61	0.63	-132.92	0.32	0.42
Bias %	-22.51	1101.13	436.03	-0.01	842.16	31.78	-44.79
CC	0.79	0.49	0.62	0.81	0.61	0.80	0.76
Cumm_flow volume (Mm ³)	1460.22	22633.40	10100.63	1884.19	17753.55	2483.12	1040.43

7.4. Impact of hydro-meteorological drivers on the streamflow

The impact of changes in hydro-meteorological drivers can be caused by land use and climate variability and eventually it can cause impact on the streamflow of the Mbarali sub-catchment and this is done by perturbing parameters derived from the CREST model parameter set. Two parameters that will be discussed are RainFact and KE.

RainFact is the multiplier on the precipitation field perturbing the precipitation reaching the soil. Precipitation is forced to the CREST model, the impact of RainFact on modelling results are related to climate variability i.e. 'what is the impact of climate variability on the rainfall? We made an assumption that if there is climate change two things can happen in rainfall, either there is increase in rainfall or there is decrease in rainfall. The assumption is that rainfall increase or decrease in the order of ($\pm 2\%$, $\pm 4\%$, $\pm 6\%$, $\pm 8\%$, $\pm 10\%$ and $\pm 12\%$). To reflect this increase or decrease of rainfall to the streamflow, CREST model is forced to run under different values of RainFact i.e. 'the parameters are changed in the order of ($\pm 2\%$, $\pm 4\%$, $\pm 6\%$, $\pm 8\%$, $\pm 10\%$ and $\pm 12\%$), the simulated results are compared with the calibrated result which is used as a reference. Figure 32 shows the impact of change in rainfall on the streamflow of the Mbarali sub-catchment, it shows that when RainFact increase there is also increase in streamflow and when it decrease there is also decrease on the streamflow as expected.

Second hydro-meteorological parameter used to investigate the impact on the streamflow is the KE, which is derived from CREST model parameter sets. KE is the factor used to convert potential evapotranspiration to actual evapotranspiration, is used to assess its impacts on the Potential Evapotranspiration and subsequently to the streamflow. The impact of the parameter on modelling results are related to land use change or climate variability i.e. what is the impact of land use change or climate variability on the evapotranspiration?, we made an assumption that, if there is land use change or climate variability two things can happen on evapotranspiration, either there is increase or decrease in evapotranspiration. If evapotranspiration increase or decrease in the order of ($\pm 2\%$, $\pm 4\%$, $\pm 6\%$, $\pm 8\%$, $\pm 10\%$ and $\pm 12\%$), to reflect this increase or decrease of evapotranspiration to the CREST model we run CREST model under different values of KE i.e. parameter value is changed in the order of ($\pm 2\%$, $\pm 4\%$, $\pm 6\%$, $\pm 8\%$, $\pm 10\%$ and $\pm 12\%$), the simulated results are compared with the calibrated results which is used as a benchmark. Figure 35 shows the impact of change in evapotranspiration on the streamflow of the Mbarali sub-catchment, it shows that when KE increase there is decrease on the streamflow and when it decrease there is increase on the streamflow as presumed.

Analysis for the impact of rainfall or evapotranspiration to the streamflow is done for 2002-2007, this period is used as the calibration period. In that period, the dry and wet year based on the hydrological year are selected for further analysis. During the calibration period, 2002/2003 is found to be the dry year while 2006/2007 is found to be the average year, there was no wet year during that calibration period we decided to take average year to represent wet year.

7.4.1. Impact of rainfall on the streamflow

Case one: for dry year 2002/03 we took hydrological year so as both high and low flow period can be captured, extremes values of RainFact -12% and +12% are chosen based on the assumption that, for RainFact of -12% there is decrease in rainfall by -12% due to climate variability and for RainFact of +12% there is increase in rainfall by +12% due to climate variability, Figure 33-A is the hydrographs produced by upper and lower values on RainFact for dry year. Runoff volume for the lower and upper values are 189.9 Mm³ and 284.69 Mm³ respectively while the runoff volume from the calibrated RainFact which is used as reference is 236.35 Mm³ this results are produced by Figure 34-A. This results show that when we decrease

the rainfall the runoff volume decreased by 19.64% and when we increased the rainfall the runoff volume increase by 20.44%, these results indicates that increase rainfall results to an increase on the streamflow and decrease the parameter has also cause decrease on the streamflow on the Mbarali sub-catchment.

For the average hydrological year 2006/07 the rainfall is increase and decrease by +12% and -12% respectively, Figure 33-B is the hydrographs resulted from the extreme values of RainFact. When the climate change cause decrease in rainfall the streamflow decreased and when the climate change increase the rainfall the streamflow increase. Further analysis is done by considering the extreme values of RainFact that is the Lowe and Upper values, runoff volume resulted from upper and lower values of RainFact are 468.22 Mm³ and 322.16 Mm³ respectively while the calibrated runoff volume is 394.65 Mm³. This shows that runoff volume decrease by 18.37% when we made an assumption that there is decrease in rainfall and it has increased by 18.64% when we made an assumption that there is increase in rainfall, these results are produced by Figure 34-B.

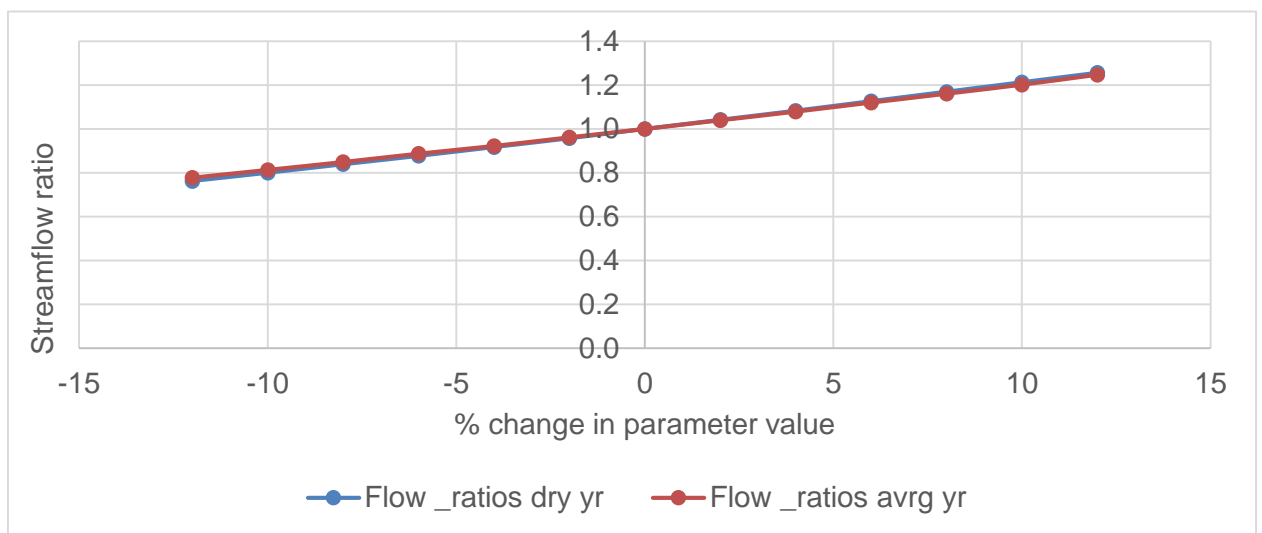


Figure 32: Graph of the streamflow (runoff ratio) and % change in RainFact parameter values. Graphs for the dry year 2002/03 and average year 2006/07. As shown in the graph when there is increase in RainFact result an increase in streamflow. And when decrease RainFact also there is decrease in the Streamflow both dry year and average year, dry year shown by blue line and average year shown by red line.

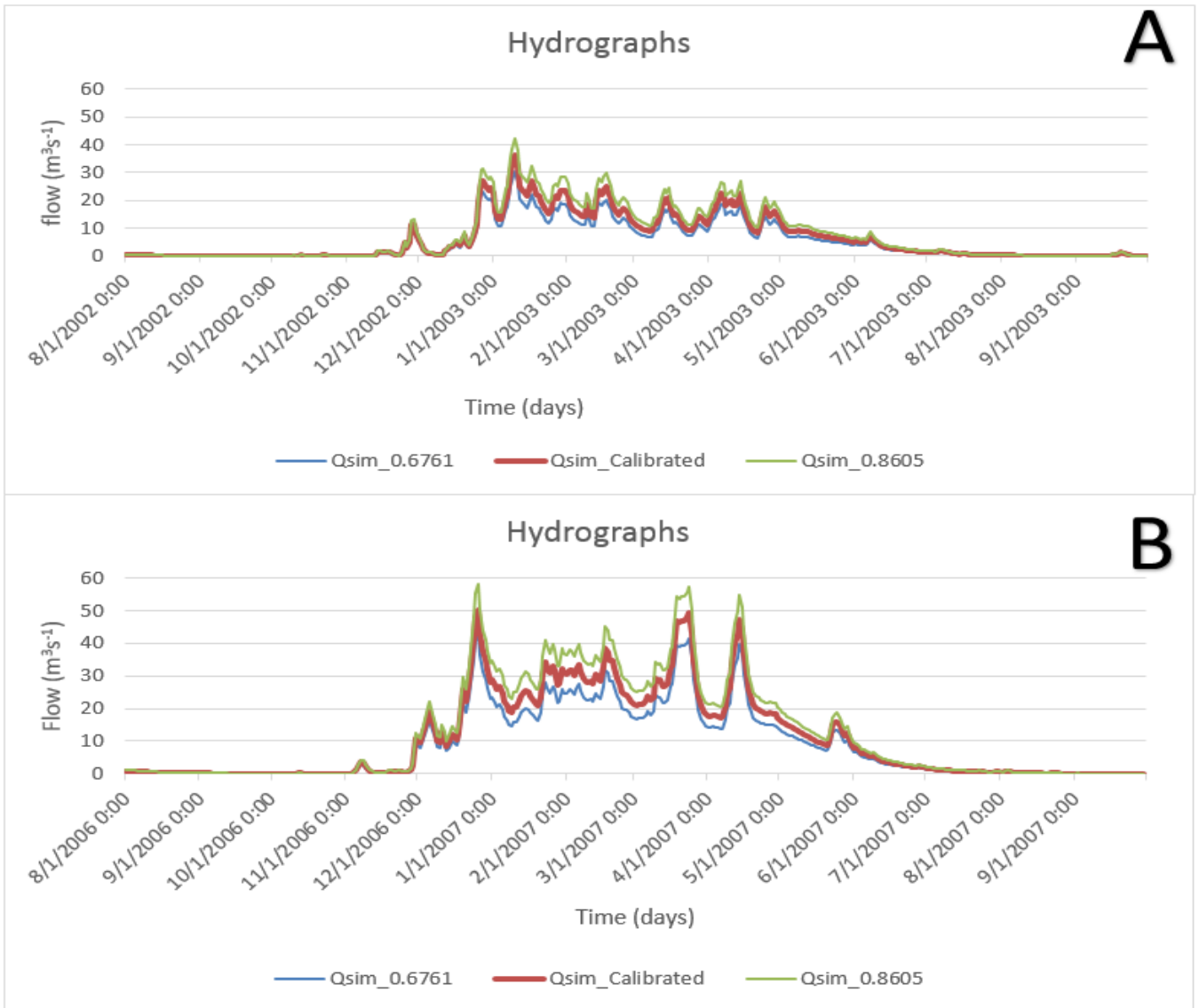


Figure 33: Hydrographs for lower and upper value of RainFact for Dry year (A) and average year (B). As shown lower RainFact produced low runoff indicated as (Qsim_0.6761) and upper RainFact produced higher runoff indicated as (Qsim_0.8605) compared to calibrated runoff indicated as (Qsim_calibrated).

Qsim_calibrated is the calibrated streamflow, which is used as a reference to make comparison if there is increase or decrease in streamflow when the rainfall is changing.

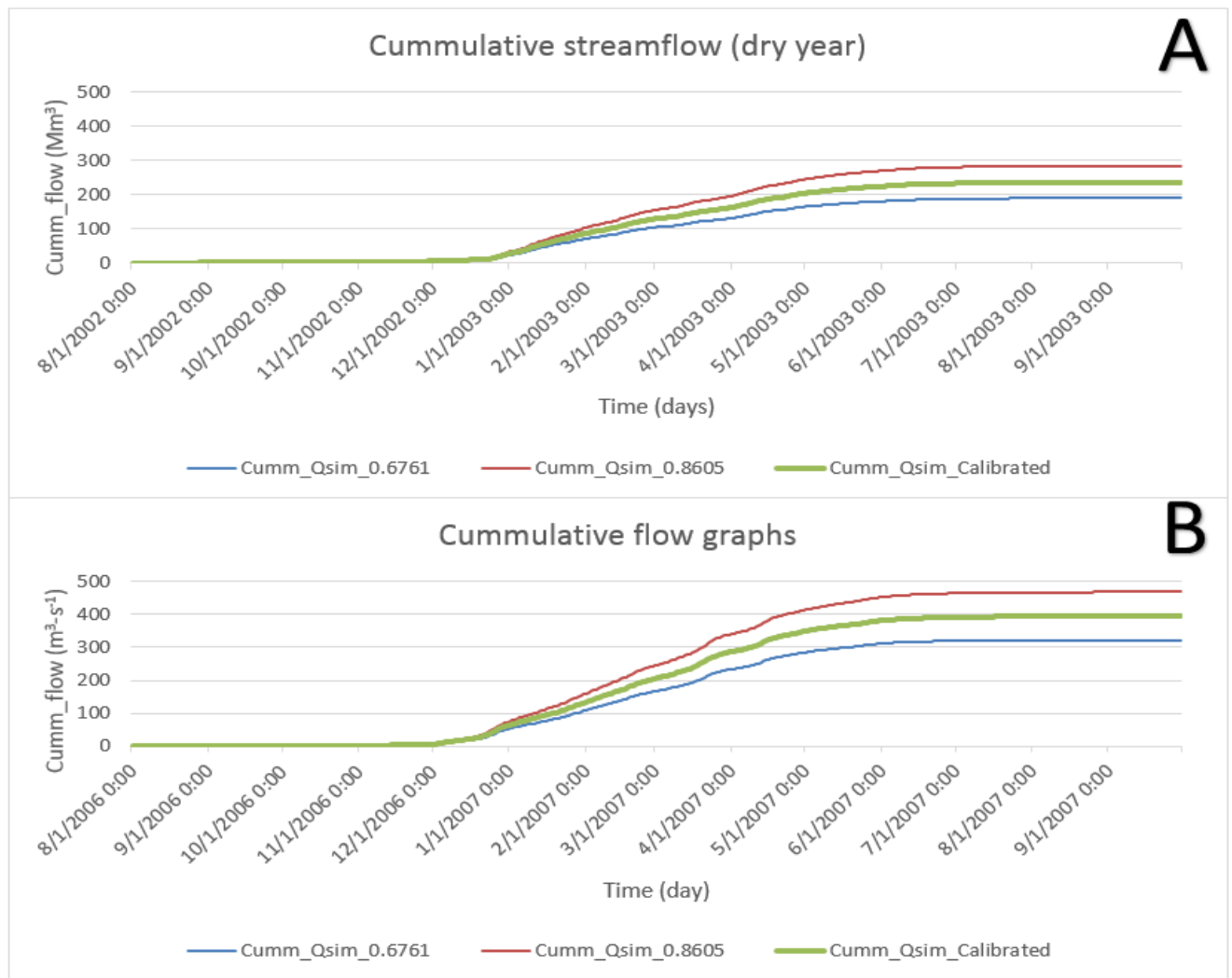


Figure 34: Shows the Cumulative runoff produced by upper and lower values of RainFact, lower value indicated as (Cumm_Qsim_0.6761) produces low cumulative runoff volume, while upper value indicated as (Cumm_Qsim_0.8605) produces higher cumulative runoff volume compared to calibrated cumulative shown as (Cumm_Qsim_calibrated) runoff volume. A shows dry year, while B indicates average year.

7.4.2. Impact of evapotranspiration on the streamflow

Case two: for dry year 2002/03 we took hydrological year so as both high and low flow period can be captured, extreme values of KE -12% and +12% are chosen based on the assumption that, for KE of -12% there is decrease in evapotranspiration by -12% this can be caused by land use change or climate variability and for KE of +12% there is increase in evapotranspiration by +12% as a results of land use change or climate variability, Figure 36-A shows the hydrographs produces by the extreme values of KE for dry year. Runoff volume for the lower and upper values are 251.98 Mm³ and 222.10 Mm³ respectively, while the runoff volume from the calibrated value of KE which is used as reference is 236.35 Mm³. This results show that when we decrease the evapotranspiration the runoff volume increase by 6.61% and when we increased evapotranspiration the runoff volume decreased by 6.03%, these analysis show that reduction of evapotranspiration cause increase on the streamflow of the Mbarali sub-catchment while increasing the

evapotranspiration decrease on the streamflow, Figure 37-A shows total volume produced by upper and lower value of KE for the period of 2002/03 dry year.

For the average hydrological year 2006/07 the evapotranspiration is increased and decreased by +12% and -12% respectively, Figure 36-B shows the hydrographs produces by the extreme values of KE for average year. Further analysis is done by considering the extreme values of KE that is the lower and upper values, runoff volume resulted from upper and lower values of KE are 374.34 M m³ and 416.08 M m³ respectively while the calibrated runoff volume is 394.65 Mm³. This shows that the runoff volume increase by 5.43% when evapotranspiration decrease by -12% and it has decrease by 5.14% when evapotranspiration increase by 12%. Figure 37-B shows total volume produced by upper and lower value of KE for the period of 2006/07 average year.

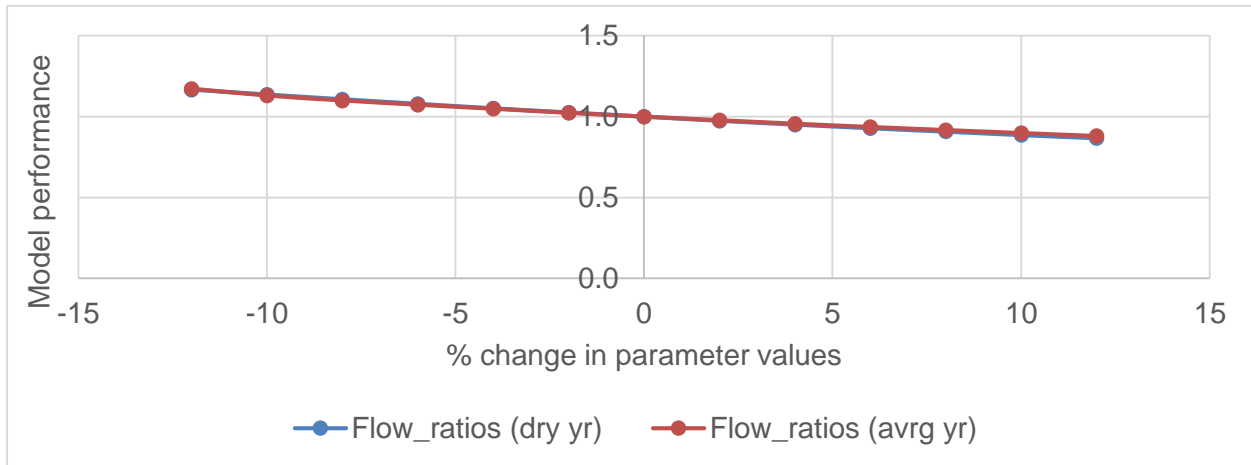


Figure 35: Graph of the streamflow (runoff ratio) versus % change in KE parameter values. Graphs for the dry year 2002/03 and average year 2006/07. As shown in the graph when there is increase in KE result decrease in streamflow. And when KE decrease there is increase in the streamflow both dry year and average year, dry year shown by blue line and average year shown by red line.

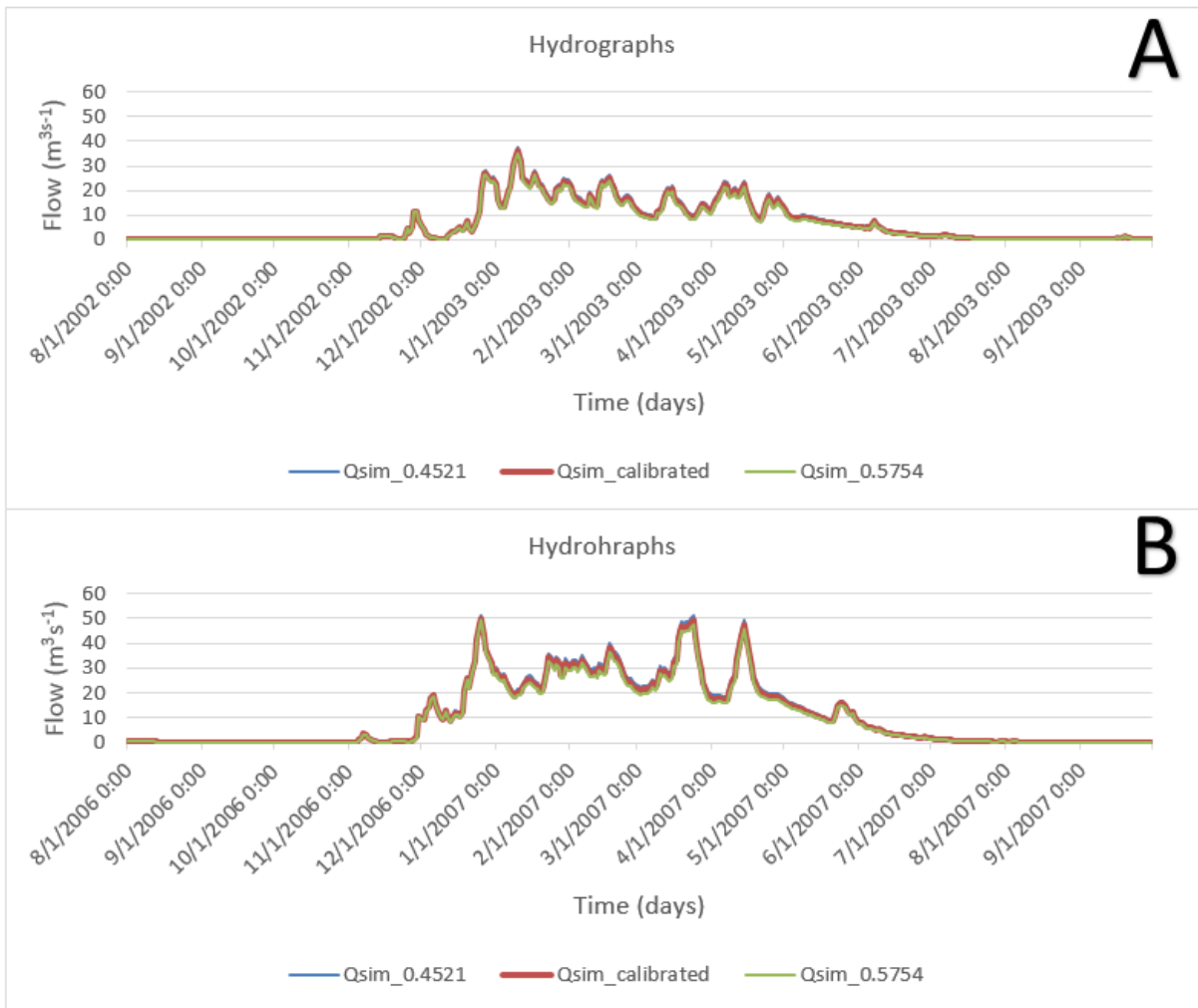


Figure 36: Hydrographs for lower and upper value of KE, A for Dry year and B is for average year. As shown lower KE indicated as (Qsim_0.4521) produced high runoff and upper KE indicated as (Qsim_0.5754) produced low runoff compared to calibrated runoff shown as (Qsim_calibrated).

Qsim_calibrated is the calibrated streamflow, which is used as a reference to make comparison if there is increase or decrease in streamflow when the rainfall is changing.

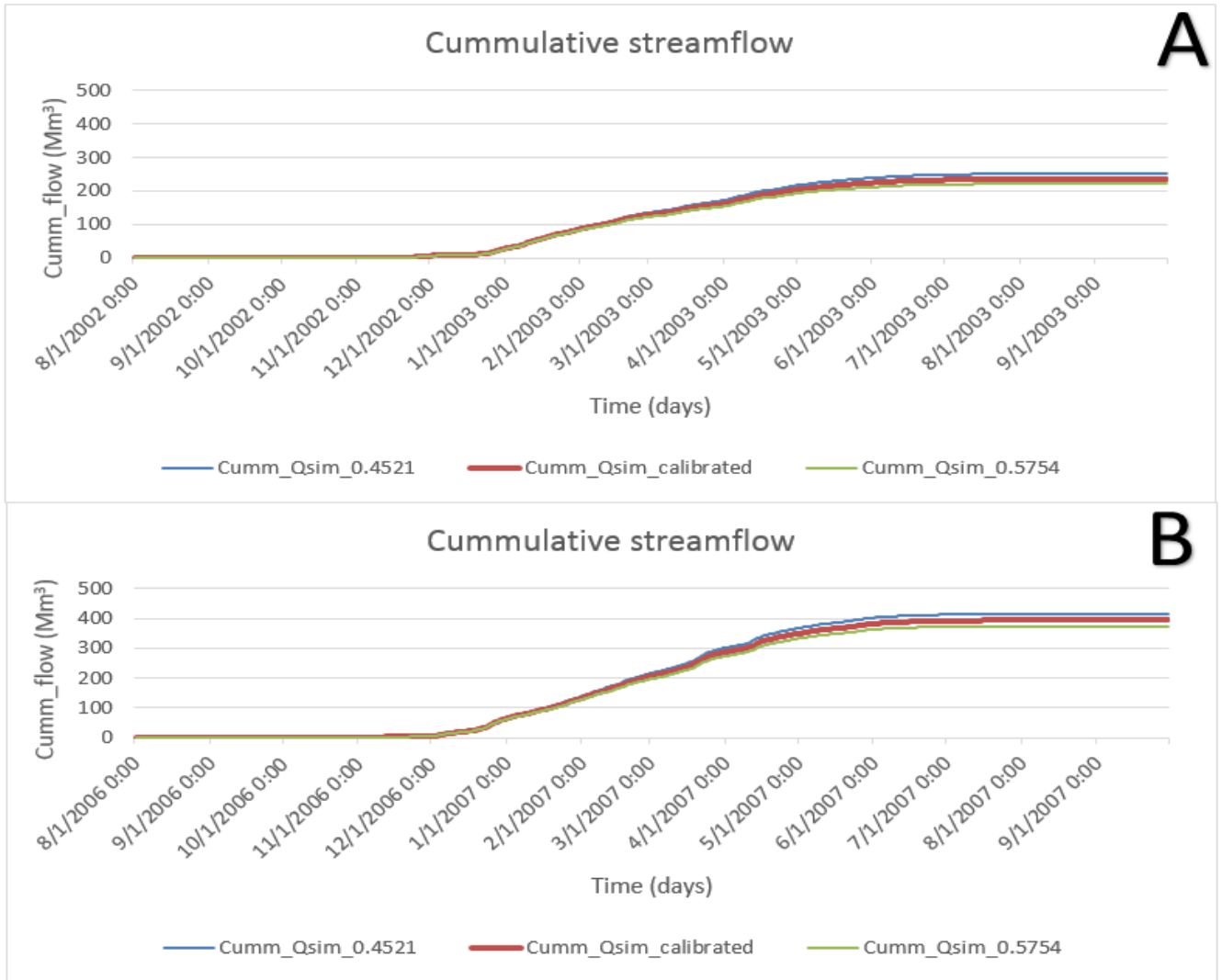


Figure 37: Shows the Cumulative runoff produced by upper and lower values of KE, lower value (Cumm_Qsim_0.4521) produced high cumulative runoff volume, while upper value (Cumm_Qsim_0.5754) produced low cumulative runoff volume compared to calibrated cumulative runoff volume (Cumm_Qsim_calibrated). This graphs A is for dry year and B is for average year.

8. CONCLUSIONS AND RECOMMENDATIONS

8.1. Conclusions

The objective of this research is to assess the impact of hydro-meteorological drivers on the streamflow of the Mbarali sub-catchment across a twelve year period (2001-2012). This will be achieved using the grid-based Coupled Routing Excess Storage (CREST) distributed hydrological model (Wang et al., 2011b) driven by atmospheric forcings derived from satellite data. The atmospheric forcings are: TRMM for rainfall and FEWSNET for potential evapotranspiration.

Mbarali sub-catchment (1,553 km²) is the part of the Usangu basin, which is the main tributary of the Great Ruaha River in Tanzania (GRR). The importance of the GRR River in Tanzania economy is built on the fact that almost 51% of the country electricity is produced from the two hydropower plants namely; Mtera and Kidatu dams situated downstream of the Usangu catchment and 30 % of the country rice is produced from the Usangu basin. Furthermore, Ruaha National park placed downstream of the catchment plays a significant role in tourist sector (Shu & Villhth, 2012). This research act as pilot study for future utilization of remote sensing data in the Usangu catchment and Tanzania River basins as whole.

Other geo-information products used for this study, the details for the product is given by Xue et al.(2013b), including topographic data, which are; (DEM, FAC and FDR derived from HydroSHEDS). Digital Elevation Model (DEM) for defining the elevation, Flow Accumulation map (FAC) for deriving the number of pixels that naturally drains into catchment outlets, Flow Direction map (FDR) for defining the natural drainage direction for every pixels in a DEM, Landcover map derived from SEVIR Eastern and Southern Africa is used for defining the water mean capacity (WM) parameter in the CREST model and for Mbarali sub-catchment is found to be 88-124 mm and Soil map obtained from Harmonized World Soil Datasets (HWSD) is used for deriving saturated soil hydraulic conductivity (K_{sat}), which is model parameter and for our study area is 146-266 mmd⁻¹. The ArcGIS and Integrated Land and Water Information System (ILWIS) tool played a dominant role for downloading and converting data to formats, which are used in the CREST model. This research shows that integrating remote sensing together with GIS and ILWIS is significant process for data handling and preparation for the distributed hydrological model.

The calibration of the CREST model is significant assignment. It involves adjusting model parameters that is difficult to be obtained in field by exact measurements, the tuning of the model parameters aiming at simulating the model results in such a way that, observed and measured become equal, by minimizing the difference between the two variables. In the calibration process that is done in our research, the automatic calibration is implemented and the results show that the baseflow is not well simulated by CREST model, also peak flow are not fully captured after calibration, and runoff volume are well captured during calibration interval as the simulated and observed volume are 1884.19 Mm³ and 1884.35 Mm³ respectively. But poorly simulated during validation duration resulting in difference of 638.52 Mm³ between simulated and observed as the simulated is 1413.44 Mm³, while observed is 2051.95 Mm³

Runoff simulation performed with the distributed hydrological model are satisfactorily corresponding to the streamflow measured in the Mbarali River at Igawa station on a daily basis. The performance assessed based on Nash-Sutcliffe model efficiency (NSCE), Relative Bias (Bias %) and Correlation of Coefficient (CC) performance indices, this indices are explained by Xue, (2012). Which are respectively found to be 0.63, -0.01% and 0.81 for the calibration time (2002-2007). 0.53, -31.12% and 0.78 respectively for the entire validation interval (2008-2012).

To further provide confidence in the calibrated model parameters a sensitivity analysis has been performed. We found three sensitive model parameters in the Mbarali sub-catchment (expM, CoeR and CoeS). The overland flow speed exponent (expM) being the parameter with high sensitivity in magnitude of 43.6727 relative sensitivity, followed by (CoeS) parameter that is used to convert overland flow speed to interflow speed with relative sensitivity of 11.5017, the third parameter with relative sensitivity of 5.8871 is (CoeR), which is the parameter that is used to convert overland flow speed to channel flow speed, definition of these parameters are given by Xue, (2012).

With the calibrated model parameters as reference, the impact of hydro-meteorological drivers on the streamflow of the Mbarali sub-catchment is assessed using the distributed hydrological model. This has been done by perturbing the RainFact and KE parameters in the hydrological model, RainFact is the multiplier on the precipitation field (Xue, 2012), which is used as a determinant factor to determined precipitation reaching the soil, while KE is the factor used to convert potential evapotranspiration to local actual evaporation (Xue, 2012), and this factor is used to determine the amount of evapotranspiration in a particular area. This analysis is done for the entire calibration period, further is analysis is done for two selected periods, which are dry year and average year. Within the calibration period 2002/03 is found to be dry year and 2006/07 average year, there is no wet year for the calibration period selected.

As expected, it is found that linearly scaling in rainfall value has positive and negative impact on the streamflow. For example for dry year 2002/03 a decrease in the rainfall of -12 % reduces the runoff volume by 19.64 %, whereas the same increase in rainfall causes an increase in runoff volume by 20.44 %. For average year 2006/07 increase rainfall to +12% resulted in the runoff volume increases by 18.64% and when decreases rainfall by the same value the runoff volume reduces by 18.37 %.

Accordingly, it is found that linearly scaling evapotranspiration has negative and positive impact on the streamflow for both average and dry year. For example for dry year 2002/03 decrease evapotranspiration to -12% increase the runoff volume by 6.61%, and increase evapotranspiration by the same value, decrease runoff volume by 6.03%. For average year 2006/07 increase evapotranspiration to +12% the runoff volume decrease by 5.14% and decrease evapotranspiration by the same value runoff volume increases by 5.43 %.

An important advantage of spatially distributed hydrological model, such as CREST is that it not only provides estimates of streamflow at the catchment outlet, but also at any location as presented by a cell or grid within the given catchment (Wang et al., 2011c). These spatially distributed streamflow are useful in water allocation because it will help water managers to know amount of water available at location within the catchment

During the calibration and validation period the CREST model underestimate the baseflow for the whole period, this can be caused by the routing method used by the CREST hydrological model. The Coupled Routing and Excess Storage (CREST) version 2.0 hydrological model use Jumped Linear Routing (JLR) as routing method during routing process, the drawback of this technique is that when it is applied where the grid cell is large and the modelling time is small, it will lead to the underestimation of the streamflow this explanation of given by Xue & Hong. (2015) in their user manual. In this research we used 1 km as grid resolution for each grid cell, to overcome the problem of underestimation of the streamflow CREST 2.1V is developed, which use another routing method called Continuous Linear Routing (CLR), the newly developed version came at the time when this research was already written so the new version can be used in other study in the same area to improve modelling results.

8.2. Recommendations

Form the findings of this research, the following recommendations can be made.

Further studies need to be carried out for the entire area of the Usangu catchment using satellite product with highest spatial and temporal resolution such as CHIRPS, which has 5 km spatial resolution available daily temporal resolution and CMORPH, which has a spatial resolution of 8 km and 30 minutes as temporal resolution. Also the study can include topographic data with high spatial resolution such as Digital Elevation Model of 30 or 90 m spatial resolution.

The main advantage of CREST distributed hydrological model is that it requires little input data, and the model performance is quite good, for the details of the results can see the work done by Xue et al. (2013b) and Wang et al. (2011b). So we recommend that the model should integrate the Landcover aspect so that further studies such as effects of landcover on runoff regime can be done using CREST model. Application of CREST model for the streamflow simulation in the Mbarali sub-catchment is appropriate since the model requires few input variable for model set-up. The model can be used for other ungauged basins in Tanzania.

As discussed in the problem definition that many studies indicate that there is decrease in the streamflow of the Usangu catchment due to increase in water use, because there is a lack of data in the catchment and using this study satellite data has shown that it can be used in data scarce area. So a detailed study, which will incorporate water use abstraction and using satellite products need to be conducted in the whole of the Usangu catchment since this research concentrated only on part of the Usangu catchment, which is the Mbarali sub-catchment.

LIST OF REFERENCES

- Al, J. E. T. (2004). CMORPH : A Method that Produces Global Precipitation Estimates from Passive Microwave and Infrared Data at High Spatial and Temporal Resolution.
- Allen, R. G. (2006). FAO Irrigation and Drainage Paper Crop by, (56).
- Anornu, G. K., & Kortatsi, B. K. (2012). Comparability Studies of High and Low Resolution Digital Elevation Models for Watershed Delineation in the Tropics : Case of Densu River Basin of Ghana, *1*(1), 9–14.
- Bahremand, a., & De Smedt, F. (2007). Distributed Hydrological Modeling and Sensitivity Analysis in Torysa Watershed, Slovakia. *Water Resources Management*, *22*(3), 393–408. doi:10.1007/s11269-007-9168-x
- Bahremand, A., & de Smedt, F. (2010). Predictive Analysis and Simulation Uncertainty of a Distributed Hydrological Model. *Water Resources Management*, *24*, 2869–2880. doi:10.1007/s11269-010-9584-1
- Bahremand, A., & Smedt, F. D. E. (2006). Parameter sensitivity and uncertainty analysis of the WetSpa model using PEST (Vol. 2006, pp. 26–35).
- Bao, Z., Liu, J., Zhang, J., Fu, G., Wang, G., Yan, X., ... Shang, M. (2011). Estimation of baseflow parameters of variable infiltration capacity model with soil and topography properties for predictions in ungauged basins. *Hydrology and Earth System Sciences Discussions*, *8*, 7017–7053. doi:10.5194/hessd-8-7017-2011
- Behrangi, A., Khakbaz, B., Jaw, T. C., AghaKouchak, A., Hsu, K., & Sorooshian, S. (2011). Hydrologic evaluation of satellite precipitation products over a mid-size basin. *Journal of Hydrology*, *397*(3-4), 225–237. doi:10.1016/j.jhydrol.2010.11.043
- Beven, K. J., Warren, R., & Zaoui, J. (1980). SHE: towards a methodology for physically-based. *IAHS Publ.*, *129*(129), 133–137.
- Birhanu, B. Z. (2009). Hydrological modeling of the Kihansi river catchment in South Central Tanzania using SWAT model, *1*(1), 1–10.
- Bloschl, G., & Sivapalan, M. (1995). Scale issued in hydrological modeling : A REVIEW. *Hydrological Processes*, *9*(September 1994), 251–290.
- Boyle, D. P., Gupta, H. V., & Sorooshian, S. (2000). Toward improved calibration of hydrologic models: Combining the strengths of manual and automatic methods. *Water Resources Research*, *36*(12), 3663–3674. doi:10.1029/2000WR900207
- Cho, S. (2002). Sensitivity consideration when modeling hydrological processes with Digital Elevation Model. *American Water Resources Association*, *37*(4), 931–934.
- Cohen Liechti, T., Matos, J. P., Ferràs Segura, D., Boillat, J.-L., & Schleiss, A. J. (2014). Hydrological modelling of the Zambezi River Basin taking into account floodplain behaviour by a modified reservoir approach. *International Journal of River Basin Management*, *12*(1), 29–41. doi:10.1080/15715124.2014.880707
- Crew, O., Vehicle, E., Summary, M. P., & Module, C. (2010). NASA facts.

- Dessu, S. B., & Melesse, A. M. (2013). Evaluation and Comparison of Satellite and GCM Rainfall Estimates for the Mara River. *Springer*, (April), 29–46. doi:10.1007/698
- Doherty, J. (2004). *HESM Instructional Materials for Training Purposes Only Parameter ESTimation Software* (pp. 1–72).
- Efstratiadis, A., & Koutsoyiannis, D. (2010). One decade of multi-objective calibration approaches in hydrological modelling: a review. *Hydrological Sciences Journal*, 55(January 2015), 58–78. doi:10.1080/02626660903526292
- Herman, J. D., Kollat, J. B., Reed, P. M., & Wagener, T. (2013). Technical Note: Method of Morris effectively reduces the computational demands of global sensitivity analysis for distributed watershed models. *Hydrology and Earth System Sciences*, 17(7), 2893–2903. doi:10.5194/hess-17-2893-2013
- Huffman, G. J., Bolvin, D. T., Nelkin, E. J., Wolff, D. B., Adler, R. F., Gu, G., ... Stocker, E. F. (2007). The TRMM Multisatellite Precipitation Analysis (TMPA): Quasi-Global, Multiyear, Combined-Sensor Precipitation Estimates at Fine Scales. *Journal of Hydrometeorology*, 8(1), 38–55. doi:10.1175/JHM560.1
- Immerzeel, W. W., & Droogers, P. (2008). Calibration of a distributed hydrological model based on satellite evapotranspiration. *Journal of Hydrology*, 349(3-4), 411–424. doi:10.1016/j.jhydrol.2007.11.017
- Irvine, U. C. (2004). Precipitation Estimation from Remotely Sensed Imagery using an Artificial Neural Network Cloud Classification System.
- J.Huffman, G. (2007). Algorithm 3B42: TRMM Merged HQ / Infrared Precipitation, 18–20.
- Jeniffer, K., Su, Z., Woldai, T., & Maathuis, B. (2010). Estimation of spatial–temporal rainfall distribution using remote sensing techniques: A case study of Makanya catchment, Tanzania. *International Journal of Applied Earth Observation and Geoinformation*, 12, S90–S99. doi:10.1016/j.jag.2009.10.003
- Jiang, S., Ren, L., Hong, Y., Yang, X., Ma, M., Zhang, Y., & Yuan, F. (2014). Improvement of Multi-Satellite Real-Time Precipitation Products for Ensemble Streamflow Simulation in a Middle Latitude Basin in South China. *Water Resources Management*, 28(8), 2259–2278. doi:10.1007/s11269-014-0612-4
- Karlsson, J. M., & Arnberg, W. (2011). Quality analysis of SRTM and HYDRO1K: a case study of flood inundation in Mozambique. *International Journal of Remote Sensing*, 32(1), 267–285. doi:10.1080/01431160903464112
- Kashaigili, J. J. (2008). Impacts of land-use and land-cover changes on flow regimes of the Usangu wetland and the Great Ruaha River, Tanzania. *Physics and Chemistry of the Earth, Parts A/B/C*, 33(8-13), 640–647. doi:10.1016/j.pce.2008.06.014
- Kashaigili, J. J., Mbilinyi, B. P., McCartney, M., & Mwanuzi, F. L. (2006). Dynamics of Usangu plains wetlands: Use of remote sensing and GIS as management decision tools. *Physics and Chemistry of the Earth, Parts A/B/C*, 31(15-16), 967–975. doi:10.1016/j.pce.2006.08.007
- Khan, S. I., Adhikari, P., Hong, Y., Vergara, H., Adler, R. F., Policelli, F., ... Okello, L. (2011). Hydroclimatology of Lake Victoria region using hydrologic model and satellite remote sensing data. *Hydrology and Earth System Sciences*, 15, 107–117. doi:10.5194/hess-15-107-2011

- Khan, S. I., Adhikari, P., Hong, Y., Vergara, H., F Adler, R., Policelli, F., ... Okello, L. (2011). Hydroclimatology of Lake Victoria region using hydrologic model and satellite remote sensing data. *Hydrology and Earth System Sciences*, 15(1), 107–117. doi:10.5194/hess-15-107-2011
- Khan, S. I., Hong, Y., Vergara, H. J., Gourley, J. J., Robert Brakenridge, G., De Groeve, T., ... Yong, B. (2012). Microwave satellite data for hydrologic modeling in ungauged basins. *IEEE Geoscience and Remote Sensing Letters*, 9(4), 663–667. doi:10.1109/LGRS.2011.2177807
- Khan, S. I., Hong, Y., Wang, J., Yilmaz, K. K., Gourley, J. J., & Adler, R. F. (2009). Satellite Remote Sensing and Hydrological Modeling for Flood Inundation Mapping in Lake Victoria Basin : Implications for Hydrologic Prediction in Ungauged Basins, 1–23.
- Khan, S. I., Vergara, H. J., Gourley, J. J., Brakenridge, G. R., De Groeve, T., Flamig, Z. L., & Policelli, F. (2012). Microwave Satellite Data for Hydrologic Modeling in Ungauged Basins. *IEEE Geoscience and Remote Sensing Letters*, 9(4), 663–667. doi:10.1109/LGRS.2011.2177807
- Kim, J., & Hogue, T. S. (2008a). Evaluation of a MODIS-Based Potential Evapotranspiration Product at the Point Scale. *Journal of Hydrometeorology*, 9(3), 444–460. doi:10.1175/2007JHM902.1
- Kim, J., & Hogue, T. S. (2008b). Evaluation of a MODIS-Based Potential Evapotranspiration Product at the Point Scale. *Journal of Hydrometeorology*, 9(April 2000), 444–460. doi:10.1175/2007JHM902.1
- Kim, S. M., Benham, B. L., Brannan, K. M., Zeckoski, R. W., & Doherty, J. (2007). Comparison of hydrologic calibration of HSPF using automatic and manual methods. *Water Resources Research*, 43(1), n/a–n/a. doi:10.1029/2006WR004883
- Kubota, T., Shige, S., Hashizume, H., Aonashi, K., Takahashi, N., Seto, S., ... Okamoto, K. (2007). Global Precipitation Map Using Satellite-Borne Microwave Radiometers by the GSMaP Project: Production and Validation. *IEEE Transactions on Geoscience and Remote Sensing*, 45(7), 2259–2275. doi:10.1109/TGRS.2007.895337
- Lawrence, D., Haddeland, I., & Langsholt, E. (2009). *Calibration of HBV hydrological models using PEST parameter estimation*.
- Lehner, B., Verdin, K., & Jarvis, A. (2006a). HydroSHEDS, 1–27.
- Lehner, B., Verdin, K., & Jarvis, A. (2006b). *HydroSHEDS* (pp. 1–27).
- Li, X., Zhang, Q., & Li, Y. (2011). Validation the applicability of satellite based rainfall data for runoff simulation and water balance analysis. *2011 International Symposium on Water Resource and Environmental Protection*, 494–496. doi:10.1109/ISWREP.2011.5893051
- Lijalem Zeray Abraham, Jackson Roehrig, D. A. C. (2007). Calibration and Validation of SWAT Hydrological Model for Meki Watershed, Ethiopia (pp. 1–5).
- Lin, K., Lian, Y., & He, Y. (2014). Effect of Baseflow Separation on Uncertainty of Hydrological Modeling in the Xinanjiang Model. *Mathematical Problems in Engineering*, 2014, 1–9. doi:10.1155/2014/985054
- Liu, J., Duan, Z., Jiang, J., & Zhu, A. (2014). Evaluation of Three Satellite Precipitation Products TRMM 3B42 , CMORPH , and PERSIANN over a Subtropical Watershed in China. *Advances in Meteorology*.

- Loukas, A., Vasilades, L., Domenikiotis, C., & Dalezios, N. R. (2005). Basin-wide actual evapotranspiration estimation using NOAA/AVHRR satellite data. *Physics and Chemistry of the Earth, Parts A/B/C*, 30(1-3), 69–79. doi:10.1016/j.pce.2004.08.023
- Mao, Y., Ye, a., Xu, J., Ma, F., Deng, X., Miao, C., ... Di, Z. (2014). An advanced distributed automated extraction of drainage network model on high-resolution DEM. *Hydrology and Earth System Sciences Discussions*, 11(7), 7441–7467. doi:10.5194/hessd-11-7441-2014
- McCartney, M. P., Kashaigili, J. J., Lankford, B. a., & Mahoo, H. F. (2008). Hydrological modelling to assist water management in the Usangu wetlands, Tanzania. *International Journal of River Basin Management*, 6(1), 51–61. doi:10.1080/15715124.2008.9635337
- Milzow, C., & Kinzelbach, W. (2010). Accounting for subgrid scale topographic variations in flood propagation modeling using MODFLOW. *Water Resources Research*, 46(10), n/a–n/a. doi:10.1029/2009WR008088
- Mishra, S. (2009). Uncertainty and sensitivity analysis techniques for hydrologic modeling. *Journal of Hydroinformatics*, 11, 282. doi:10.2166/hydro.2009.048
- Moriasi, D. N., Arnold, J. G., Liew, M. W. Van, Bingner, R. L., Harmel, R. D., & Veith, T. L. (2007a). *Model Evaluation and Guidelines for Systematic Quantification of Accuracy in Watershed Simulation* (Vol. 50, pp. 885–900).
- Moriasi, D. N., Arnold, J. G., Liew, M. W. Van, Bingner, R. L., Harmel, R. D., & Veith, T. L. (2007b). *Model Evaluation Guidelines for Systematic Quantification of Accuracy in Watershed Simulation. Soil and Water Division of ASABE*, 50(3), 885–900.
- Morris, M. D., & May, N. (2007). Factorial Sampling Plans for Preliminary Computational Experiments. *Technometrics*, 33(2), 161–174.
- Mwakalila, S. (2011a). Assessing the Hydrological Conditions of the Usangu Wetlands in Tanzania. *Journal of Water Resource and Protection*, 03(12), 876–882. doi:10.4236/jwarp.2011.312097
- Mwakalila, S. (2011b). Assessing the Hydrological Conditions of the Usangu Wetlands in Tanzania. *Journal of Water Resource and Protection*, 03(December), 876–882. doi:10.4236/jwarp.2011.312097
- N.Yastikli, G. Kocak, G. B. (2003). Accuracy and morphological analyses of GTOPO 30 and SRTM X-C band DEMs in the test area Instabul, (2002).
- Ochieng, W. O., & Kimaro, T. A. (2009). Comparative study of performance of satellite derived rainfall estimate : Case Study of Mara River Basin.
- Proposal, S. R. (2011). Tropical Rainfall Measuring Mission.
- Rango, A., & Shalaby, A. I. (1998). Operational applications of remote sensing in hydrology: success, prospects and problems. *Hydrological Sciences Journal*, 43(6), 947–968. doi:10.1080/02626669809492189
- Rientjes, T. H. M., Muthuwatta, L. P., Bos, M. G., Booij, M. J., & Bhatti, H. a. (2013). Multi-variable calibration of a semi-distributed hydrological model using streamflow data and satellite-based evapotranspiration. *Journal of Hydrology*, 505, 276–290. doi:10.1016/j.jhydrol.2013.10.006

- Shafii, M., & Smedt, F. De. (2009). Multi-objective calibration of a distributed hydrological model (WetSpa) using a genetic algorithm. *Hydrology and Earth System Sciences*, (2006), 2137–2149.
- Shook, K. R. (2012). River Basins. *GEOG 827: Principles of Hydrology*.
- Shu, Y., & Villholth, K. (2012). Analysis of Flow and Baseflow Trends in the Usangu Catchment, Tanzania. ... *Water Management Institute, Pretoria, South Africa*, 1–13. Retrieved from http://www.ru.ac.za/static/institutes/iwr/SANCIAHS/2012/documents/047_Shu.pdf
- Singh, R., Senay, G., Velpuri, N., Bohms, S., & Verdin, J. (2014). On the Downscaling of Actual Evapotranspiration Maps Based on Combination of MODIS and Landsat-Based Actual Evapotranspiration Estimates. *Remote Sensing*, 6(11), 10483–10509. doi:10.3390/rs61110483
- Singh, S. K., Liang, J., & Bárdossy, A. (2012). Improving the calibration strategy of the physically-based model WaSiM-ETH using critical events. *Hydrological Sciences Journal*, 57(8), 1487–1505. doi:10.1080/02626667.2012.727091
- SMUWC. (2001a). *Sustainable Management of the Usangu Wetland and its Catchment*.
- SMUWC. (2001b). *Sustainable Management of the Usangu Wetlands and its Catchment*.
- Sorooshian, S., Hsu, K., Imam, B., & Hong, Y. (n.d.). Global Precipitation Estimation from Satellite Image Using Artificial Neural Networks.
- Tang, T., Reed, P., Wagener, T., & van Werkhoven, K. (2006). Comparing sensitivity analysis methods to advance lumped watershed model identification and evaluation. *Hydrology and Earth System Sciences Discussions*, 3, 3333–3395. doi:10.5194/hessd-3-3333-2006
- Todini, E. (2007). Hydrological catchment modelling: past, present and future. *Hydrology and Earth System Sciences*, 11(1), 468–482. doi:10.5194/hess-11-468-2007
- Vrugt, J. a., Gupta, H. V., Bastidas, L. a., Bouten, W., & Sorooshian, S. (2003). Effective and efficient algorithm for multiobjective optimization of hydrologic models. *Water Resources Research*, 39(8), n/a–n/a. doi:10.1029/2002WR001746
- Vrugt, J. a., Gupta, H. V., Bouten, W., & Sorooshian, S. (2003). A Shuffled Complex Evolution Metropolis algorithm for optimization and uncertainty assessment of hydrologic model parameters. *Water Resources Research*, 39(8), n/a–n/a. doi:10.1029/2002WR001642
- Wang, J., Hong, Y., Li, L., Gourley, J. J., Khan, S. I., Yilmaz, K. K., ... Okello, L. (2011a). The coupled routing and excess storage (CREST) distributed hydrological model. *Hydrological Sciences Journal*, 56(1), 84–98. doi:10.1080/02626667.2010.543087
- Wang, J., Hong, Y., Li, L., Gourley, J. J., Khan, S. I., Yilmaz, K. K., ... Okello, L. (2011b). The coupled routing and excess storage (CREST) distributed hydrological model. *Hydrological Sciences Journal*, 56(1), 84–98. doi:10.1080/02626667.2010.543087
- Wang, J., Hong, Y., Li, L., Gourley, J. J., Khan, S. I., Yilmaz, K. K., ... Okello, L. (2011c). The coupled routing and excess storage (CREST) distributed hydrological model. *Hydrological Sciences Journal*, 56(February 2015), 84–98. doi:10.1080/02626667.2010.543087
- Xue, X. (2012). Hands-on Session : Visualization of the CREST Model Results.

- Xue, X., & Hong, Y. (2013). *CREST Coupled Routing and Excess Storage-User Manual*.
- Xue, X., & Hong, Y. (2015). *Coupled Routing and Excess Storage (CREST) v2.0 User Manual - CREST User Manual (v2.0).pdf* (pp. 8–9). Retrieved from [http://hydro.ou.edu/files/Crest_Workshops/Kenya_Xianwu_2012/CREST User Manual \(v2.0\).pdf](http://hydro.ou.edu/files/Crest_Workshops/Kenya_Xianwu_2012/CREST%20User%20Manual%20(v2.0).pdf)
- Xue, X., Hong, Y., Limaye, A. S., Gourley, J. J., Huffman, G. J., Khan, S. I., ... Chen, S. (2013a). Statistical and hydrological evaluation of TRMM-based Multi-satellite Precipitation Analysis over the Wangchu Basin of Bhutan: Are the latest satellite precipitation products 3B42V7 ready for use in ungauged basins? *Journal of Hydrology*, *499*, 91–99. doi:10.1016/j.jhydrol.2013.06.042
- Xue, X., Hong, Y., Limaye, A. S., Gourley, J. J., Huffman, G. J., Khan, S. I., ... Chen, S. (2013b). Statistical and hydrological evaluation of TRMM-based Multi-satellite Precipitation Analysis over the Wangchu Basin of Bhutan: Are the latest satellite precipitation products 3B42V7 ready for use in ungauged basins? *Journal of Hydrology*, *499*, 91–99. doi:10.1016/j.jhydrol.2013.06.042
- Yang, J., Castelli, F., & Chen, Y. (2014). Multiobjective sensitivity analysis and optimization of distributed hydrologic model MOBIDIC. *Hydrology and Earth System Sciences*, *18*(10), 4101–4112. doi:10.5194/hess-18-4101-2014
- Zhang, X., Waters, D., & Ellis, R. (2013). Evaluation of Simhyd , Sacramento and GR4J rainfall runoff models in two contrasting Great Barrier Reef catchments. In *20th International Congress on Modelling and Simulation, Adelaide, Australia* (pp. 1–6).


```
cmd / c C:\Ilwis372_Dec2013\Extensions\ISOD-Toolbox\toolbox_batchroutines\trmm_3B42_025d_day.bat %1%230 x x H: Working_dir
C:\Ilwis372_Dec2013\Extensions\ISOD-Toolbox\GDAL\bin C:\Ilwis372_Dec2013 C:\Ilwis372_Dec2013\Extensions\ISOD-Toolbox\util
cmd / c C:\Ilwis372_Dec2013\Extensions\ISOD-Toolbox\toolbox_batchroutines\trmm_3B42_025d_day.bat %1%231 x x H: Working_dir
C:\Ilwis372_Dec2013\Extensions\ISOD-Toolbox\GDAL\bin C:\Ilwis372_Dec2013 C:\Ilwis372_Dec2013\Extensions\ISOD-Toolbox\util
```

Appendix B: Script used to convert TRMM data from MPE to ASCII

```
export ArcInfoNAS(trmm_3b42_20010101_day.mpr,trmm_3b42_20010101_day)
export ArcInfoNAS(trmm_3b42_20010102_day.mpr,trmm_3b42_20010102_day)
export ArcInfoNAS(trmm_3b42_20010103_day.mpr,trmm_3b42_20010103_day)
export ArcInfoNAS(trmm_3b42_20010104_day.mpr,trmm_3b42_20010104_day)
export ArcInfoNAS(trmm_3b42_20010105_day.mpr,trmm_3b42_20010105_day)
export ArcInfoNAS(trmm_3b42_20010106_day.mpr,trmm_3b42_20010106_day)
export ArcInfoNAS(trmm_3b42_20010107_day.mpr,trmm_3b42_20010107_day)
export ArcInfoNAS(trmm_3b42_20010108_day.mpr,trmm_3b42_20010108_day)
export ArcInfoNAS(trmm_3b42_20010109_day.mpr,trmm_3b42_20010109_day)
export ArcInfoNAS(trmm_3b42_20010110_day.mpr,trmm_3b42_20010110_day)
export ArcInfoNAS(trmm_3b42_20010111_day.mpr,trmm_3b42_20010111_day)
export ArcInfoNAS(trmm_3b42_20010112_day.mpr,trmm_3b42_20010112_day)
export ArcInfoNAS(trmm_3b42_20010113_day.mpr,trmm_3b42_20010113_day)
export ArcInfoNAS(trmm_3b42_20010114_day.mpr,trmm_3b42_20010114_day)
export ArcInfoNAS(trmm_3b42_20010115_day.mpr,trmm_3b42_20010115_day)
export ArcInfoNAS(trmm_3b42_20010116_day.mpr,trmm_3b42_20010116_day)
export ArcInfoNAS(trmm_3b42_20010117_day.mpr,trmm_3b42_20010117_day)
export ArcInfoNAS(trmm_3b42_20010118_day.mpr,trmm_3b42_20010118_day)
export ArcInfoNAS(trmm_3b42_20010119_day.mpr,trmm_3b42_20010119_day)
export ArcInfoNAS(trmm_3b42_20010120_day.mpr,trmm_3b42_20010120_day)
export ArcInfoNAS(trmm_3b42_20010121_day.mpr,trmm_3b42_20010121_day)
export ArcInfoNAS(trmm_3b42_20010122_day.mpr,trmm_3b42_20010122_day)
export ArcInfoNAS(trmm_3b42_20010123_day.mpr,trmm_3b42_20010123_day)
export ArcInfoNAS(trmm_3b42_20010124_day.mpr,trmm_3b42_20010124_day)
export ArcInfoNAS(trmm_3b42_20010125_day.mpr,trmm_3b42_20010125_day)
export ArcInfoNAS(trmm_3b42_20010126_day.mpr,trmm_3b42_20010126_day)
export ArcInfoNAS(trmm_3b42_20010127_day.mpr,trmm_3b42_20010127_day)
export ArcInfoNAS(trmm_3b42_20010128_day.mpr,trmm_3b42_20010128_day)
export ArcInfoNAS(trmm_3b42_20010129_day.mpr,trmm_3b42_20010129_day)
export ArcInfoNAS(trmm_3b42_20010130_day.mpr,trmm_3b42_20010130_day)
export ArcInfoNAS(trmm_3b42_20010131_day.mpr,trmm_3b42_20010131_day)
```

Appendix C: Script used to convert PET data from MPE to ASCII

```
Export ArcInfoNAS (pet_20111201.mpr, pet_20111201)
Export ArcInfoNAS (pet_20111202.mpr, pet_20111202)
Export ArcInfoNAS (pet_20111203.mpr, pet_20111203)
Export ArcInfoNAS (pet_20111204.mpr, pet_20111204)
Export ArcInfoNAS (pet_20111205.mpr, pet_20111205)
Export ArcInfoNAS (pet_20111206.mpr, pet_20111206)
Export ArcInfoNAS (pet_20111207.mpr, pet_20111207)
Export ArcInfoNAS (pet_20111208.mpr, pet_20111208)
```

Export ArcInfoNAS (pet_20111209.mpr, pet_20111209)
Export ArcInfoNAS (pet_20111210.mpr, pet_20111210)
Export ArcInfoNAS (pet_20111211.mpr, pet_20111211)
Export ArcInfoNAS (pet_20111212.mpr, pet_20111212)
Export ArcInfoNAS (pet_20111213.mpr, pet_20111213)
Export ArcInfoNAS (pet_20111214.mpr, pet_20111214)
Export ArcInfoNAS (pet_20111215.mpr, pet_20111215)
Export ArcInfoNAS (pet_20111216.mpr, pet_20111216)
Export ArcInfoNAS (pet_20111217.mpr, pet_20111217)
Export ArcInfoNAS (pet_20111218.mpr, pet_20111218)
Export ArcInfoNAS (pet_20111219.mpr, pet_20111219)
Export ArcInfoNAS (pet_20111220.mpr, pet_20111220)
Export ArcInfoNAS (pet_20111221.mpr, pet_20111221)
Export ArcInfoNAS (pet_20111222.mpr, pet_20111222)
Export ArcInfoNAS (pet_20111223.mpr, pet_20111223)
Export ArcInfoNAS (pet_20111224.mpr, pet_20111224)
Export ArcInfoNAS (pet_20111225.mpr, pet_20111225)
Export ArcInfoNAS (pet_20111226.mpr, pet_20111226)
Export ArcInfoNAS (pet_20111227.mpr, pet_20111227)
Export ArcInfoNAS (pet_20111228.mpr, pet_20111228)
Export ArcInfoNAS (pet_20111229.mpr, pet_20111229)
Export ArcInfoNAS (pet_20111230.mpr, pet_20111230)
Export ArcInfoNAS (pet_20111231.mpr, pet_20111231)